Model based predictive control for load following of a pressurised water reactor

Gerhardus Human
B.Ing. Electrical & Electronic Engineering
(Randse Afrikaanse Universiteit, 2004)

Dissertation submitted for the partial fulfilment of the requirements for the degree Magister in Engineering in Nuclear Engineering of the Post Graduate School for Nuclear Science and Engineering, North West University, Potchefstroom Campus

Supervisor: Dr. K.R. Uren

Co-Supervisor: Prof. G. van Schoor

November 2009
Potchefstroom

ABSTRACT

By September 2009 the International Atomic Energy Agency reported that the number of commercially operated nuclear reactors in 30 countries across the world is 436, around 50 reactors are currently being constructed, 137 reactors have been ordered or is already planned, and there are around 295 proposed reactors. Pressurised water reactors (PWRs) make up the majority of these numbers. The growing number of carbon emissions and the ongoing fight against fossil fuel power stations might see the number of planned nuclear reactors increase even more to be able to satisfy the world's need for cleaner energy. To ensure that technology keeps pace with this growing demand, ongoing research is essential. Not only is the research of new reactor technologies (i.e. High Temperature Reactors) important, but improving the current technologies (i.e. PWRs) is critical. With the increased contribution of nuclear generated electricity to our grids, it is becoming more common for nuclear reactors to be operated as load following units, and not base load units as they are more commonly being operated. Therefore a need exists to study and develop new strategies and technologies to improve the automatic load following capabilities of reactors.

PWR power plants are multivariable systems. In this study a multivariable, more specifically, a model predictive controller (MPC) is developed for controlling the load following of a nuclear power plant, more specifically a PWR plant. In developing this controller system identification is employed to develop a model of the PWR plant. For the identification of the model, measured data from a computer based PWR simulator is used as the input. The identified plant model is used to develop the MPC controller. The controller is developed and tested on the plant model. The MPC controller is also evaluated against another set of measured data from the simulator. To compare the performance of the MPC controller to that of the conventional controller the ITAE performance index is employed. During the process Matlab®, the System Identification Toolbox™, the MPC Toolbox™ and Simulink® are used.

The results reveal that MPC is practicable to be used in the control of non-linear systems such as PWR plants. The MPC controller showed good results for controlling the system and also outperformed the conventional controllers. A further

result from the dissertation is that system identification can successfully be used to develop models for use in model based controllers like MPC controllers. The results of the research show that a need exists for future research to improve the methods to eventually have a controller that can be applied on a commercial plant.

Keywords: control, model predictive, advanced, MIMO, nuclear reactor, pressurised water reactor, system identification.

OPSOMMING

In September 2009 is daar deur die Internasionale Atoom Energie Agentskap geraporteer dat daar ’n totaal van 436 kommersiele kern reactore in 30 lande wêreld wyd bedryf word. Daar is ook ongeveer 50 reactore wat tans onder konstruksie is, 137 reactore wat reeds beplan is, en ongeveer 295 voorgestelde reaktore. Die grootste getal hiervan word opgemaak deur drukwaterreaktore (DWRe). Die getal beplande reaktore kan binne die volgende paar jare steeds toeneem as in ag geneem word die toenemende koolstof vrystellings en die aanhoudende geveg teen fossielbrandstof stasies en die nood vir skoner energie. Aanhoudende navorsing is nodig om te verseker dat nuwe tegnologieë pashou met die groeiende energie aanvraag. Nie net is navorsing nodig in nuwe reaktor tegnologieë nie (bv. Hoë Temperatuur Reaktore), maar bevordering van reeds bestaande tegnologieë (bv. DWRe) is ook baie belangrik. Met die toenemende bydra van kern krag stasies tot elektriese netwerke reg oor die wereld, word dit ook meer algemeen om kern reaktore as lasvolg eenhede te bedryf. Daar is dus ‘n nood om nuwe strategieë en tegnologieë te bestudeer om die beheer van die las volg eenhede te verbeter.

DWRe is meerveranderlike stelsels. In die studie is ’n meerveranderlike beheerder, en meer spesifiek, ‘n modelvoorspellende beheerder ontwikkel om die druiwing van die kern aanleg te beheer. Die proses van stelsel identifikasie is gebruik om n model van die aanleg af te lei. Om die stelsel identifikasie te doen is gemete data van ’n rekenaar sagteware pakket van n DWR simulator gebruik. Die geidentifiseerde model is daarna gebruik om die modelvoorspellende beheerder te ontwikkel. Die model van die aanleg is gebruik om die beheerder te toets. Die beheerder is ook vergelyk met n stel data wat van die DWR simulator geneem is. Om die vertoning van die modelvoorspellende beheerder te evalueer teenoor die van die konvensionele beheerder, is die “ITAE” vertoning indeks gebruik. In die proses is Matlab® se System Identification Toolbox™, die MPC Toolbox™ asook Simulink® gebruik.

Die resultate het getoon dat dit prakties moontlik is om modelvoorspellende beheer te gebruk om nie-lineêre stelsels soos DWRe te beheer. Die modelvoorspellende beheerder het goeie resultate vertoon en ook beter vertoon as die konvensionele

beheerders. Die studie het ook verder bewys dat stelselidentifikasie sukksesvol aangewend kan word om modelled af te lei wat vir die ontwikkeling van modelvoorspellende beheer gebruik kan word. Die resultate van die studie dui daarop dat daar ‘n behoefte bestaan om verdere navorsing in die rigting van modelvoorspellende beheer om uiteindelik ’n beheerder te ontwikkel wat in kommersieele aanlegte geimplimenteer kan word.

ACKNOWLEDGEMENTS

All thanks to God, for providing the opportunities, resources, knowledge, strength and determination to succeed.

Thanks to Dr. Kenny Uren for your guidance and experience to make this a success.

“The mind is like a parachute. It doesn’t work unless it’s open”

Thanks to Prof. George van Schoor for your advice and support and willingness to listen to my proposal.

“A wise man does not need advice and a fool won’t take it”

TABLE OF CONTENTS

LIST OF FIGURES

LIST OF TABLES

LIST OF ABBREVIATIONS

ARX	-	Autoregressive Exogenous
BWR	-	Boiling Water Reactor
DSn	-	Data set n for $n = 1, 2, 3, 4, 5, 6, 7$
DWR	-	Drukwaterreaktor
EDF	-	Electricité de France
EPR	-	European Pressurised Reactor
GUI	-	Graphical User Interface
HP	-	High Pressure
IAEA	-	International Atomic Energy Agency
IHX	-	Intermediate Heat Exchanger
ITAE	-	Integral Time Absolute Error
KAERI	-	Korea Atomic Energy Research Institute
LBE	-	Lead Bismuth Eutectic
LP	-	Low Pressure
LQR	-	Linear Quadratic Regulator
LQG	-	Linear Quadratic Gaussian
LTI	-	Linear Time-Invariant
MIMO	-	Multi-Input Multi-Output
MIT	-	Massachusetts Institute of Technology
MPC	-	Model Predictive Control
PBMM	-	Pebble Bed Micro Model
PBMR	-	Pebble Bed Modular Reactor
PWR	-	Pressurised Water Reactor
SISO	-	Single-Input Single-Output
VVER	-	Voda-Vodyanoi Energetichesky Reaktor (Russian: Pressurised Water Reactor
XADS	-	Experimental Accelerator Driven System

LIST OF SYMBOLS

T	Temperature	^oC
T_{Hot}, T_{co}	Reactor outlet temperature	^oC
$T_{Cold,}$ T_{ci}	Reactor inlet temperature	^oC
T_{Avg}, T_m, T_c, T_p, T_{pc}	Reactor average temperature	^oC
T_{ref}	Reference Temperature	^oC
T_{po}	Steam generator primary outlet temperature	^oC
T_{pi}	Steam generator primary inlet temperature	^oC
T_s	Steam generator steam temperature	^oC
T_w	Steam generator feedwater temperature	^oC
T_{SG}	Average secondary circuit temperatures	^oC
T_f	Fuel temperature	^oC
P_c	Reactor core pressure	Pa
P_s	Steam generator secondary pressure	Pa
P_t	Pump inlet pressure	Pa
P_e	Pump outlet pressure	Pa
$\dot{m}$	Mass flow rate	kg/s
d, $\dot{m}_g$	Steam mass flow	kg/s
F, $\dot{m}_c$	Primary coolant flow rate	kg/s
$\dot{m}_f$	Feedwater mass flow	kg/s
P, P_l	Reactor power	kW
$P(t)$	Reactor power at time, t	kW
P_0	Reactor power at time $t = 0$	kW
P_f , $P_f(t)$	Power from fission	kW
$P_{di}(t)$	Power from decay heat	kW
$\dot{Q}$	Heat transfer rate across boundaries	kW
$\dot{Q}_s$	Supplied heat transfer rate	kW
$\dot{Q}_R$	Rejected heat transfer rate	kW

$\dot{W}$	Net work transfer rate across boundaries	kW
E	Energy in steam	kJ
U_{sg}	Steam generator internal energy	kJ
E_{evap}	Evaporation energy	kJ
W_{loss}	Heat loss	kJ
ε	Fast fission factor	
P_f	Fast non-leakage factor	
p	Resonance escape probability	
P_{th}	Thermal non-leakage factor	
f	Thermal utilisation factor	
η	Reproduction factor	
N_0	Fast neutrons from thermal fission	
k_{eff}	Effective multiplication factor	
F_0	Neutrons in initial generation	
F_n	Neutrons in next generation	
$\sum_a^f$	Fuel absorption cross-section	cm^{-1}
$\sum_a^D$	Poisons absorption cross-section	cm^{-1}
β	Delayed neutron fraction	
l^*	Prompt neutron life-time	s
λ_i	*i-th* precursor group decay constant	
C_i	*i-th* precursor group concentration	
N	Number of delayed neutron precursor groups	
$n(t)$	Neutron population	
$\tau(t)$	Reactor period	
$\lambda_e(t)$	Effective multi-group decay parameter	
ρ_t , $\rho(t)$	Net reactivity	Δk/k
ρ_c	Reactivity from control rod movement	Δk/k
$\dot{\rho}(t)$	Rate of change of the reactivity	Δk/k/s
α_f	Fuel temperature coefficient	Δk/k/^{o}C

α_c	Coolant temperature coefficient	$\Delta k/k/^oC$
Ψ_i	Portion of decay heat power	kW
n	Neutron flux	n/cm^2
κ	Power per unit of flux	kW
$\bar{h}_f$, h_i	Enthalpy for saturated water	kJ/kg
$\bar{h}_g$, h_e	Enthalpy for saturated steam	kJ/kg
C_f	Fuel specific heat	$kJ/kg.^oC$
C_c	Coolant specific heat	$kJ/kg.^oC$
C_{sg}	Water & steel specific heat	$kJ/kg.^oC$
c_p^w	Water specific heat	$kJ/kg.^oC$
c_p^s	Vapour specific heat	$kJ/kg.^oC$
h_{fc}	Fuel to coolant heat transfer coefficient	$kW/m^2.^oC$
m_f	Fuel mass	kg
m_c	Coolant mass	kg
m_{sg}	Primary steam and water mass in steam gen.	kg
m_f	Mass of water in secondary side	kg
m_g	Mass of steam in secondary side	kg
v_1, v_2	Control rod vertical position	m
D	Diameter	m
Δv_w	Change in velocity in whirl direction	m/s
A_{fc}	Fuel to coolant heat transfer area	m^2
V_{sg}	Steam generator secondary side volume	m^3
v_f	Fluid specific volume	m^3/kg
v_g	Steam specific volume	m^3/kg
N	Rotational speed	rev/min
f_s	Frequency of the output voltage	Hz
t	time	s
n	Generator number of pole pairs	

u	Input
x	State
y	Output
r	Reference
$\hat{y}$	Simulated or predicted output
$\bar{y}$	Mean of the measured output
$\boldsymbol{u}$	Input vector
$\boldsymbol{x}$	State vector
$\boldsymbol{y}$	Output vector
A, B, C, D, K, O	*M*atrices
x_i	i^{th} controlled variable
r_i	i^{th} reference variable
u_i	i^{th} manipulated variable

CHAPTER 1. INTRODUCTION

In this chapter a broad introduction to this study is given. Background is provided on the operations of a PWR power plant along with a basic explanation of the control strategy of a PWR power plant. This is followed by an overview of the issues to be addressed along with the accompanying methodology. This chapter concludes with an outline of the chapters of the thesis.

1.1 Background

In order to operate any large-scale process safely, for example a nuclear power plant, control system engineering is extremely important. Today a majority of plant control systems are still based on classical control loops. Modern advanced multi-input multi-output (MIMO) controllers receive very little attention. Although MIMO controllers are more complex to implement, if applied correctly they can considerably improve plant performance.

During the first few operational years only a small fraction of electrical power on grids around the world were supplied by nuclear power plants. Because of their high capital costs, and also lack of operating experience in nuclear calculations as well as in plant behaviours, it was preferred to operate nuclear power plants at constant full load. Lately however, electrical grids across the world are increasing the percentage of electrical power supplied by nuclear plants. Examples of such grids are the grids of Northern Germany (Hamburg) and Southern Germany (Bavarian), each having 80% and 60% nuclear generated electricity respectively, and also the grid of Electricité de France (EdF) with 80% nuclear generated electricity. This growth led to an increased interest in control strategies that would enhance plant operating during load-following conditions. Today there is an even bigger drive to increase the percentage of nuclear generated electricity in order to reduce carbon emissions.

Two points are therefore highlighted. Firstly nuclear power plants, especially PWRs, are expected to increase in numbers in the next few years, and secondly conventional control is still the preferred method of plant control. Advanced MIMO controllers can replace these conventional controllers with significantly improved performance. For this reason methods for developing advanced MIMO controllers

require ongoing researche to firstly demonstrate that these controllers will in reality present the improved performance that they are expected to produce, and further to show that these controllers are reliable.

The next few sections (1.1.1 and 1.1.2) provide a basic overview of PWR plants and its associated control. Also provided is an introduction to the PWR simulator in 1.1.3 and an overview of MIMO control in 1.1.4.

1.1.1 The pressurised water reactor

A pressurised water reactor (PWR) is a light water nuclear reactor. The PWR is the most common nuclear reactor for power generation. A light water reactor is a reactor that uses light water as a coolant and also as the neutron moderator. The term light water is used to distinguish between heavy water and light water. Light water refers to the commonly known water (H_2O) opposed to what is known as heavy water or deuterium (^2H_2O). The most common two types of light water reactors (LWRs) are the PWR and the boiling water reactor (BWR). The difference between conventional coal fire power plants and LWRs are the source of heat. Both use steam to turn power turbines for generating electricity. In a nuclear reactor however the heat is generated by nuclear fissions and transferred to the turbine in various ways. A PWR utilises a combined cycle, splitting the plant into a primary loop and a secondary loop. The reactor heats up water in the primary loop and transfers the heat to the water in the secondary loop through a steam generator. The water in the primary loop of a PWR is not allowed to boil. For it to reach the high temperatures of around 320^oC required the entire primary system is placed under very high pressures of around 155bar or 15.5MPa. The steam generator produces the steam to turn the turbine. A boiling water reactor uses a direct cycle, meaning that the steam is generated directly inside the reactor and the same steam is used to turn the turbine. The PWR is discussed further in more detail as it is the focus of this study. Figure 1 shows a conceptual diagram of a PWR power plant. A PWR plant uses water under pressure as the heat transfer medium. The water absorbs heat created by the reactor core and transfers the heat to the secondary loop in the steam generator generating the steam used to drive the turbine. The same water used to transport the heat is also used as the moderator in the PWR. A moderator slows down the fast (high energy) neutrons to slow (thermal energy) neutrons therefore helping the

nuclear fission reaction. A pressuriser controls the coolant pressure. The fluid flow is controlled by large electric pumps. Reactor power is controlled by neutron absorbing control rods inserted at specific depths into the reactor core. This is used to keep the average coolant temperature at a specific set point. Neutron flux signals and turbine power signals are used to control the reactor/turbine power during load variations. Neutron absorbing boric acid added to the reactor coolant is used for long term neutron absorbing regulation. The coolant temperature in a PWR is also used as a control input to perform reactor control and steam dump operations [4], [25].

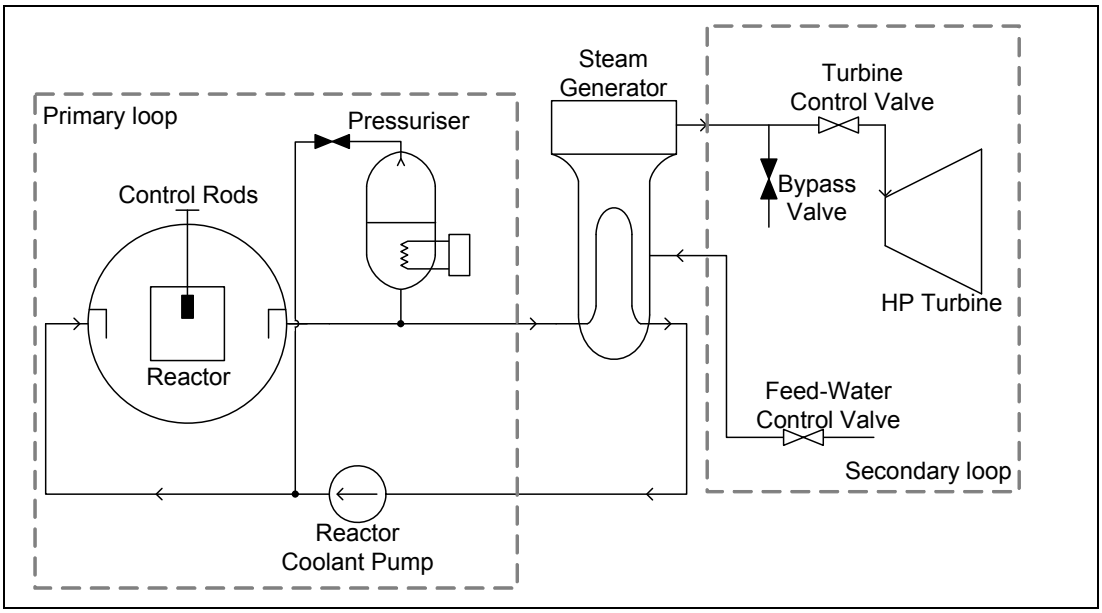

Figure 1: PWR power plant

1.1.2 Nuclear power plant control

The power control of a PWR is performed by the turbine/generator control system (governor) along with the reactor control system. These two systems work together through design and also through limiting functions to control the system. A balanced collaboration is required between the two systems for start-up, power operations and also disturbance situations. Figure 2 illustrates an example where the reactor control unit receives its reference from the turbine power. Figure 2 shows that the average temperature, turbine power and the reference temperature from the turbine power are used as inputs to the reactor control unit. Average temperature is the average between the reactor outlet temperature (T_{Hot}) and the reactor inlet temperature (T_{Cold}).

There are two plant control philosophies of operation:

- **Reactor follows turbine mode**, where the power is controlled according to the demand using a reference value and/or a value derived from the frequency deviation. The average coolant temperature control is normally used to adjust the reactor power.
- **Turbine follows reactor mode** is normally used when the plant is not yet connected to the grid, for example during start-up [3].

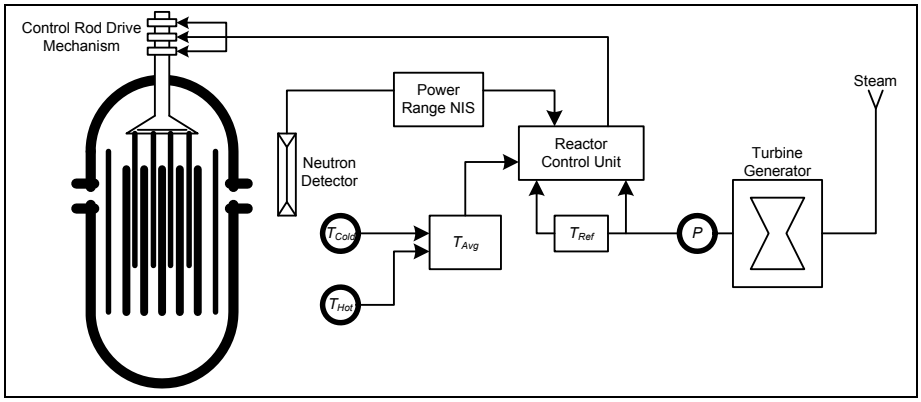

Figure 2: Reactor power dependant on turbine load [9]

1.1.2.1 Governor operations

When the mechanical loading on the generator increases, the speed will drop slightly for the rotor current to increase in order to supply the increased torque. The stator windings will then draw more current from the supply. Increased current flow in the stator causes a braking effect on the rotor, decreasing its speed slightly. The governor responds to this speed reduction and allows more steam to enter the turbine. The turbine speed and power is increased allowing the generator to deliver the required load. The increased steam flow will gradually reduce the pressure in the steam generators. Control is then required to adjust the power from the reactor in order to increase the heat transferred to the steam generators and thereby restoring the pressure.

In all governor systems the turbine-generator shaft speed is used as the basis on which to alter the working fluid. The working fluid in the case of a PWR power plant is steam from the steam generators [1].

1.1.2.2 Steam generator water level control

The main purpose of the steam generator control system is to maintain the water level in the steam generator by regulating the feedwater flow. The control system is often called the “feedwater control system”. Control of the water level in a steam generator is a very important part of the power plant control, as about 25% of nuclear power plant reactor shutdowns are as a result of ineffective feedwater control. These shutdowns cause severe economic loss [5].

1.1.2.3 Reactor control

A nuclear reactor is controlled by controlling the rate of fission reactions in the reactor. Power output is directly proportional to the rate of fission reactions.

A reactor’s fission rate is controlled by inserting and withdrawing control rods made of a neutron-absorbing material, such as boron. These are interspersed with the fuel rods. Figure 3 shows a PWR cluster control assembly and single fuel rod schematic.

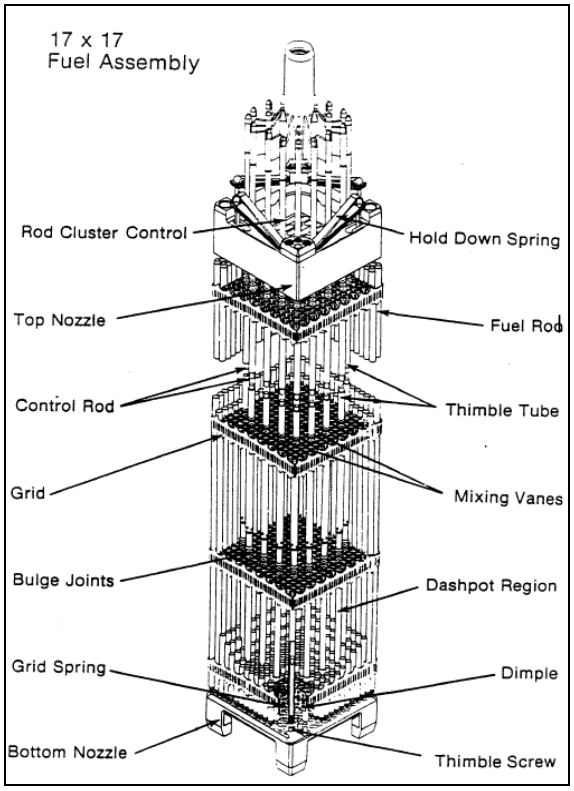

Figure 3: PWR cluster control assembly and single fuel rod schematic [9]

In PWRs boron can also be added to the water in the form of boric acid. This is however only done to aid in long term reactivity control.

By lowering and raising the control rods the rate of fission reactions can be controlled. The control rods absorb neutrons available for fission reactions.

Control rods are moved up and down to minimise the difference between the reactor power and the turbine load. Figure 4 is an example of a conventional reactor regulating system. Figure 4 shows that control rod position is also dependant on the average temperature from the coolant loops and the temperature reference set-point obtained from the turbine load.

Automatic power control is normally only performed by control rod movement. Boric acid control is used mainly for control rod worth and fuel burn-up compensation at the start of fuel and rod lifetimes [2].

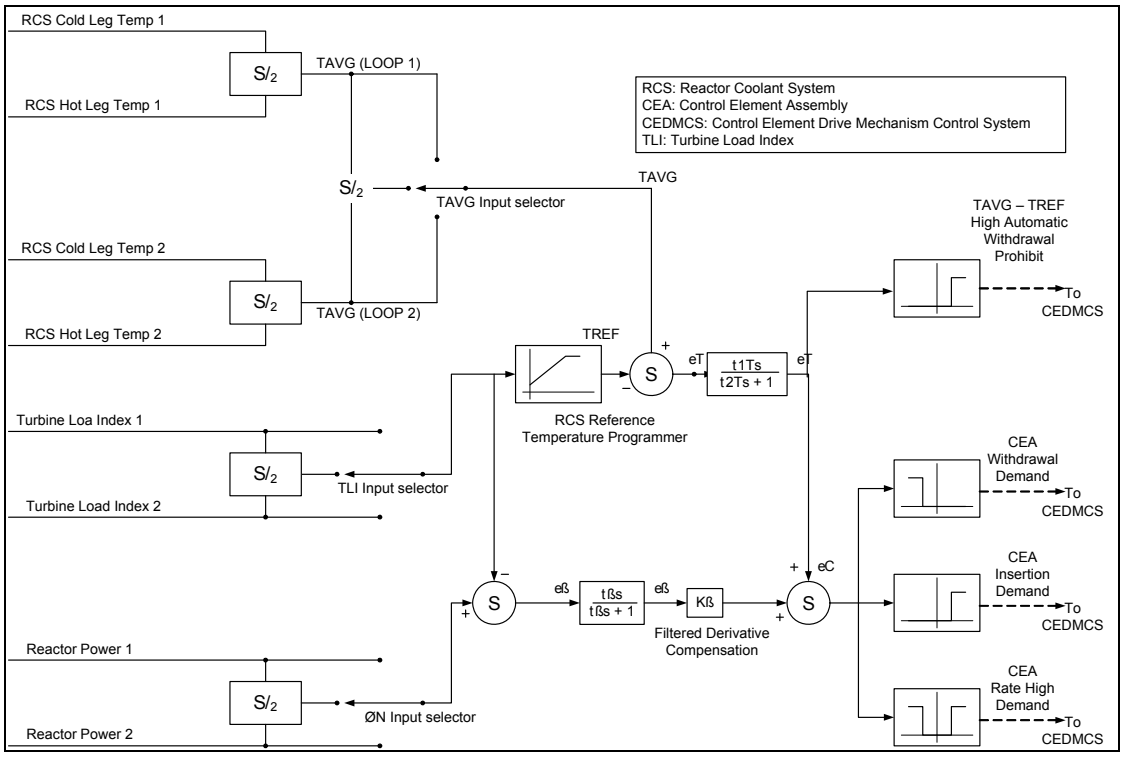

Figure 4: Conventional reactor regulating system [19]

1.1.3 Pressurised water reactor simulator

For the purpose of this study a PWR simulation code is used. The simulator is PC-based simulator software and can be used to predict transient behaviours. The simulator is based on a plant model of the Westinghouse 3-loop PWR 900MW_e type reactor. The simulator is developed by Micro-Simulation Technology [38] and provides the possibility of saving the plot data from all the variables available into an

excel spreadsheet. This information can easily be transferred to the Matlab® environment for necessary processing and development of the controller. Figure 5gives a screen shot of the PCTran simulator used.

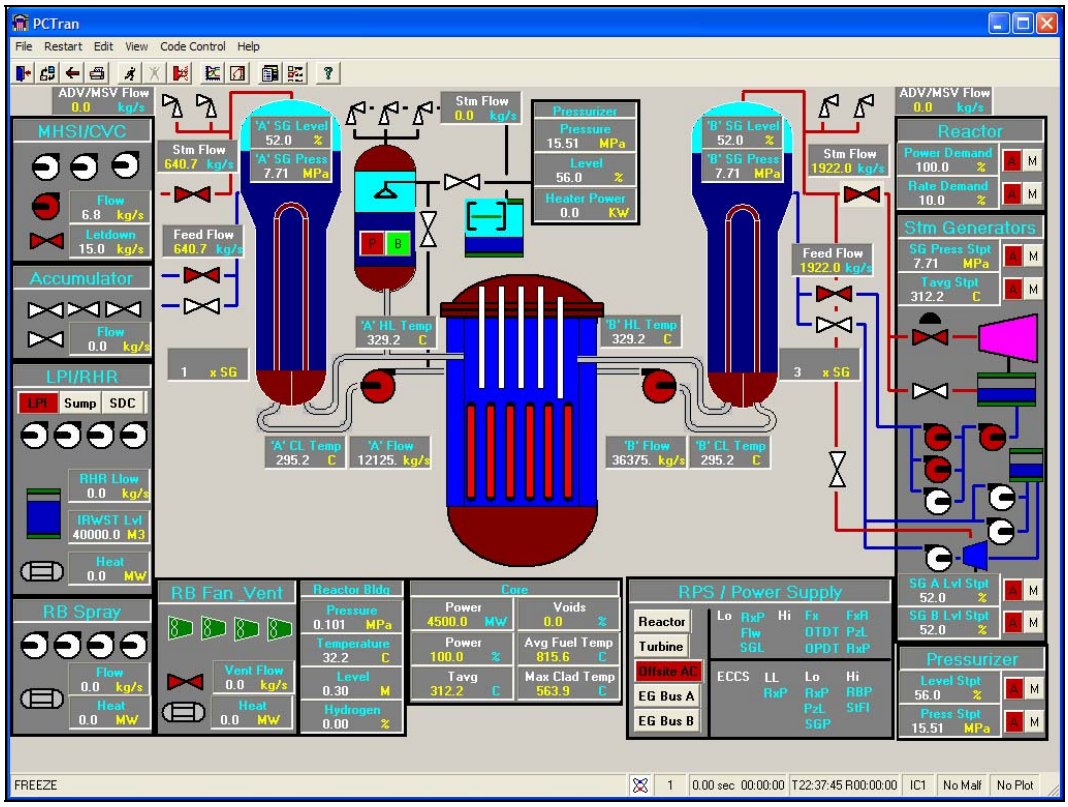

Figure 5: PCTran Simulator

1.1.4 MIMO controllers

A multivariable system is defined as a system having a multiple number of inputs and a multiple number of outputs. This is often also referred to as a MIMO.

Before designing a MIMO control strategy, the process first needs to be modelled, either analytically using sets of differential equations to describe a system, or empirically using data obtained from measured data fitted to a specified model structure.

Various types of MIMO control strategies are available. The most common and also the ones to be considered for this study are MPC, robust MIMO control, linear-quadratic-regulator (LQR) control, and linear-quadratic-Gaussian (LQG) control.

1.2 Purpose of research

The purpose of this study is to develop a MIMO controller for load following of a PWR power plant. A single controller must be developed to include all control functions of a PWR power plant as far as possible. The control of the nuclear reactor power, the steam generator water level, and the power turbine steam supply are the control actions that are identified as control functions that are required to be included.

1.3 Issues to be addressed and methodology

1.3.1 Obtain a plant model

To develop model based controllers a plant model is required. A PWR PC-based simulation code is used to generate input-output data sets. The measured data is used to develop the plant model using system identification techniques. For this, different approaches to system identification and available model structures are studied. The System Identification Toolbox™ in Matlab® is used to derive models from the measured input-output data.

1.3.2 Verify this model, select the best performing model

The models obtained using the system identification techniques is verified on how well they predict the outputs of the system for a given set of inputs. The best fit approach available in the System Identification Toolbox™ is used. The model with the best fit is used for the controller development.

1.3.3 Develop the controller

Literature on the PWR power plant is studied to gain a deeper understanding of the working and limitations of the plant. Different MIMO control techniques are studied and the most suitable MIMO control strategy is used. A MIMO controller will then be derived from the best system model obtained.

1.3.4 Verify the controller and measure performance

The MIMO controller is tested and the outputs compared to that of the conventional controller for the same input disturbances. The model from the simulator is used as a platform for controller evaluation.

The performance of the controller will be assessed using the Integral of Time Multiplied by the Absolute Value of Error performance index available in Matlab®:

$$ITAE = \int_0^\infty t\left|e(t)\right|dt\,, \tag{1.1}$$

where t represents time and $e(t)$ represents the difference between the set-point and controlled variable.

A comparison will be made between the performance results of the classical controller and the MIMO controller.

1.4 Outline of the thesis

The procedure followed to develop the MPC controller is presented in Figure 6.

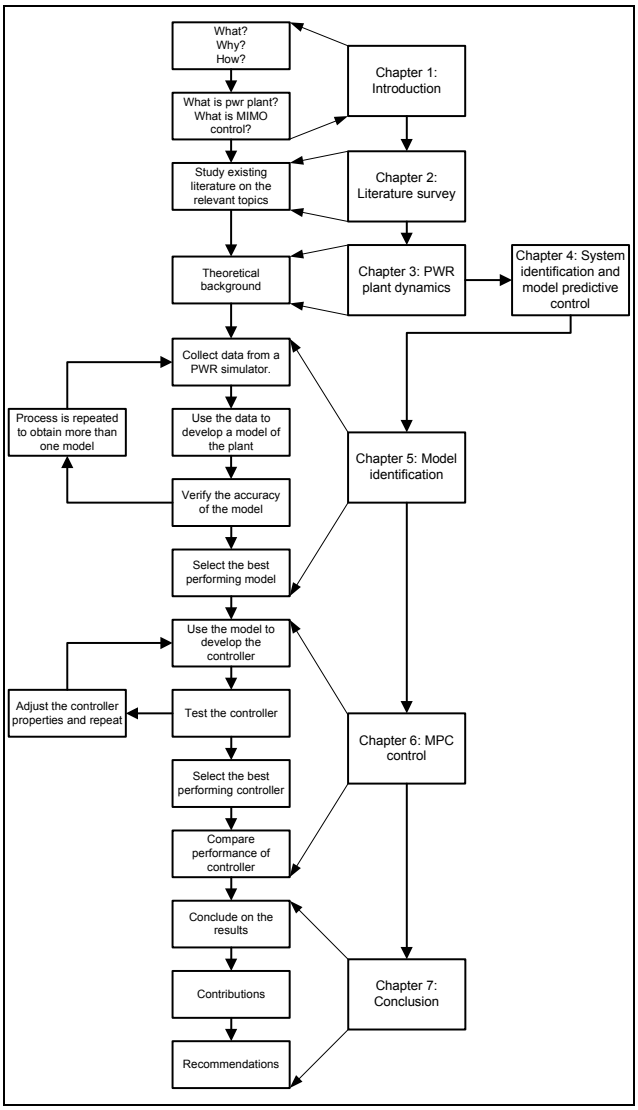

Figure 6: Chapter layout

Chapter 2: Literature survey

In this chapter the reader will be given an overview of similar research that has been completed and describes how the results of each are relevant to the current dissertation.

Chapter 3: PWR plant dynamics

In chapter three a detailed description is provided on PWR plant dynamics and also the plant control functions. This chapter provides an understanding of how a PWR operates.

Chapter 4: System identification and MPC

In chapter four a detailed description is given on system identification and MPC. This chapter provides information regarding the application of system identification and MPC and also provides information regarding the software to be used during this study.

Chapter 5: System modelling

Chapter five will include the procedures and models of the system identification and its validation. This chapter gives an explanation on how the system identification procedure is applied and the model obtained and verified.

Chapter 6: Model predictive control

Chapter six includes the procedures for developing the controller and its validation. This chapter gives an explanation on how the controller is developed and applied and eventually tested and compared to the traditional control strategy.

Chapter 7: Conclusion

Chapter seven provides the reader with the closing conclusion, gives the contributions that is made by this study, and also provides the information regarding future research that can follow from this work.

CHAPTER 2. LITERATURE SURVEY

The literature survey is focused on providing information of previous work done on system identification and/or MPC of nuclear facilities. This literature survey will be limited to applications focused specifically on the nuclear facilities and components thereof. The survey will however not be limited only to PWR types but reactor power plants of all types.

2.1 Power plant system identification

Two approaches for modelling systems have been developed and applied in many applications over the years. The first of these approaches is based on obtaining a model from first principles. This approach normally involves many man hours and complex mathematical formulations. The second approach is based on obtaining a system model by using data from the specific system. This is known as the system identification approach. If measured data of the required system model is available a model of the system can be obtained in a relatively short time.

The following three sections (2.1.1, 2.1.2 and 2.1.3) describe work done where system identification was applied on a nuclear plant. Section 2.1.4 gives a conclusion on how these contribute to the work of this research. The references mentioned here have been selected to be discussed in more detail. Some more references that were studied regarding reactor modelling is [30], [32], [33], [34], [35].

2.1.1 Modelling of PBMM using SISO models

System identification has previously been researched for modelling the Pebble Bed Modular Reactor (PBMR) [10]. Data from the pebble bed micro model (PBMM) was used to develop single-input single-output (SISO) models for three subsystems of the PBMM. The models were obtained through system identification techniques.

The power conversion unit of the PBMM is based on a three-shaft closed-loop recuperative Brayton cycle. Figure 7 shows the basic layout of the recuperative Brayton cycle [10].

Separate linear time-invariant SISO models were obtained for the low pressure injection system, the high pressure extraction system, and the bypass valve

regulation system. The System Identification Toolbox™ in Matlab® was used. The models obtained were of high quality and these models could essentially be used to design a control system for the PBMM and ultimately the PBMR.

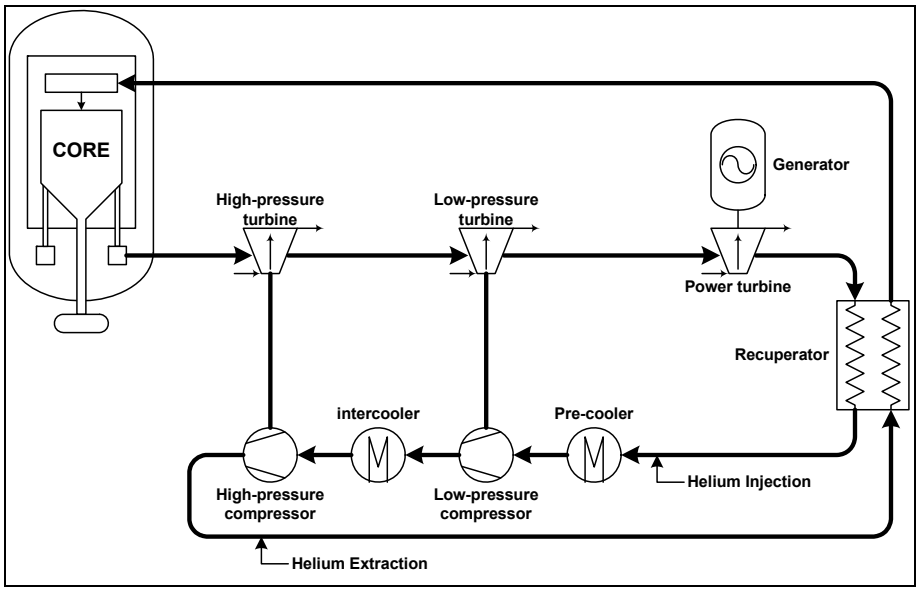

Figure 7: The recuperative Brayton cycle [10]

2.1.2 Linearising a non-linear model for PWR controller design

System identification has been used for deriving linear models of a set of system data obtained from a non-linear model. In [11] system identification was used to derive a linear model of a non-linear PWR plant. A method was described for designing a control system for a plant having continuous non-linearities using system identification techniques and robust controller design methods. The identification of the plant was done at different operating points. The bounds to the robust controller design were obtained by using the variations of the identified coefficients of the transfer functions obtained from the two different operating points. The Horowitz-technique was used for the robust controller design. This method was then tested in the design of the controllers of the steam supply system of a PWR. These controllers were also evaluated on a non-linear simulation of the PWR. The system was identified at two power levels. This was 20% power and 90% power. The conclusion was that the approach followed here could be very useful, especially for systems containing non-linearities. The non-linear model had to be used for verification as there was no physical plant available for the controller design to be tested on in South Africa. Better simulations can however be developed that would produce

simulations much closer to reality. A conclusion from [11] mentioned that in future studies more attention could be given to the system identification approach. In [11] the effects of the pressuriser were ignored. The assumption was made that the pressuriser controller would maintain the required pressure at all times. Effects of boric acid addition and neutron poison effects were also ignored. If a controller for a physical plant were to be developed these effects would not be ignored. An approximation of xenon values would be useful in achieving this goal.

2.1.3 Identification and H_∞ control design for a PWR

Controller design following the system identification route for a PWR from observed data have been attempted before [20]. The objective was to design controllers for a PWR using model based control techniques. The physical system data was identified from experimental data using a MIMO state-space description. An H_∞ controller was designed using a lower order model of the plant. From a PWR standpoint the required power corresponds to a specific steam flow input that may be viewed as a measurable disturbance. The identification experiments were carried out using a realistic nonlinear simulator developed by Electricité de France (EDF). The model obtained was validated on a different data set from the one with which it was estimated. The results achieved were successful over a very large operating range. The large operating range was achieved mainly due to the static inversion performed at the plant input. Figure 8 shows the basic components of the reactor and steam generator.

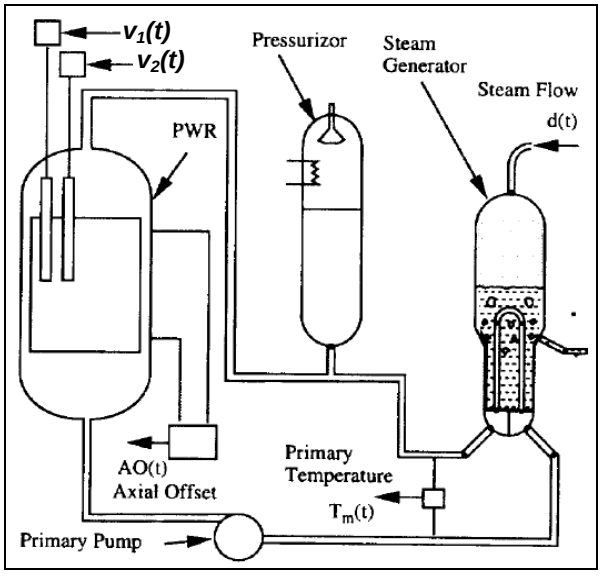

Figure 8: Primary circuit and steam generator [20]

Figure 9 gives the block diagram of the plant system with the inputs and outputs that were used for the system identification.

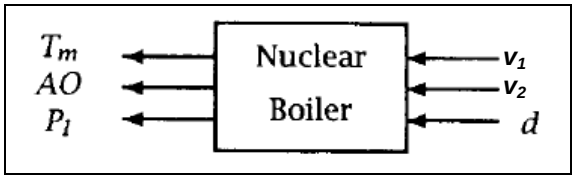

Figure 9: Plant system [20]

where T_m is the average temperature, AO is the axial offset, P_I is the power, d is the steam flow and v_1 and v_2 are the vertical positions of the rods.

2.1.4 Conclusion

The contribution of system identification to the present research is to develop a system model that could be used to design a controller for the specific PWR plant.

In [10] system identification was used to develop three separate SISO models for the PBMM. These were the low pressure injection system, the high pressure injection system and the bypass valve regulation system. The same basic method would be used to identify the systems for the current study. The difference is that for the present research the entire plant is included, i.e. all components of the primary and secondary loops. The model will also be a single MIMO model and not separate models for each system.

In [11] system identification was used to derive linear models from data of a non-linear model of a PWR plant. By doing this the non-linearities were eliminated. The results obtained in [11] were very useful and it was noted that specifically the approach of system identification could be given some more attention. Therefore in the present research the use of system identification to develop a model of the plant would be a large contribution to future research. The development of a controller can be simplified and development time reduced.

In [20] system identification was used to generate a system model of a PWR. The inputs and outputs used were average temperature (T_m), the axial offset (AO), the reactor power (P_I), the steam flow (d) and the respective vertical positions of the control rod assemblies $(v_1$ and $v_2)$. (Refer to Figure 8 & Figure 9). The system model

obtained was a relatively low order state-space model. Only the reactor variables were controlled. For the present research the entire power plant is to be controlled. This requires much more inputs and outputs and will deliver a higher order system model. A much narrower operating range will be achieved but a controller for the entire plant will be realised.

2.2 Controller development

MPC is an effective method for dealing with MIMO control problems. MPC has also received a great deal of attention in industrial process system control and MPC has been applied successfully in nuclear power plants with very good results.

The following two sections (2.2.1 and 2.2.2) describe two different studies where MPC was applied in the nuclear industry. Section 2.2.3 concludes on how these contribute to the current study. The references mentioned here have been selected to be discussed in more detail. Some more references that were studied regarding reactor control is [29], [31], [36], [37].

2.2.1 Model predictive controller of an experimental reactor

A model predictive controller has previously been proposed for controlling the Italian LBE-cooled 80MWth experimental accelerator driven system (XADS) [16]. The objective was to minimise the difference between the average temperature of the diathermic oil and its reference value. The main goal was essentially to minimise the variations in the control input. The response of the LBE-XADS was evaluated with reference to a 20% reduction in reactor power from nominal power. The main design data for the Italian LBE-XADS is given in Table 1, followed by a layout of the plant in Figure 10. A description of the plant is can be found in [16].

The conclusion was that despite the demanding transient that was used (20% reduction from nominal) the proposed controller was very effective in satisfying their requirements. It was noted that the adoption of the MPC strategy could be even more useful if several constraints on the physical variables of the plant components have to be fulfilled during the transients. These variables could include the temperature and/or the velocity of the LBE coolant in the core, in addition to the average temperature of the diathermic oil and the air mass flow rate.

Table 1: Main design data of the Italian LBE-XADS [16]

Core power MW_{th}	80
Primary coolant	Lead bismuth eutectic
Core inlet temperature ^{o}C	300
Core outlet temperature ^{o}C	400
Coolant flow rate in the core kg/s	5471
Coolant velocity in the core m/s	~0.4
Secondary coolant	Organic diathermic fluid
IHX secondary coolant inlet temperature ^{o}C	280
IHX secondary coolant outlet temperature ^{o}C	320
IHX secondary coolant flow rate kg/s	796.8
Effective core sub-criticality (Beginning-of-life)	0.97
Effective core sub-criticality (End-of-life)	0.94
Fuel	UO_2-PuO_2 mixed oxides
Target Material	Lead bismuth eutectic
Proton energy MeV	600
Maximum beam current mA	6

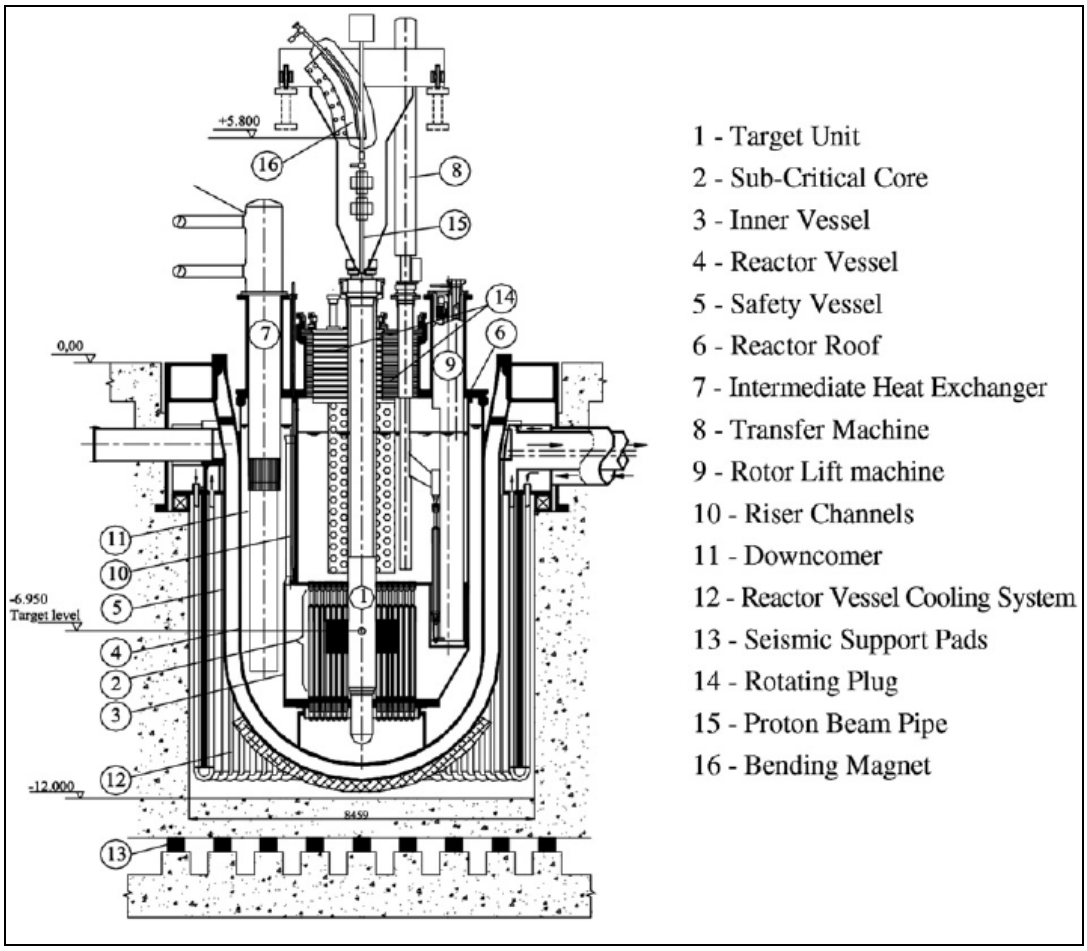

Figure 10: LBE-XADS reactor layout [16]

2.2.2 Model predictive controller design for a PWR

MPC techniques have been proposed for PWR plants [19]. The core dynamics of a PWR is identified online by a recursive least-squares method. Based on the identified reactor model consisting of the control rod position and the core average temperature, the future average coolant temperature is predicted. A MPC strategy is applied for designing an automatic controller for the thermal power control of PWR reactors. The objectives of the proposed MPC are to minimise both the difference between the predicted core coolant temperature and the desired temperature, as well as minimising the variation of the control rod positions. The proposed controller for a nuclear reactor was verified using a three-dimensional nuclear reactor analysis code, MASTER, developed by the Korea Atomic Energy Research Institute (KAERI). From the results of a numerical simulation carried out to verify the proposed controller performance, from a 5%/min ramp increase of a desired load and a 10% step increase of a desired load, it was found that the proposed controller could track the desired power level very good when compared to the nuclear power level controlled. Figure 11 shows the schematic diagram of the proposed MPC controller.

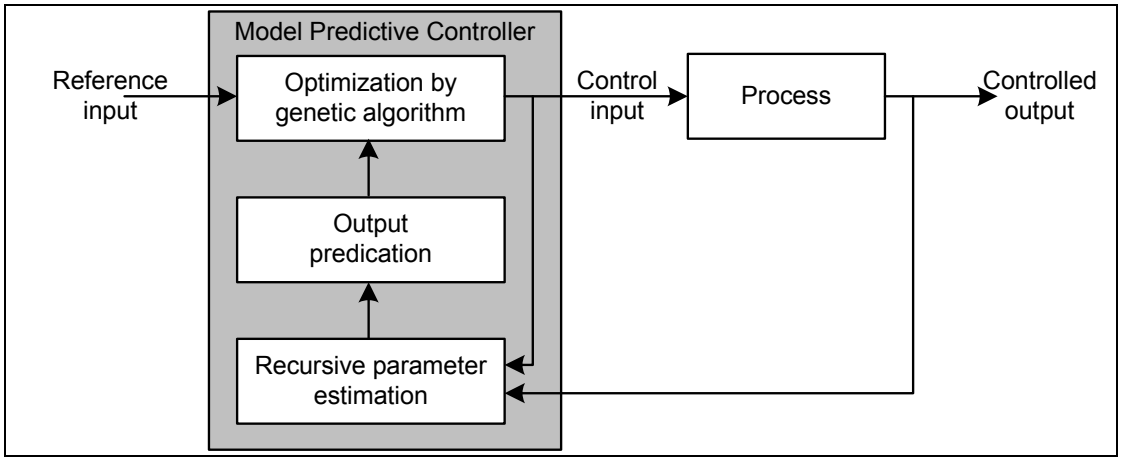

Figure 11: Proposed MPC schematic block diagram [19]

2.2.3 Conclusion

The contribution of MPC to the present research is to develop a MIMO controller for the entire power plant. MPC is a proven MIMO control strategy. A valuable feature of MPC is its capability to reject disturbances very well. This is due to its built-in optimisation algorithms and predictive characteristics.

In [16] a controller was designed and proposed for the Italian LBE-XADS. (Refer to Table 1 and Figure 10 for detail.) The controller was very successful in achieving the set requirements. The model obtained however did not capture all the dynamics of the system. This may be due to certain assumptions concerning the selected input data. In this study all possible inputs will be considered for capturing as much dynamic inputs as possible.

In [19] a MPC was proposed for a PWR. The reactor model was identified and a MPC designed to control the reactor power. The proposed controller could track the desired power very well. For the present research the controller will control multiple variables for each of the sub-systems of the PWR plant.

CHAPTER 3. PWR PLANT DYNAMICS

In this chapter detailed description is given of the PWR power plant dynamics. Focus is placed on the reactor core, primary cycle and its components, the steam generator and its components and the secondary cycle and its components. More detail is also provided on the PWR power plant load changing constraints and limitations.

3.1 PWR overview

In this section the entire nuclear power plant is described starting with the plant control concepts and load following constraints, followed by detailed descriptions of the individual components of a PWR. Figure 12 is a simplified representation of a PWR. Figure 12 is a more detailed version of Figure 1. This is required for the purpose of this section. It is however still a simplified representation from the real plant.

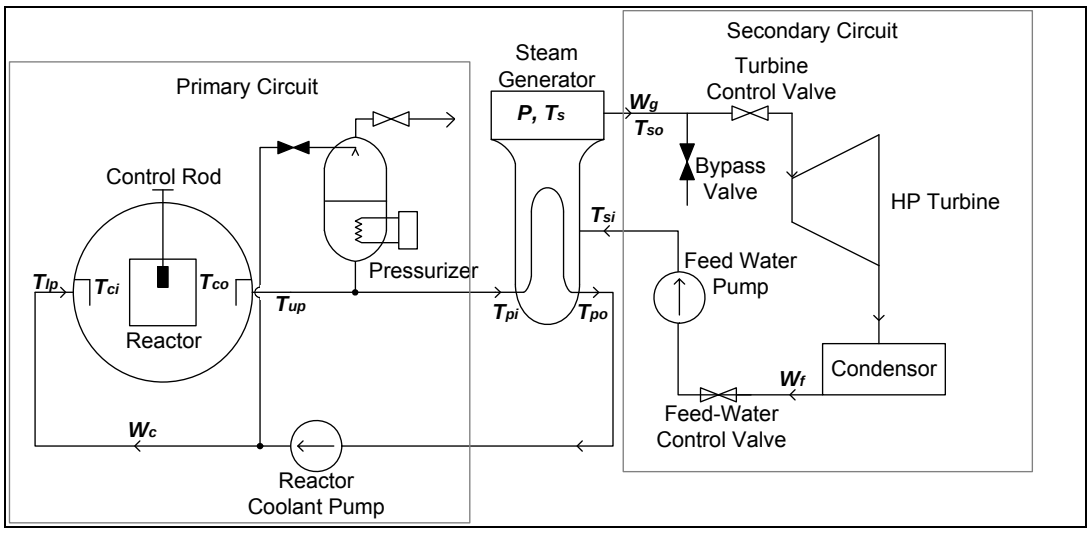

Figure 12: Simplified representation of a PWR

As seen in Figure 12 the PWR Nuclear Plant consists of the following main parts: The primary circuit, the secondary circuit and the steam generator. The primary circuit consists of the following basic components: The reactor core, the pressuriser and the reactor coolant pump and necessary piping. The secondary circuit consists of the following basic components: The power turbine, the condenser and the feedwater pump and necessary piping.

The steam generator forms part of both primary and secondary systems essentially being the interface between the primary and secondary circuits. The steam generator separates the closed loop primary coolant and the secondary feed water where the steam is generated to drive the turbine [7], [24].

3.2 Plant control concepts

3.2.1 Levels of control required

PWR plants required a number of control actions and these are separated into levels depending on their function and importance. There are basically three levels that are important to mention. The first level is having adequate control margins for reactivity during normal operation, start-ups and malfunctions. The second level ensures sufficient excess reactivity for three conditions: The reactivity that is lost when heating the reactor up from a cold start, the reactivity that is lost due to reactor poisons, and the reactivity that is lost as a result of fuel burn up and the forming of isotopes. The third level provides instant reactivity control for, firstly reactor start-ups and shutdowns, secondly adjustments to the distribution of temperature control, and control of the changes in the load.

The first two levels of control are not very important for the considerations of this study, however, the last level mentions providing instant reactivity control for control of the changes in the load [8].

3.2.2 Reactor control systems

A reactor normally has four main control systems, and these are required to operate a reactor safely. The first of these control systems is the all important reactor protection system. No control functions are actually performed with the protection system. Protection systems constantly monitor all measured variables and reactor conditions to determine if an unsafe condition is created. The protection systems will upon detection of such an unsafe condition also safely shutdown the reactor. A second control system found in all nuclear plants is the radiation monitoring system. This system constantly measures the levels of radiation in and around the plant. The third important control system is the plant process control systems. These systems would be for example the deionisation of make-up water. The fourth is the operating control system. This is the important system to be considered. The operating control

system is responsible for meeting load demands, varying between say 30-100% of full load for a typical PWR. Operating of the reactor at low power is not discussed as it is not considered as the normal load changing operation of the reactor. Low power operating is essentially important during reactor start-up and shutdown.

Further it is proposed to only look at specific working points during load changing operations. Therefore slower acting control devices such as Xenon effects are omitted. The focus is placed on the timescale of seconds and minutes when control is required for varying load demands.

The general control actions of the operating control system are illustrated in Figure 13.

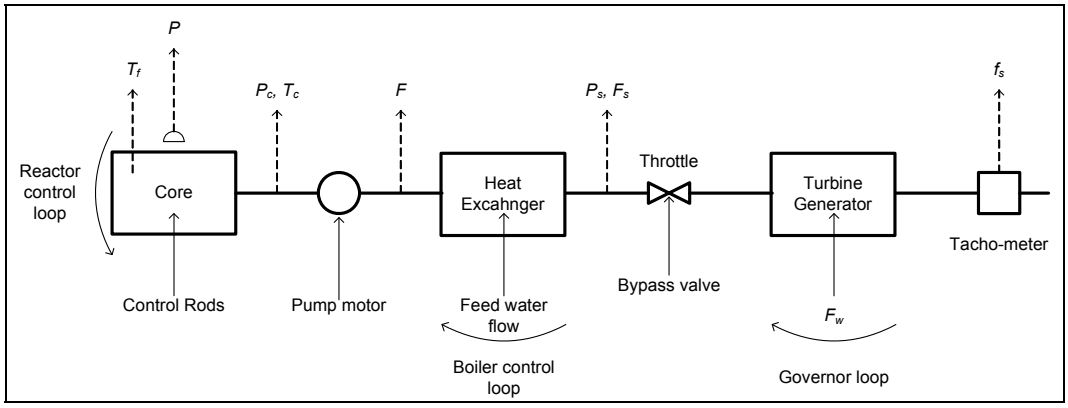

Figure 13: Schematic of a nuclear power plant control loops [8]

The following signals are available for automatic control (Refer to Figure 13):

- The neutron or flux measurements give the reactor power, P. Also possible but less convenient is to obtain the reactor power from combined temperature increments and coolant flow measurements.
- The pressure, P_c, and also the temperature, T_c, of the primary coolant exiting the reactor and entering the steam generator.
- The primary circuit flow rates, F.
- The turbine and generator shaft speed, f_s. This is normally expressed as the system frequency.
- The pressure, P_s, and also the temperature, T_s, of the steam generator secondary loop exit, and the entrances to the high and intermediate turbines.
- The secondary water level in the steam generator.

These measured signals are applied to perform the control functions for the entire plant. Control signals are applied to control the control rods. The control rods are responsible for controlling the reactor core reactivity and power. Control signals can also be used to control the primary coolant pump speed. This controls the primary coolant temperature and since the coolant is also the moderator it indirectly changes the reactivity. Control signals are also applied to control the secondary steam flow rate from the turbine throttle opening. This also controls the feedwater pump as the steam flow to the steam generator is quite important to control with changes in the throttle [8].

3.2.3 Sequence of events for load following

To meet the increasing demand, the control valves are opened to allow more steam into the turbine. As a result the water level in the steam generator drops. To restore the water level in the steam generator the feed water flow will increase. Reactor coolant temperature and pressure will decrease due to the mismatch between the reactor power level and steam generator load. Moderating fluid (water) density decreases as a result. Therefore the neutron multiplication rate increases which is the initial increase in the reactor power. From the lower coolant temperature the control system will withdraw the control rods to raise the reactor power. The coolant pressure control will activate the pressuriser heaters as a response to the pressure change. Eventually pressuriser water level will be restored and a new steady state condition is reached, and therefore equilibrium between the generator electrical power and the reactor power level. A decrease in load demand is similar to that of a load increase [2].

3.3 PWR load following constraints

3.3.1 Constraints due to design limitations

In the past, load changing operations used to cause fuel failures [2]. This was because of a lack of knowledge of fuel performance. Therefore, the failures where mainly caused by operator induced stresses. Fuel failures depend upon the overall fuel design and manufacturing process, the water chemistry, the control strategy applied and also the modes of operation.

A combination of any of the following can cause a fuel failure:

- The local reactor power density is raised too fast for new fuel elements.
- The reactor power is raised quickly following operation at low power for a long period.
- The local reactor power density operated above a certain conditioning level.

Conditioning levels are dependant on fuel burn-up. In Light Water Reactors conditioning of fresh fuel elements can prevent abovementioned fuel performance. For conditioning, the rate of power increase after refuelling is limited to very low values, for example 0.5 to 2% per hour of the reactor nominal power. This means that nominal power can not be available for any thing from a few days to weeks depending on the design. During this time provision should be made to cater for this conditioning period. This needs to be done for every reactor.

Fuel failure can be avoided if start-up is performed slowly. This refers to the conditioning period mentioned. Quick ramps must be avoided after periods of operation at low reactor power, and failure can also be avoided if large changes in fuel power density are avoided.

These days, fuel elements are designed with better knowledge of fuel behaviour. Utilities are also provided with the reactor limitations regarding fuel changing capabilities specifically looking at the above mentioned failure points and it can be ensured that reactors are operated within these limitations/margins [2].

3.3.2 Restrictions due to reactivity

To maintain reactor power, reactivity balance (equilibrium) must be achieved. Reactivity is a measure of the deviation of a reactor from critical condition. Reactivity is zero in the critical condition. When the reactivity is positive (adding positive reactivity) the reactor output power increases. When the reactivity is negative (adding negative reactivity) the reactor output power decreases. In some conditions it may not be possible to raise the power because of a lack of positive reactivity. Reasons can be that the designed operating limits are reached, all available reactivity is required for transient Xenon-135 poisoning or it might be that the reserved capacity for liquid control is depleted due to previous load changes. Liquid

control refers to the boric acid added to the coolant as a neutron poison [2] [4]. Section 3.5.1.4 also discusses Xenon poisoning which is a reactivity restriction.

3.3.3 Restrictions due to material thermal stresses

Thermal stresses in materials are caused by the rate of change of the power levels. What is important is to know that these stresses are cumulative and add up over the life time of the component. These types of stress damages are mainly located in pipe and component walls, nozzles, tanks of small mass-to-flow ratio, points of large temperature changes and also welded joints. The extents of these damages depend on the size and rate of temperature and pressure changes, the number of load cycles and the size and rating of components.

Turbines have two types of stresses that are required to be specified: Mechanical stresses, and thermal stresses. These have to do with plant start-up and load following operations.

Designs of Nuclear power plants include manufacturer specified loading and unloading limits to ensure proper life expectancies of materials. Such specifications would be for example be that rapid load changes of a certain size may be limited to once a day for the lifetime of the reactor, and for each size of power change there will be limitations to the amount of changes of this size over certain periods of the reactor operating life-time.

Additional provision must be made for unforeseen events such as power transients from the grid that may cause certain conditions inside the reactor that could lead to material stresses [2].

3.4 Nuclear power plants load following capabilities

Nuclear power plants are primarily operated as base load stations for economical reasons. Load following is however considered as an important requirement of modern nuclear power plants. The most important plants are listed below with their typical load changing capabilities.

Heavy Water Reactors (HWRs) – HWRs have the ability to adjust power between 60 and 100% of its full power. The natural uranium however with its large Xenon poisoning, limits power adjustments in the lower power ranges.

Gas Cooled Reactors (GCRs) – GCRs have almost the same load change ability as HWRs mentioned above.

LWRs – LWRs are divided into the two known types already discussed. BWRs have the ability to change load very quickly. Around 1%/second in the range of about 70 to 100% of rated power, and around 3 to 5%/minute from 30% of rated power and upwards is possible. PWRs have the ability of changing load in the range of 15/30 to 100% of rated power at a rate of around 1 to 3%/minute. However, 5 to 10%/minute is possible in a limited range [2], [4], [24].

3.5 Reactor core dynamics

In order to fully understand the concept of the behaviour and effects of a nuclear reactor during operation it might be necessary to explain a few concepts related to reactor reactivity. These concepts are that of the effective multiplication factor, the six factors of the six factor formula, reactivity, the point kinetics equations and the dynamic period equation. These are explained in the following subsections in sufficient detail and the affects they have on each other and the reactor power.

3.5.1 Neutron physics

3.5.1.1 The six factor formula

There are six factors that are defined that could affect the life of a neutron. These factors are:

- Fast fission factor – ε
- Fast non-leakage factor – P_f
- Resonance escape probability – p
- Thermal non-leakage factor – P_{th}
- Thermal utilisation factor – f
- Reproduction factor – η

For explanation of the six factors mentioned, assume that N_0 is the number of fast neutrons that are produced from thermal fission. The six factors mentioned above then get the following meanings:

- $N_0\varepsilon$ - Number of fast neutrons produced from fast and thermal fission.
- $N_0\varepsilon P_f$ - Number of fast neutrons that remain in the core.
- $N_0\varepsilon P_f p$ - Number of thermalised neutrons.
- $N_0\varepsilon P_f pP_{th}$ - Number of thermal neutrons that are absorbed in the core.
- $N_0\varepsilon P_f pP_{th}f$ - Number of thermal neutrons absorbed by the fuel.
- $N_0\varepsilon P_f pP_{th}f\eta$ - Number of fast neutrons that are produced from thermal fission for the next generation.

From the six factors as they are described above it is now possible to formulate the effective multiplication factor, k_{eff}, known as the six factor formula as it is shown by

$$k_{eff} = \varepsilon.P_f.p.P_{th}.f.\eta\,. \tag{3.1}$$

The physical meaning of the six factor formula is given by

$$k_{eff} = \frac{Number\ of\ neutrons\ in\ one\ generation}{Number\ of\ neutrons\ in\ the\ next\ generation}. \tag{3.2}$$

Therefore, k_{eff} is defined as the ratio between the number of fissions in one generation and the number of fissions in the next generation. Now assume that F_0 is the number of neutrons in the initial generation and F_1 is the number of neutrons in the next generation. Now the following is true: $F_1 = k_{eff}F_0$, and $F_2 = k_{eff}F_1$. Therefore the result is $F_2 = k_{eff}^2F_0$. The following relationship is now derived: $F_n = k_{eff}^nF_0$. From the value of k_{eff} for a specific condition of the reactor it is then possible to estimate the criticality condition of the reactor core. Figure 14 illustrates the effects of the six different factors during a neutron lifecycle [4], [9].

3.5.1.2 Criticality conditions

The three criticality conditions are defined as listed below:

- *Reactor is Critical:* If a reactor has a k_{eff} equal to one, the reactor is Critical. This is the preferred normal operating condition of a reactor.
- *Reactor is Supercritical:* If a reactor has a k_{eff} greater than one, the reactor is Supercritical. Super criticality is not a dangerous or abnormal condition for a reactor. The reactor is to be made supercritical in order to be able to increase the power of the reactor. k_{eff} can become too large and the reactor power increase will then be too large to be able to control it.
- *Reactor is Subcritical:* If a reactor has a k_{eff} of less than one, the reactor is Subcritical. This condition of sub criticality is also not abnormal but is required in order to reduce the reactor power or to shut the reactor down [4], [9].

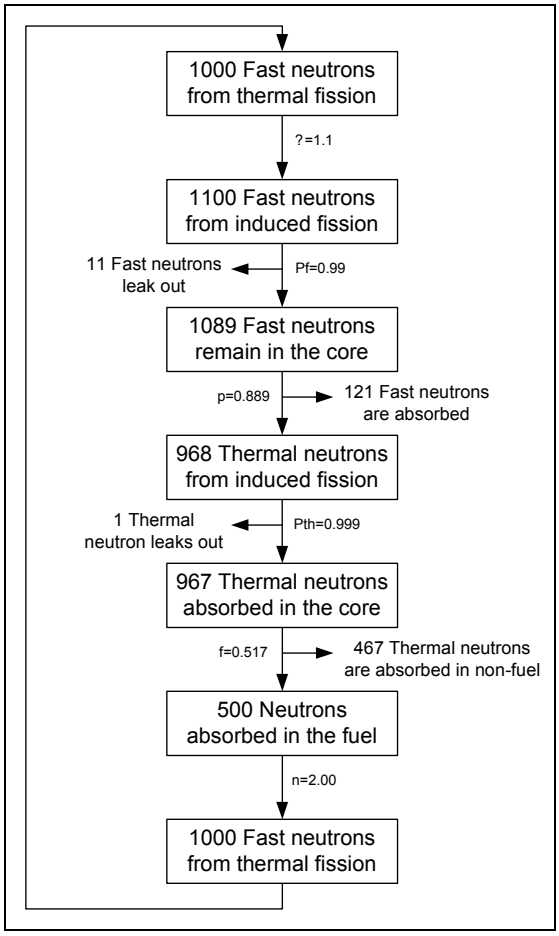

Figure 14: The neutron fission chain [9]

3.5.1.3 Reactivity

The value of k_{eff} in an operating reactor is usually close to 1. Normal transients are in the order of 0.99 to 1.001 for k_{eff}. The effective multiplication factor (k_{eff}) is however not used as it is not convenient. Reactivity (ρ) is used instead. Reactivity is defined as the fractional change of k_{eff} from the criticality condition ($k_{eff} = 1$). The formula for reactivity is given by

$$\rho = \frac{k_{eff} - 1}{k_{eff}}. \qquad \textbf{(3.3)}$$

Table 2 describes the three criticality conditions and the effect of the change in k_{eff} with ρ.

Table 2: Effective multiplication factor vs. reactivity

Reactor Condition	Effective Multiplication Factor	Reactivity
Supercritical	k_{eff} > 1	ρ > 0
Critical	k_{eff} = 1	ρ = 0
Subcritical	k_{eff} < 1	ρ < 0

For simplicity reactivity (ρ) can be used rather than k_{eff} since the numbers are easier to use, and a change in ρ is calculated much faster than a change in k_{eff}.

k_{eff} is affected by a number of parameters. These include fuel temperature, coolant temperature, control rod position and a few more. Each of the reactivity (ρ) contributions due to changes in these parameters are calculated individually. The total change in reactivity (ρ) is then obtained from the sum of the individual reactivity (ρ) changes given by

$$\Delta\rho = \Delta\rho_A + \Delta\rho_B + \Delta\rho_C + \ldots. \qquad \textbf{(3.4)}$$

Parameters that affect the effective multiplication factor (k_{eff}) are:

- Core aging in the form of fuel depletion.
- Reactor poisons.
- Control rods.
- Fuel temperature.

- Moderator temperature.

Each of these parameters will now be discussed in some detail [9].

Fuel depletion

It is necessary for a nuclear power plant to maintain the reactor at criticality in order to produce power for a long period of time. There is however many contributing factors that cause the core parameters to change. The reactor operators are then required to manipulate the reactor controls to maintain criticality at the desired conditions. Most of the control mechanisms used to control the reactor criticality alters the thermal utilisation (f).

Without the operator taking action, the fuel depletion causes the fuel absorption cross-section to decrease; this effectively decreases the number of fissions in the successive generations. Fission products are also produced in the fuel. Fission products increase the absorption cross-section of the non-fuel elements inside the reactor core. Considering only these changes, the thermal utilisation factor (f) decreases over the core life. In order to maintain criticality at unity, the operator needs to control the reactor by compensating for variations in the six factors over the fuel life.

The changes of the six factors with the core aging effects taken into consideration are as given as follows [9]:

ε - No change.

P_f - No significant change.

p - Slight decrease. The production of Pu-240 increases the resonance absorbers in the core.

P_{th} - No significant change.

f - Slight increase. Methods used to control the reactor primarily affect f.

η - No significant change.

Reactor poisons

Reactor poisons are non-fissionable nuclides. These non-fissionable nuclides absorb neutrons. There are various reasons for the presence of poisons in the core. Poisons include the metals used for the core structure. Neutrons are captured by the moderator/coolant and therefore the water in the core is a poison. Poisons are added to the core in the form of moveable control rods, burnable poison rods and chemicals dissolved in the water. Certain fission products that are produced from reactor operation are also poisons. The main effect of poisons in the reactor is that they contribute negatively to the reactivity by reducing the thermal utilisation factor (f). Thermal utilisation is calculated by using

$$f = \frac{\sum_a^f}{\sum_a^f + \sum_a^D}, \qquad \textbf{(3.5)}$$

where $\sum_a^f$ is the macroscopic thermal absorption cross-section of the fuel, and $\sum_a^D$ is the macroscopic thermal absorption cross-section of the poisons.

As the macroscopic absorption cross-section of the poisons increase, more thermal neutrons are absorbed by the poisons reducing k_{eff}. The greater the macroscopic absorption cross-section of the poisons, the more negative reactivity is inserted by the poisons. Figure 15 is an illustration of the effect of the thermal utilisation factor and the ratio of poison cross-section to fuel cross-section.

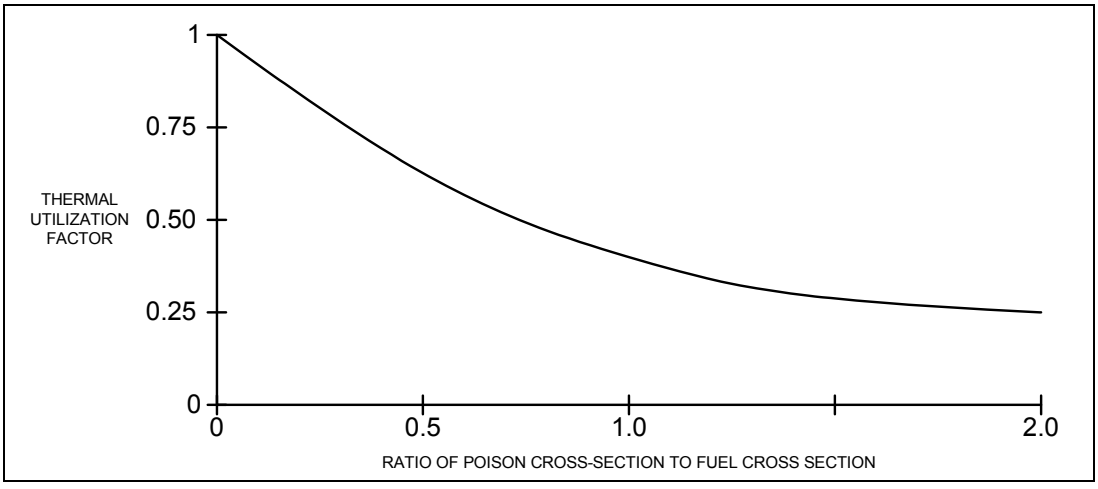

Figure 15: Thermal utilisation and reactor poisons

Figure 15 clearly shows that as the ratio of poison cross-section to fuel cross-section increases the thermal utilisation factor is decreasing.

The fission product poison Xenon-135 has a significant effect on the reactivity. The effect of fission product poison Xenon-135 is a lengthy discussion on its own and is therefore discussed later on in section 3.5.1.4.

The changes of the six factors with the effects of poisons taken into consideration are as given as follows [9]:

ε - No change.

P_f - No significant change.

p - Small decrease. Some poisons have resonance peaks.

P_{th} - No significant change.

f - Decrease. An increase in the presence of poisons causes an increase in the number of neutrons that are absorbed.

η - No change.

Control rods

Control rods are devices that affect the reactivity of the core by moving them into or out of the core. Control rods are made of a material with a high absorption cross-section. Such materials include boron steel, hafnium and cadmium metallic elements and silver. As mentioned previously control rods are poisons introduced into the core on purpose. Therefore, by inserting a control rod into the core, the poison absorption cross-section is increased and the thermal utilisation factor is decreased.

When a control rod is inserted into the core, it adds negative reactivity to the core. When a control rod is pulled out of the core, it adds positive reactivity to the core.

The changes of the six factors with the effects of control rods taken into consideration are given as follows [9]:

ε - No change.

P_f - Decreases. The fast neutron leakage factor is reduced.

p - Decrease. Control rod materials have resonance peaks.

P_{th} - Decreases. The effective leakage surface increases.

f - Decrease. Control rods are poisons that are added to the core.

η - No change.

Fuel temperature

The temperature inside a fuel assembly can reach temperatures of up to 2200°C. Fuel resonance absorption cross-sections are affected by temperature variations inside the fuel element. This effect of temperature on the fuel, known as Doppler broadening, increases the absorption cross-section of the fuel and decreases the fission cross-section. Therefore less neutron fissions are caused.

The changes of the six factors with the effects of the Doppler Broadening taken into consideration are given as follows [9]:

ε - No change.

P_f - Decreases. Absorbs more neutrons.

p - Decreases. Absorbs more neutrons.

P_{th} - Decreases. Absorbs more neutrons.

f - Decreases. Absorbs more neutrons.

η - Decreases. Absorbs more neutrons.

Moderator temperature

As the moderator (water in the case of a PWR) temperature increases the density of the moderator decreases. This decrease in density causes the moderation of the neutrons to reduce and fewer neutrons are thermalised. This causes the fission rate of the thermal neutrons to reduce. Figure 16 illustrates the decrease of the water density at higher temperatures.

Figure 17 is a representation of how the six factors of the six factor formula vary with a change in the moderator-to-fuel ratio.

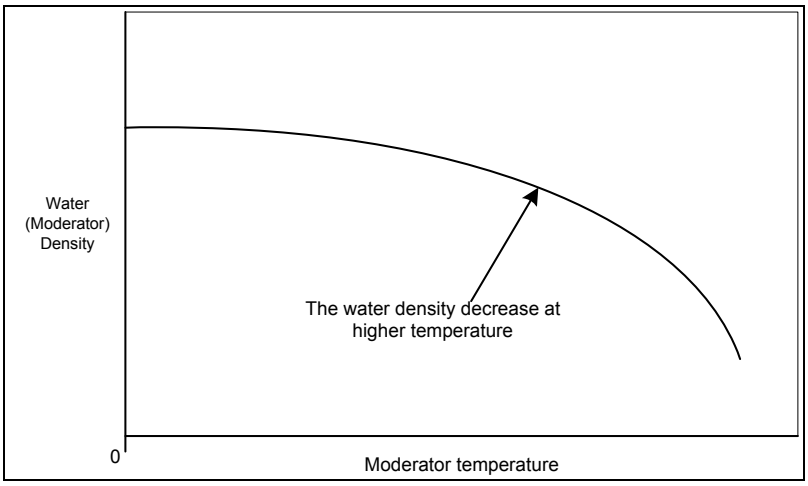

Figure 16: Water density vs. temperature

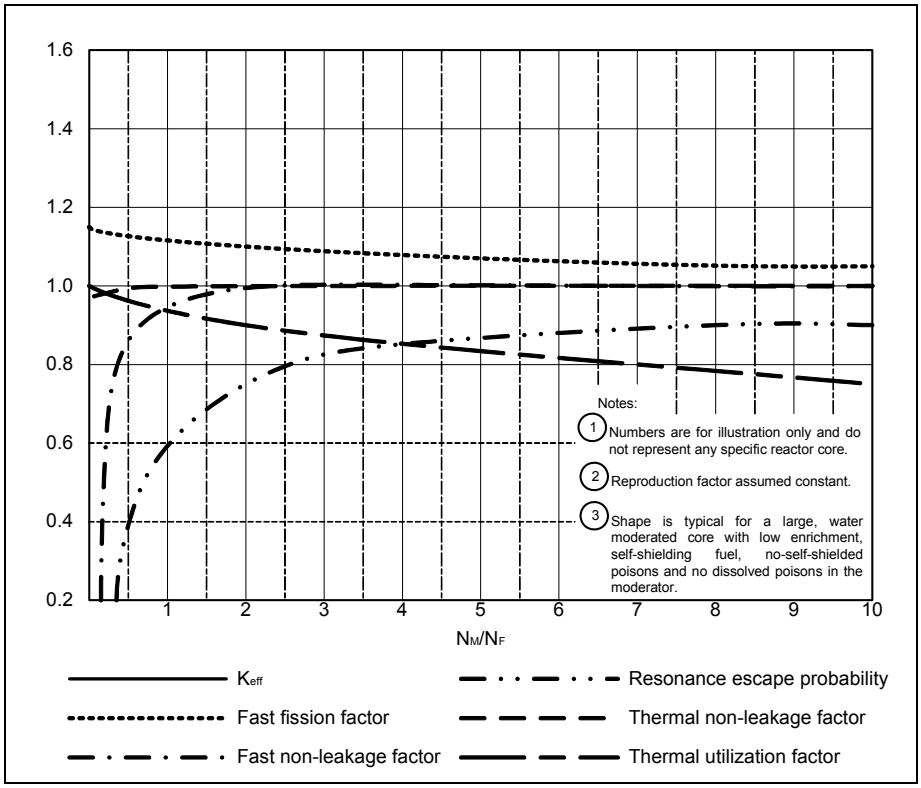

Figure 17: Variation of the six-factors with moderator-to-fuel ratio

The changes of the six factors with the effects of the moderator temperatures taken into consideration are given as follows [9]:

ε - Small decrease. The moderator to fuel ratio is increased. More moderator is now available to thermalise neutrons.

P_f - No significant change.

p - Increase. The moderator to fuel ratio is increased. More neutrons are slowed-down into the resonance region.

P_{th} - No significant change.

f - Decreases. The moderator to fuel ratio is increased. More neutrons are absorbed by the moderator.

η - No change.

3.5.1.4 Xenon poisoning

The biggest concern when considering reactor power changes is the build-up of fission product poisons in reactor fuel. A poison is a substance consisting of a large neutron absorption cross-section. This is not desirable in nuclear reactors. Some poisons like Boron, Hafnium, etc. are added to the reactor coolant in for example a boric acid solution. This is done to avoid criticality incidents (emergency shutdowns) and also to compensate for excess reactivity. Other poisons are produced directly from the nuclear fission process or by the decay of nuclides generated from fission.

The most significant fission product poison is Xenon-135. Xenon-135 has an absorption cross-section 4000 times that of Uranium-235. Although very undesirable it is completely unavoidable and therefore the reactor needs to be controlled while taking poisons, especially Xenon-135 into account.

Approximately 6.6% of all fissions produce a Xenon-135 nuclide. Of this, 5% of Xenon-135 is directly from fission:

$$ {}^{1}_{0}n + {}^{235}_{92}U \rightarrow {}^{99}_{38}Sr + {}^{135}_{54}Xe + 2\,{}^{1}_{0}n + \gamma\,, \qquad \textbf{(3.6)} $$

and 95% of Xenon-135 is produced from the decay of the fission product Iodine-135:

$$ {}^{135}_{53}I \xrightarrow[T_{1/2}=6.6hr]{} {}^{135}_{54}Xe + \beta\,. \qquad \textbf{(3.7)} $$

Iodine-135 is produced in 6.3% of all fissions. Although Iodine-135 itself has a negligible absorption cross-section, all Iodine-135 decays to Xenon-135 and as mentioned Xenon-135 has a very large absorption cross-section. The reactor's control device is to be adjusted to compensate for the reactor equivalent of the poisons to keep the reactor at its power level.

Xenon-135 is removed from the reactor also by two processes. The first is by nuclear decay. This accounts for around 10% of Xenon-135 removal:

$$^{135}_{54}Xe \xrightarrow[T_{1/2}=9.1hr]{} {}^{135}_{55}Cs + \beta . \quad \textbf{(3.8)}$$

The second is by neutron absorption (radiative capture). This accounts for around 90% of Xenon-135 removal from the reactor:

$$^{1}_{0}n + {}^{135}_{53}Xe \rightarrow {}^{136}_{54}Xe + \gamma . \quad \textbf{(3.9)}$$

Xenon-135 slowly builds up to an equilibrium level following a start-up. Equilibrium level depends on the steady state power and is reached after a few hours. Once equilibrium is reached Xenon-135 is produced and removed from the reactor at the same rate. After equilibrium is reached, Xenon-135 only changes when the reactor power level is changed. Figure 18 shows how Xenon-135 contributes to the reactivity inside the reactor directly after start-up.

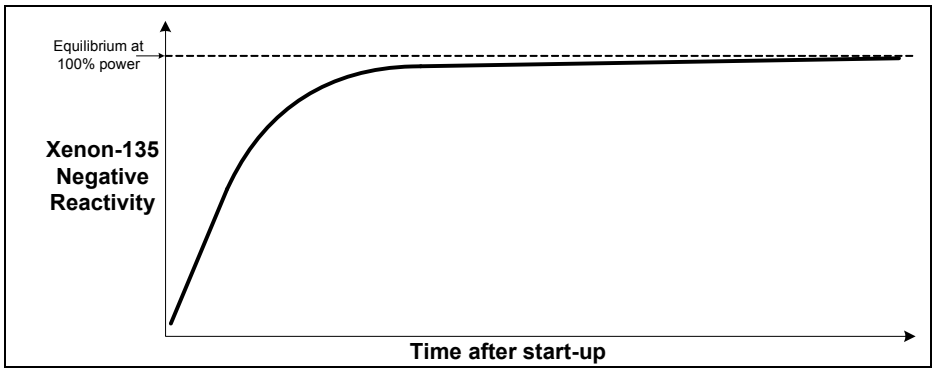

Figure 18: Xenon-135 contribution at start-up

Figure 19 shows how Xenon-135 contributes to the reactivity inside the reactor directly following a trip.

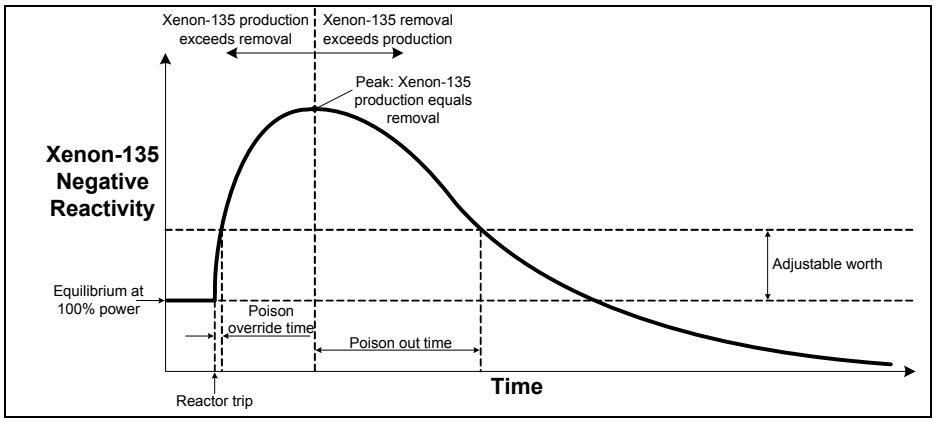

Figure 19: Xenon-135 contribution following a trip

Figure 20 shows how Xenon-135 contributes to the reactivity inside the reactor following an action of lowering the reactor power. (Negative reactivity added).

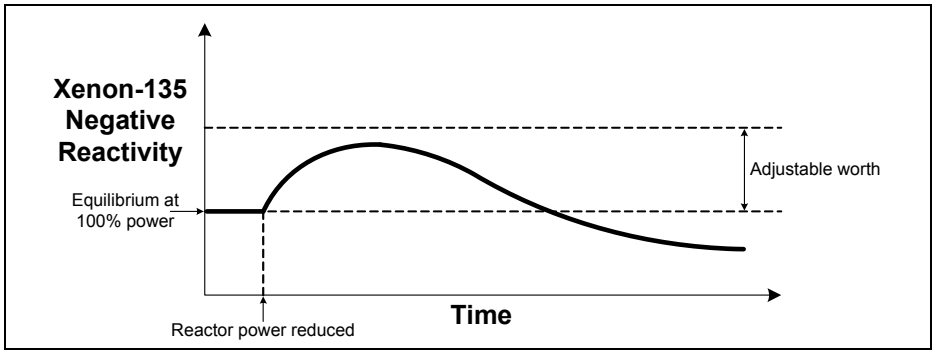

Figure 20: Xenon-135 contribution for power reductions

The amount of reactivity from Xenon-135 is directly proportional to the Xenon concentration as indicated by

$$\rho = -\frac{\sigma_a N_{Xe}}{\sum_a^{U-235}}. \qquad \textbf{(3.10)}$$

Figure 21 is an illustrative example of the reactivity changes for a 100% power to 50% power, back to 100%, again to 50% power and finally back to 100% power again. Figure 21 shows the effect of the net reactivity and also the reactivity due to Xenon [4].

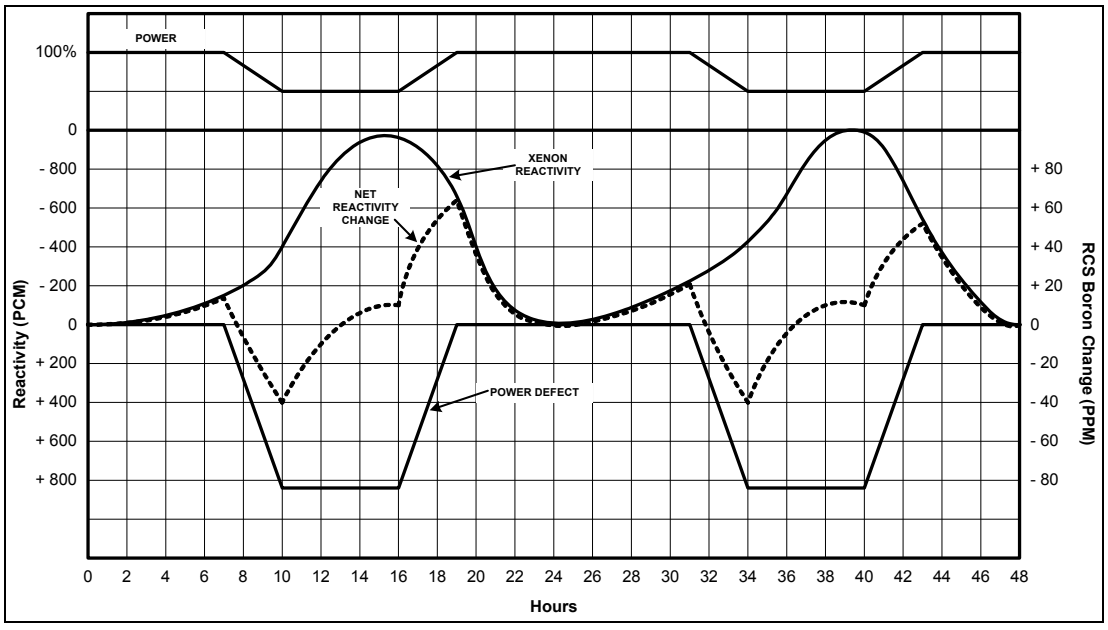

Figure 21: Load following [9]

3.5.2 Reactor kinetics

3.5.2.1 Point kinetics equations

The behaviour of the prompt and delayed neutron populations with changes in reactivity is given by the point kinetics equations. The point kinetics equations are space-independent in order to make the mathematics less complex. This approach is acceptable for most applications, except for reactor design analysis and for certain safety studies. The reactor point kinetics equations are given by

$$\frac{dn(t)}{dt} = \frac{(\rho(t)-\beta)}{l^*} n(t) + \sum_i^N \lambda_i C_i(t) \text{, and} \quad \textbf{(3.11)}$$

$$\frac{dC_i(t)}{dt} = \frac{\beta_i n(t)}{l^*} - \lambda_i C_i(t), \quad \textbf{(3.12)}$$

where $n(t)$ is the reactor power, $\rho(t)$ is the net reactivity, β is the delayed neutron fraction, l^* is the prompt neutron life-time ($\pm 10^{-4} s$), λ_i is the decay constant of the $i-th$ precursor group, C_i is the concentration of the $i-th$ precursor group, and N is the number of delayed neutron precursor groups.

The meaning of the terms in the point kinetics equations are:

- $\rho(t)$ is the fractional change in the total neutron population (delayed + prompt) per generation and β is the fraction of the number of neutrons that are delayed. Therefore, $\rho(t)-\beta$ is the fractional change in the prompt neutron population per generation.

- $1/l^*$ is the number of neutron generated per second and $n(t)$ is the total neutron population. Therefore $\frac{(\rho(t)-\beta)}{l^*} n(t)$ is the change in the prompt neutron population per unit time.

- $\lambda_i C_i$ is the rate of decay of delayed neutron precursors. This equals the rate of appearance of delayed neutrons.

- $\frac{\beta_i n(t)}{l^*}$ is the rate of production of delayed neutron precursors per unit time.

The point kinetics equations can be summarised as shown in Figure 22.

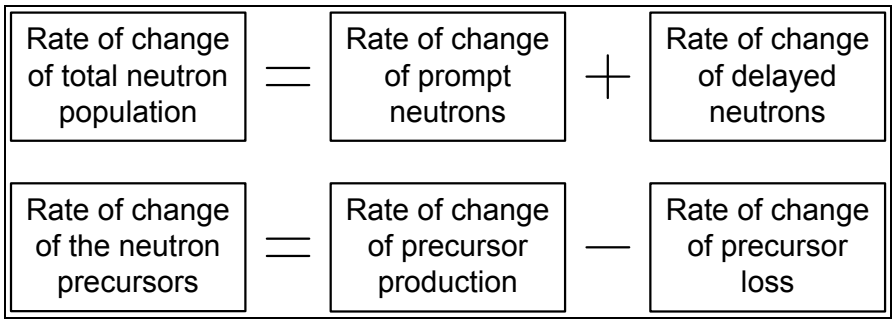

Figure 22: Meaning of the point kinetics equations [7]

3.5.2.2 The dynamic period equation

The problem with the point kinetics equations is that the precursors are not measurable. And also, visualising the consequences of two simultaneous differential equations is difficult. The two point kinetics equations ((3.11) and (3.12)) can be simplified through differentiation and combining the two to obtain the dynamic period equation which is used by reactor operators. The dynamic period equation relates reactor period which is measurable to the reactivity. A simplified version of the dynamic period equation is given by

$$\tau(t) = \frac{\beta - \rho(t)}{\dot{\rho}(t) + \lambda_e(t)\rho(t)}, \qquad \textbf{(3.13)}$$

where $\tau(t)$ is the reactor period, $\dot{\rho}(t)$ is the rate of change of the net reactivity, $\lambda_e(t)$ is the standard effective multi-group decay parameter, $\beta - \rho(t)$ is the fractional change in the prompt neutron population per generation.

The meaning of the terms in the dynamic period equation is:

- $\dot{\rho}(t)$ is proportional to prompt neutron population. Changing of a control device has an immediate effect on the period.
- $\lambda_e(t)\rho(t)$ is proportional to the delayed neutron population.

A control devices position has to be altered or burnable poison concentration has to be adjusted. This takes time. The reactor period depends on the rate of change of reactivity $\dot{\rho}(t)$ and the total reactivity $\rho(t)$.

The reactor power change is an exponential function of time and is given by

$$P(t) = P_0 e^{t/\tau}, \quad \textbf{(3.14)}$$

where $P(t)$ is the reactor power at time, t, P_0 is the reactor power at time $t = 0$ and τ is then the reactor period as described in the dynamic period equation. The reactor period is dependant on the fraction of delayed neutrons to prompt neutrons. The delayed neutrons in a reactor are used to control the reactor and not the prompt neutrons. Although delayed neutrons make up only a small fraction of the total neutron population, the delayed neutron life-time ($\pm 12.2\,\mathrm{s}$) is much longer than that of prompt neutrons ($\pm 10^{-4}\,\mathrm{s}$). The delayed neutron contribution to the reactor period in neutron life-time is therefore much stronger than their contribution in the fraction of the total neutrons. The reactor is therefore controlled with delayed neutrons. The fraction of delayed neutrons present in a reactor is controlled mainly by the type of reactor and its design parameters. The reactor can not be controlled with prompt neutrons only. Nuclear fission chains controlled by prompt neutrons will only be found in nuclear explosive devices. Reactors are designed so that this is not possible. Nuclear reactors can therefore not explode like a nuclear explosive device; they can only melt the core [7, 8].

3.5.2.3 Net reactivity in the core

The net reactivity in the reactor core is given by

$$\rho_t = \rho_c - \alpha_f (T_f - T_{f0}) - \alpha_c (T_c - T_{c0}), \quad \textbf{(3.15)}$$

where ρ_t is the net reactivity $[\Delta k/k]$, ρ_c is the reactivity from control rod movement $[\Delta k/k]$, α_f is the fuel temperature coefficient $\left[\Delta k/k/^0C\right]$, α_c is the coolant temperature coefficient $\left[\Delta k/k/^0C\right]$, $T_f - T_{f0}$ is the temperature difference between the temperature T_f from the nominal temperature T_{f0} [^0C] and $T_c - T_{c0}$ is the temperature difference between the temperature T_C from the nominal temperature T_{c0}[^0C] [5].

3.5.2.4 Power from fission

The power generated by the fission of the neutrons is given by

$$P_f = \left(1 - \Psi_1 - \Psi_2\right) n\kappa \,, \tag{3.16}$$

where P_f is the power produced by fission [kW], Ψ_i is the portion of power produced by decay heat, n is the neutron flux and κ is the power per unit of flux [kW] [5].

3.5.2.5 Total core power

The total power inside the reactor core is given by

$$P_t(t) = P_f(t) + P_{d1}(t) + P_{d2}(t) \,, \tag{3.17}$$

where $P_t(t)$ is the total power in the reactor core [kW], $P_f(t)$ is the power produced by fission [kW] and $P_{di}(t)$ is the power produced by decay heat [kW] [5].

3.5.2.6 Fuel temperature

The total power in the core is then transferred to thermal power (heat) of the fuel. The temperature change of the fuel is given by

$$\frac{dT_f}{dt} = \frac{1}{\left(m_f C_f\right)}\left(P_t - h_{fc}.A_{fc}\left(T_f - T_c\right)\right), \tag{3.18}$$

where T_f is the temperature of the fuel [^oC], m_f is the fuel weight [kg], C_f is the specific heat capacity of the fuel [$kJ/kg.^oC$], h_{fc} is the heat transfer coefficient from the fuel to the coolant [$kW/m^2.^oC$], A_{fc} is the heat transfer area between the fuel and the coolant [m^2] and T_c is the average Coolant Temperature [^oC] [5].

3.5.2.7 Coolant temperature

This thermal power is then transferred to the cooling water circulated through the core. The temperature change of the coolant is given by

$$\frac{dT_C}{dt} = \frac{1}{\left(m_C C_C\right)}\left(h_{fC}.A_{fC}\left(T_f - T_C\right) - \dot{m}_C.C_C\left(T_{Co} - T_{Ci}\right)\right), \tag{3.19}$$

where m_C is the coolant mass [kg], C_C is the specific heat capacity of the coolant [$kJ/kg.^oC$], $\dot{m}_c$ is the mass flow rate of the coolant [kg/s], T_{co} is the core outlet temperature [^oC] and T_{ci} is the core inlet temperature [^oC] [5].

3.6 Primary cycle

The rest of the primary circuit consists of the pressuriser and the reactor coolant pump and the related piping. The steam generator is excluded here as it forms the interface between the primary and secondary circuit and is described separately. The primary circuit can be described by the following equations [5]:

Upper Plenum:

$$\frac{dT_{up}}{dt} = \frac{1}{\tau_{up}}\left(T_{co} - T_{up}\right) \tag{3.20}$$

Hot leg:

$$\frac{dT_{h1}}{dt} = \frac{1}{\tau_{h1}}\left(T_{up} - T_{h1}\right) \tag{3.21}$$

Steam Generator inlet:

$$T_{pi} = T_{h1} \tag{3.22}$$

Cold leg:

$$\frac{dT_{c1}}{dt} = \frac{1}{\tau_{c1}}\left(T_{po} - T_{c1}\right) \tag{3.23}$$

Bottom plenum:

$$\frac{dT_{1p}}{dt} = \frac{1}{\tau_{1p}}\left(T_{ci} - T_{1p}\right) \tag{3.24}$$

Reactor inlet:

$$T_{ci} = T_{1p} \tag{3.25}$$

3.7 Steam generator

A steam generator transfers heat generated from the fission inside the reactor via the primary and secondary heat transfer fluids to the steam generator on the secondary side. The steam generator allows the isolation of the secondary system from radioactive exposure.

3.7.1 Primary temperature

The difference between the power extracted from the coolant and the power transferred to the secondary side is the change in ΔT across the steam generator primary side. The temperature change of the coolant is given by

$$\frac{dT_p}{dt} = \frac{1}{\left(m_{sg}C_{sg}\right)}\left(\dot{m}_c.C_c\left(T_{pi} - T_{po}\right) - h_{ps}.A_{ps}\left(T_p - T_s\right)\right), \quad \textbf{(3.26)}$$

where T_p is the average primary coolant temperature [$^{o}\mathrm{C}$], T_s is the secondary saturated steam temperature [$^{o}\mathrm{C}$], m_{sg} is the steam and water mass in the steam generator [kg], C_{sg} is the specific heat capacity of water and steel [$\mathrm{kJ/kg.^{o}C}$], T_{po} is the steam generator primary outlet [$^{o}\mathrm{C}$] and T_{pi} is the steam generator primary inlet [$^{o}\mathrm{C}$] [5].

3.7.2 Secondary energy

The energy available on the secondary side of the steam generator is given by

$$E = m_f\bar{h}_f + m_g\bar{h}_g - V_{sg}P, \quad \textbf{(3.27)}$$

where E is the total energy in steam the generator secondary side [J], m_f is the weight of the water in the secondary side [kg], m_g is the mass of the steam in the secondary side [kg], $\bar{h}_f$ is the enthalpy for saturated water [$\mathrm{kJ/kg.^{o}C}$], $\bar{h}_g$ is the enthalpy for saturated steam [$\mathrm{kJ/kg.^{o}C}$], v_f is the specific volume of water in steam generator secondary side [$\mathrm{m^3/kg}$], v_g is the specific volume of steam in steam generator secondary side [$\mathrm{m^3/kg}$], V_{sg} is the steam generator secondary side volume [$\mathrm{m^3}$] and P is the steam generator secondary side Pressure [P].

The Maxwell and Clausius equation is given by

$$dQ = d\bar{h} - vdP, \quad \textbf{(3.28)}$$

where dQ is the change in energy, dh is the change in enthalpy, v is specific volume and dP is the change in pressure.

Combining (3.27) and (3.28) gives the relation

$$\frac{dE}{dt} = \frac{d}{dt}\left(m_f\bar{h}_f + m_g\bar{h}_g\right) - V_{sg}\frac{dP}{dt}. \quad \textbf{(3.29)}$$

The rate of change in energy, $\frac{dE}{dt}$, can also be given by the difference in the power transferred from the primary side to the feedwater, and the power transferred to turbine in the form of steam. The relation is given by

$$\frac{dE}{dt} = \left(\dot{m}_f \bar{h}_{fin} + \dot{m}_g \bar{h}_g\right) - h_{ps}.A_{ps}\left(T_p - T_s\right), \quad \textbf{(3.30)}$$

where $\dot{m}_f$ is the feed water mass flow [m^3/kg] and $\dot{m}_g$ is the steam mass flow to the turbine [m^3/kg] [5].

3.7.3 Conservation balances

The water level controller of the steam generator when assumed ideal will ensure that the secondary inlet water mass flow rate and the secondary outlet steam mass flow rate are kept equal. The energy balance for the working fluid in the steam generator is given by

$$\frac{dU_{SG}}{dt} = c_p^w.\dot{m}.T_w - c_p^s.\dot{m}.T_s - \dot{m}.E_{evap} + K_T.(T_{PC} - T_{SG}) - W_{loss}, \quad \textbf{(3.31)}$$

where U_{SG} is the internal energy, c_p^w and c_p^s are the water and vapour specific heats respectively, T_w and T_s are the inlet and outlet temperatures respectively, $\dot{m}$ is the secondary side mass flow rate, E_{evap} is the evaporation energy, T_{PC} and T_{SG} are the average primary and secondary circuit temperatures respectively and W_{loss} is the heat loss [14].

3.8 Secondary cycle

3.8.1 Physical description of the secondary system

The secondary side of the nuclear plant is responsible for driving the turbine connected to the electrical generator in order to generate electricity. To generate electricity the secondary side of the nuclear plant acts as a heat engine. A heat engine can be defined as a piece of equipment operating in a thermodynamic cycle and does a certain amount of net positive work as a result of heat transferred from a high temperature body to a low temperature body. Figure 23 gives a more detailed version of the secondary system as compared to Figure 12.

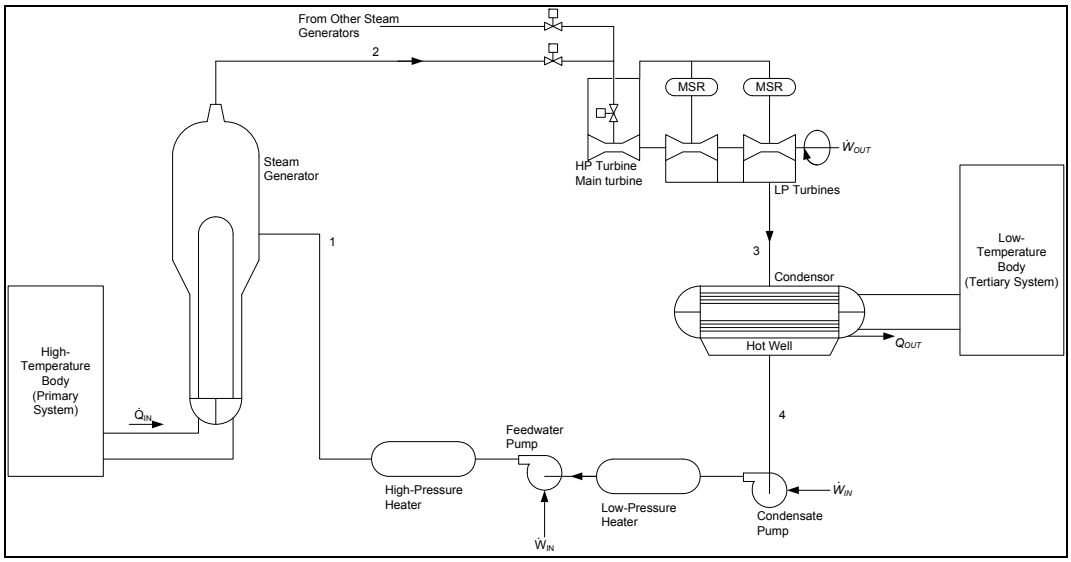

Figure 23: Secondary system as a heat engine [9]

The main turbine does positive work in the system. The condensate and feedwater pumps do negative work on the system. Heat is added to the system in the steam generators, while heat is extracted from the system by the condenser. Figure 23 also indicates that the basic secondary system includes high-pressure and low-pressure heaters. These heaters use high-pressure steam from the high- and low pressure turbines to raise the temperature of the feedwater. This mechanism enhances plant efficiency. Plant efficiency can also be enhanced by means of moisture separator re-heaters. These remove any moisture from the steam. The remaining steam is superheated. This is done in the moisture separator re-heaters with steam directly from the steam generators. For the system illustrated in Figure 23 the steam usage throughout the secondary system can be as follows:

- 8% of the steam from the steam generators is diverted to the moisture separator re-heaters for superheating the steam of the HP-Turbine outlet.
- 92% of the steam then enters the main HP-Turbine.
- 15% of the original steam is extracted from the HP-Turbine and used to heat feedwater in the high-pressure heaters.
- 77% of the steam exits the HP-Turbine and enters the moisture separator re-heaters. 9% of this mass is moisture and extracted from the system.

- 68% of the original steam enters the LP-turbines.
- 11% is extracted to the low-pressure heaters to heat feedwater.
- 57% of the steam is then condensed in the condenser.

All the steam is eventually condensed and re-enters into the main feedwater flow. The mass flow rate of water entering and steam leaving the steam generator is equal.

The cycle's thermal efficiency is the net work performed to the heat energy supplied as shown by

$$\eta_{th} = \frac{Work(net)}{Heat\ \sup plied} = \frac{\dot{Q}_s + \dot{Q}_R}{\dot{Q}_s}. \quad \textbf{(3.32)}$$

The net work of the system is equal to the sum of the heat supplied $\dot{Q}_s$ and the heat rejected $\dot{Q}_R$ [9], [25].

3.8.2 The Rankine cycle

The operation of the steam power plant as a heat engine is represented by the Rankine cycle.

The PWR heat engine operated in a Rankine cycle has the following basic components: The steam generator, the turbine, the generator, and the pump.

Although there are many more components, these four are the main components. The remaining components are for increasing the plant efficiency. These components will not be discussed in detail.

Figure 24 shows the $T-s$ diagram of the Ideal Rankine Cycle. The numbers 1 to 4 in Figure 24 corresponds to the numbers 1 to 4 in Figure 23 indicating each stage of the process.

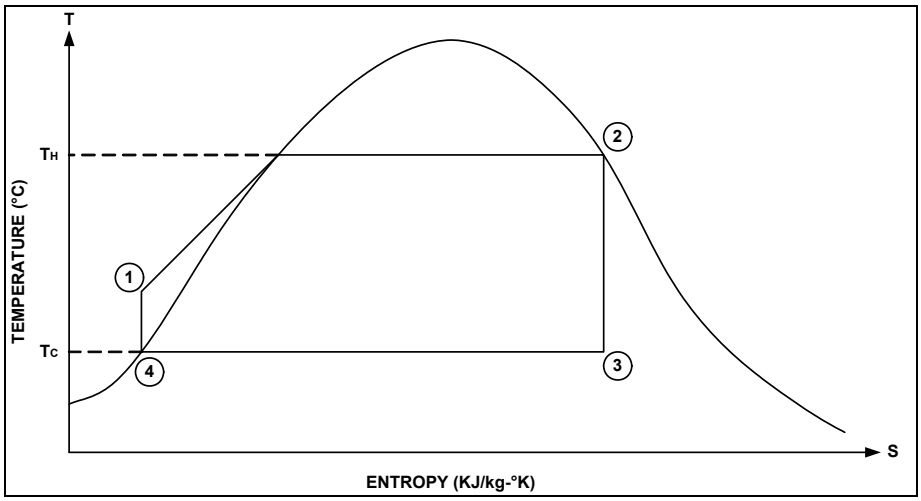

Figure 24: Ideal Rankine cycle on a T-s diagram [9]

Within the ideal Rankine cycle there are four basic stages. The first of these is the transfer of heat into sub cooled liquid at constant pressure. This heat transfer occurs in the steam generator. Referring to both Figure 23 and Figure 24, point 1 represents steam generator inlet. As can be seen the temperature rises on the constant pressure line as heat is added until the saturation temperature for the specific pressure is reached. Further heat being added causes vaporisation and eventually the water is turned into 100% saturated steam. The equation for the rate of heat transfer across a steam generator is given by (3.34).

The second stage begins at point 2 where the saturated steam exits the steam generator and enters the turbine. The enthalpy of the saturated steam is converted to work inside the turbine. As energy gets extracted from the steam, the steam temperature drops. The equation for the rate of turbine work is given by (3.35). The steam exiting the turbine at point 3 is a saturated mixture with a certain steam quality. This saturated mixture enters the condenser. The fluid condenses to 100% saturated liquid as heat is extracted from the system in the condenser. The equation for the rate of heat transfer across a condenser is given by (3.36).

The condensed saturated liquid exits the condenser and enters the pump at point 4. Work is now performed on the system by the pump. The pump increases the pressure in the system, and therefore also increases its internal energy. The working fluid is pressurised to a compressed liquid. The equation for the rate of pump work is given by (3.37) and (3.38).

The sub cooled liquid water exits the pump and re-enters the steam generator at point 1. The working fluid is now again at its original state and the process will be repeated. This is then the complete steam cycle of the power plant.

The efficiency is the ratio of the available energy to the total energy as given by (3.32) [9], [11], [25].

3.8.3 Evaluating the individual stages of the ideal Rankine cycle

From the combination of the ideal Rankine cycle's net work, heat transfer and cycle efficiency and each component's energy equation, the secondary system can be evaluated. Parameters requiring evaluation includes steam quality at the turbine exit, turbine work, steam saturation pressure in the steam generator, and the pressure change of the working fluid in the pump. The energy equation describing the secondary system is given by

$$\dot{Q}+\dot{m}\left(\frac{\overline{V}_i^2}{2}+gZ_i+u_i+P_iv_i\right)=\dot{W}+\dot{m}\left(\frac{\overline{V}_e^2}{2}+gZ_e+u_e+P_ev_e\right), \quad \textbf{(3.33)}$$

where $\dot{Q}$ is the net heat transfer rate across the system boundaries, $\dot{W}$ is the net work transfer rate across system boundaries, $\dot{m}$ is the mass flow rate across the system boundaries, $\frac{\overline{V}^2}{2}$ is the kinetic energy per unit mass of the mass across the system boundaries, gZ is the specific potential energy of the mass crossing the system boundaries, u is the specific internal energy of the mass crossing the system boundaries and Pv is the specific flow energy of the mass crossing the system boundaries [9], [25].

3.8.3.1 Steam generator

Section 3.7 gives a more detailed description of the steam generator. Heat transferred to the secondary water across the steam generator is given by

$$\dot{Q}=\dot{m}\left(h_e-h_i\right), \quad \textbf{(3.34)}$$

where $\dot{Q}$ is the heat transferred to the secondary working fluid from the primary working fluid in the steam generator, $\dot{m}$ is the mass flow rate through the steam

generator, h_e is the specific enthalpy of the steam exiting the steam generator and h_i is the specific enthalpy of the water in the steam generator [9], 25].

3.8.3.2 Turbine

The energy for work done by a steady-flow turbine is given by

$$\dot{W} = \dot{m}\left(h_i - h_e\right), \tag{3.35}$$

where $\dot{W}$ is the work done by the turbine per unit time, $\dot{m}$ is the mass flow rate through the turbine, h_i is the specific enthalpy of the steam entering the turbine and h_e is the specific enthalpy of the steam exiting the turbine [9], [25].

3.8.3.3 Condenser

The condenser is a heat exchanger that rejects heat from the system. The general steady-flow equation for a condenser is given by

$$\dot{Q} = \dot{m}\left(h_e - h_i\right), \tag{3.36}$$

where $\dot{Q}$ is the heat rejected from the secondary system, $\dot{m}$ is the mass flow rate through the condenser, h_e is the specific enthalpy of the steam entering the condenser and h_i is the specific enthalpy of the saturated water leaving the condenser [9] , [25].

3.8.3.4 Pump

The purpose of the pump is to increase the pressure of the water in the secondary system to provide a driving force for the flow of the working fluid through the system. The pump returns the water to the steam generator in its original state, therefore completing the cycle. The energy equation for the pump is given by

$$\dot{W} = \dot{m}\left(h_i - h_e\right), \tag{3.37}$$

where $\dot{W}$ is the work done by the pump per unit time, $\dot{m}$ is the mass flow rate through the pump, h_i is the specific enthalpy of the water entering the pump and h_e is the specific enthalpy of the water leaving the pump. An alternative formulation of the energy for the pump, is given by

$$\dot{W} = \dot{m}\nu\left(P_i - P_e\right), \tag{3.38}$$

where ν is specific volume. Since the fluid (water) is assumed incompressible, $\nu_i = \nu_e$. P_i is the pressure at the pump inlet and P_e is the pressure at the pump exit [9] , [25].

3.9 Conclusion

The PWR is the core of this study. The chapter provided information on what a PWR is, how the plant control is accomplished, what the load following constraints are, what the PWRs main contributing components are, how these components work and what are their characteristics, and how the different PWR plant components and their characteristics influence each other during load following. This information is important to obtain an understanding of a PWRs components and their dynamics, allowing for a model of the system to be derived that will include all the characteristics required to develop a successful controller. In the developing, testing and verification of the system model and controller these plant characteristics described during this chapter will be observed. Now that an understanding of the PWR plant is provided, theory on deriving the model of the system and developing the controller is given in CHAPTER 4.

CHAPTER 4. SYSTEM IDENTIFICATION & MPC

This chapter provides a detail description of system identification techniques used to derive a dynamic model of the PWR. A description of MPC follows. MPC is a MIMO control technique that utilises a dynamic model of the system to make predictions that aids in improving the control of the system.

4.1 System identification

4.1.1 Introduction

System Identification is a tool used to derive dynamic models from the measured data obtained from a physical system. This dynamic model is a mathematical description of the system's dynamic behaviour.

The conventional method of obtaining models of systems is usually by deriving it from first principles. These models become harder to derive as the complexity of the system increases, and the increasing complexity deriving mathematical models are becoming time-consuming.

An alternative approach towards deriving a model from first principles is system identification. Figure 25 depicts the basic concept of systems identification.

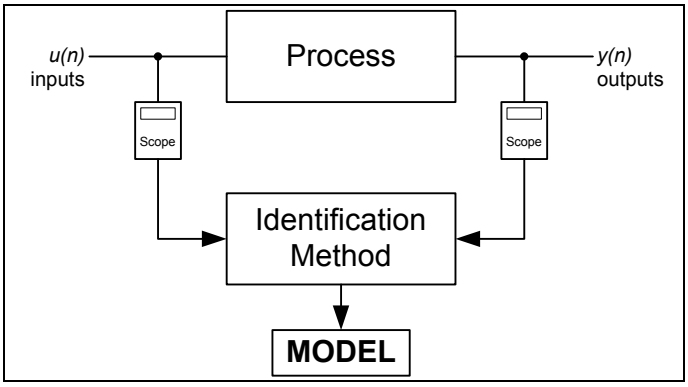

Figure 25: System identification concept [10]

Input-output data of the actual system is used to derive a parametric model of the system. This can be done without any knowledge of the system's internal details.

4.1.2 The system identification procedure

Obtaining a model from measured data requires three basic ingredients explained in the following points:

- Firstly, a set of measured data is required. Input-output data sets can be obtained from experiments, existing systems and also from existing simulations obtained from complex first principle models. The input-output signals that are measured for the data-set can be selected by the user. This has the advantage of the possibility for the user to select the most informative set of measured variables. These most informative variables can be determined through careful consideration of the system but will eventually be through repeated experiments.

- A *set of candidate model structures* is to be obtained. This is done by specifying a collection of models that is to be looked at for determining a suitable one. Of the entire system identification procedure, this proves to be the most difficult choice, and at the same time it is also the most important choice to be made.

- Rules for *assessing the candidate models* are where the best model in the set is selected. This is the identification method. Each model is basically assessed by evaluating how well the models reproduce the measured data.

The system identification is a logical process; firstly, collect the measured data; secondly, select a suitable model set; and finally, choose the best performing model in this set [12].

4.1.3 Matlab® system identification workflow

System identification is an iterative process. Performance of different models that are estimated is compared. The least complicated model that sufficiently describes the system dynamics will be selected. The models derived using system identification is compared according to a performance specification. The models are required to be of low order and should represent the dominant dynamics of the system.

4.1.3.1 Four stages of system identification

There are four stages through the system identification process. The first stage involves the preparation of the data for system identification. This stage involves the following actions:

i. Importing the data into the workspace.
ii. Plotting the data to examine its features. The data can then be analysed for features like offsets, delays and feedback.
iii. Pre-processing of the data. This involves removing the offsets and linear trends.

Stage two involves estimating and validating the model. The Matlab® System Identification Toolbox™ supports various linear and nonlinear models. The nonlinear models that are supported are the nonlinear ARX model and the Hammerstein-Wiener model. When a model does not achieve satisfactory results a new model will be trained. Both linear and nonlinear models will be evaluated for the purpose of this study.

Stage three involves the post processing and transformation of models. The models are transformed between discrete- and continuous time descriptions. Model orders are reduced. Models are converted to linear time-invariant models and imported to Simulink®.

The fourth stage involves the implementation of the model in a simulation environment. The model can now be used to design a controller for a nonlinear plant [12].

4.1.3.2 Black-box model structures

There are a number of Model Structures. The linear parametric models include the ARX model structure, the ARXMAX model structure, the Output Error model structure, the Box-Jenkins model structure and the State-Space model structure. Two types of nonlinear Black-Box model structures are available to choose from. They are the nonlinear ARX model structure and the Hammerstien-Wiener model structure.

4.1.3.2.1 Linear ARX model structure

The linear difference equation is the simplest representation between the inputs and outputs of a system. The linear difference equation is given as follows:

$$y(t)+a_1y(t-1)+\ldots+a_ny(t-n)=b_1u(t-1)+\ldots+a_mu(t-m). \quad \textbf{(4.1)}$$

At time t the systems inputs are denoted by $u(t)$ and the outputs by $y(t)$. The system is observed in discrete time. The reason is that all observed data are always collected by sampling. The next output can be determined by writing (4.1) in the following form shown:

$$y(t)=-a_1y(t-1)-\ldots-a_ny(t-n)=b_1u(t-1)+\ldots+a_mu(t-m). \quad \textbf{(4.2)}$$

(4.2) can be rewritten as follows:

$$y(t)=\phi^T(t)\theta \text{, where} \quad \textbf{(4.3)}$$

$$\theta=\begin{bmatrix} a_1 & \ldots & a_n & b_1 & \ldots & b_m \end{bmatrix}\text{, and} \quad \textbf{(4.4)}$$

$$\phi(t)=\begin{bmatrix} -y(t-1) & \ldots & -y(t-n) & u(t-1) & \ldots & u(t-m) \end{bmatrix}. \quad \textbf{(4.5)}$$

Where y is also dependant on θ (4.3) can be represented as follows [10, 12]:

$$\hat{y}(t/\theta)=\phi^T(t)\theta. \quad \textbf{(4.6)}$$

4.1.3.2.2 State-space model structure

The State-space form gives the relationship between inputs, noise and outputs. It is written as a system of first order differential equations.

The discrete state-space system is described by

$$x(n+1)=Ax(n)+Bu(n)\text{, and} \quad \textbf{(4.7)}$$

$$y(n)=Cx(n)+Du(n). \quad \textbf{(4.8)}$$

where $u(n)$ is the inputs, $x(n)$ is the states and $y(n)$ is the outputs. The four matrices, A, B, C, and D must have dimensions as illustrated in Figure 26:

According to Figure 26, the A matrix is a $n\times n$ matrix, the B matrix is a $n\times m$ matrix, the C matrix must be a $r\times n$ matrix and the D matrix is a $r\times m$ matrix,

where n is the number of states, m is the number of inputs and r the number of outputs [10, 12].

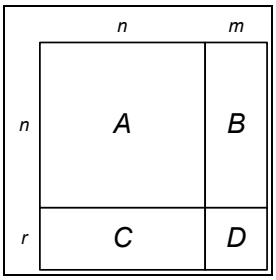

Figure 26: State-Space Matrix Sizes

4.1.3.2.3 Nonlinear ARX model structure

Parallel combinations of nonlinear and linear blocks are used to describe nonlinear structures. Regressors are used to describe the nonlinear and linear functions.

The model output is a function of regressors as given by

$$\hat{y} = g\left(y(t-1), u(t-1), y(t-2), \ldots\right), \tag{4.9}$$

where g is generally a combination of a linear and a nonlinear function. Figure 27 illustrates the predicted outputs obtained [13].

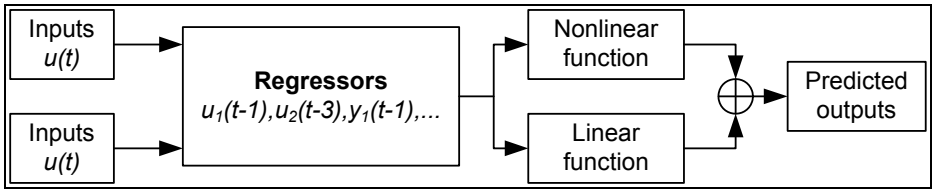

Figure 27: Predicted outputs for a nonlinear ARX model [13]

4.2 Model verification

Matlab® has a number of verification techniques available to validate the model structures that are identified. Validation is required to verify that the model structure replicates the behaviour of the identified system within acceptable levels. Validation methods available in Matlab® are:

- Comparing simulated and predicted output to the measured output based on the best fit approach.

- Analysing the cross-correlation and autocorrelation of the residuals with the inputs.
- Analysing the model response using input response and step response plots, and frequency response models.
- Plotting the poles and zeros of the linear parametric models.
- For non-linear models it is possible to plot the linear and nonlinear blocks.

For this study the best fit approach was decided on to validate the model structures. The reason for this is that both linear parametric models and nonlinear methods are used in the model identification. The selected method of validation supports both linear parametric and non-linear models. The performance of how well the output that the model reproduces fits to the measured output is measured. A best fit value is calculated using the following equation:

$$Best\ \ fit = \left(1 - \frac{\left| y - \hat{y} \right|}{\left| y - \bar{y} \right|} \right) \times 100\%, \qquad \textbf{(4.10)}$$

where y is the measured output, $\hat{y}$ is the simulated or predicted output and $\bar{y}$ is the mean of the measured output.

A fit of 100% corresponds to a perfect fit, and 0% indicates that the fit could be a guessed value of a constant output.

4.3 MIMO controller theory

4.3.1 Introduction

Most advanced control applications involve plants having a multiple number of inputs and outputs. These are MIMO systems and advanced control is preferred in these applications. SISO refers to single-input single-output systems and forms part of classical control system theory. For MIMO systems, each one of the outputs can be influenced by any one or more of the inputs and outputs simultaneously. The MIMO problem can have unequal numbers of inputs and outputs. MIMO is therefore a more

realistic approach. Figure 28 shows the general structure of a MIMO control system [15], [28].

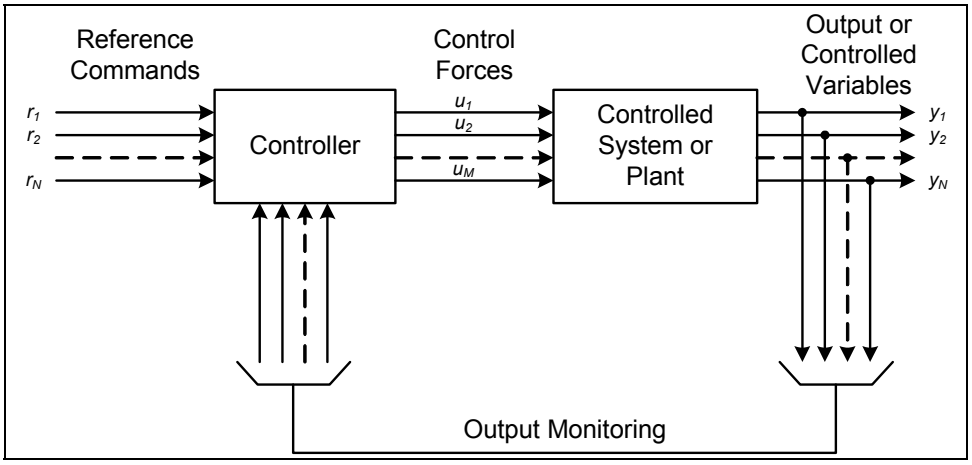

Figure 28: MIMO control system structure [15]

The system to be controlled is known as the plant. The plant is a component of the system whose physical characteristics can not be controlled. There are N number of measured plant outputs $y_1(t),\ y_2(t),\ \ldots,\ y_N(t)$. A controlling device, generally known as the plant controller, directly controls the plant by means of M number of controlled plant inputs $u_1(t),\ u_2(t),\ \ldots,\ u_M(t)$. The controller uses N number of reference commands $r_1(t),\ r_2(t),\ \ldots,\ r_N(t)$ along with information obtained from the output variables to generate the control actions. [15], [28].

4.3.2 MIMO example

Consider the following example of a MIMO system. Take for example a hot water supply. To control the water at the outlet at a specified temperature and flow rate, the flow rate of the cold water supply and the hot water supply are required to be controlled. The hot water and cold water supplies have constant temperatures, but their flow rates can be adjusted and controlled. Figure 29 is an illustration of the example.

A state-space model for this example, relates the system's inputs and outputs to:

$$\dot{x} = f(x,u), \text{ and} \quad \textbf{(4.11)}$$

$$y = g(x,u), \quad \textbf{(4.12)}$$

where u is the inputs, y is the outputs and x is the state of the system.

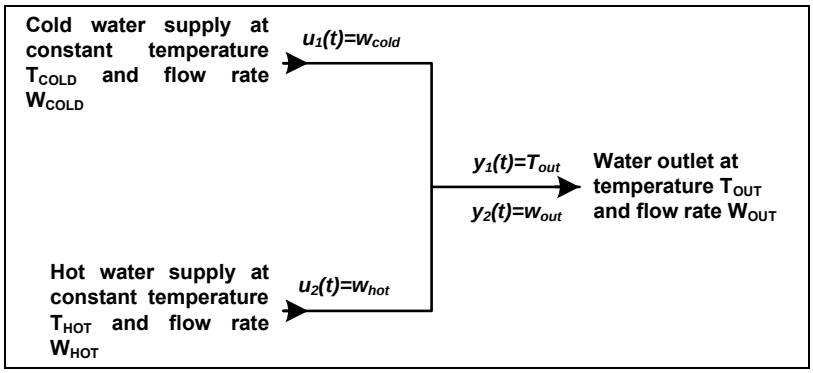

Figure 29: Illustration of MIMO control example

Restricting the example to linear time-invariant (LTI) systems, (4.11) and (4.12) can be written in the following form:

$$\dot{x} = Ax + Bu \text{ , and} \quad \textbf{(4.13)}$$

$$y = Cx + Du \text{ ,} \quad \textbf{(4.14)}$$

where ***A*** is a $n \times n$ matrix, ***B*** a $n \times m$ matrix , ***C*** a $k \times n$ matrix, and ***D*** a $k \times m$ matrix. m is the number of inputs, for this example two, and k is the number of outputs, for this example again two. To control the outlet temperature and outlet flow rate the flow rates of the cold and hot water need to be adjusted. If the outlet temperature starts to increase, it would be required that either the hot water or cold water be adjusted to correct the temperature change. Adjusting either of the two inputs will however also change the outlet flow rate and again an alteration will be required and this will keep on until the outlet temperature and flow rate is stabilised at the set points. To avoid this affect on the outlet, the inputs are required to be adjusted and controlled simultaneously. This will then result in the system reaching steady state much faster. A MIMO controller will be able to achieve this.

4.3.3 Matlab® and MIMO controllers

4.3.3.1 Matlab® MPC Toolbox™

MPC is an advanced method of controlling a process. Dynamic models of the process are required for these types of controllers. Usually these models are linear empirical models obtained through system identification techniques.

The dynamic models are used to predict the outputs of the system. Predictions are done with respect to the system's inputs. Inputs are referred to as independent variables and the outputs as dependant variables. The MPC will send the outputs to

a corresponding controller as a set point value. MPC controller are usually implemented at supervisory level. Figure 30 illustrates an example where a MPC is used at the supervisory level. This type of cascade configuration has the advantage of the MPC algorithm sitting on top of the PID control. The MPC therefore does not interfere with the closed loop control system [23].

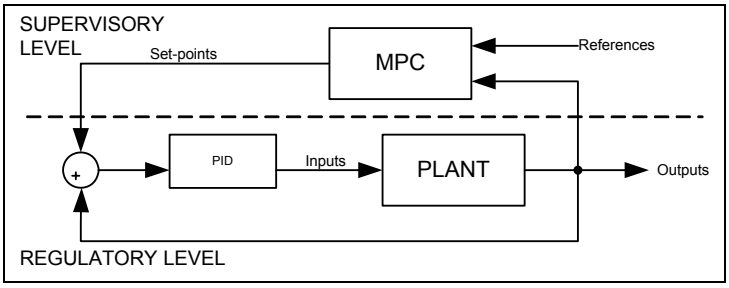

Figure 30: Example of supervisory MPC [23]

Most processes are non-linear, but can be linearised around an operating point. MPCs can make use of linearised state-space models to predict the future response for a given control input at the current time step.

MPC is a MIMO control algorithm. This requires three components to determine the optimum control output set points. These three components are, a dynamic model of the process, history of previous control actions, and an optimisation cost function J.

The optimisation cost function is given by

$$J = \sum_{i=1}^{N} w_{x_i} \left(r_i - x_i \right)^2 + \sum_{i=1}^{N} w_{u_i} \Delta u_i^{\,2}, \qquad \textbf{(4.15)}$$

where x_i is the i^{th} control variable, r_i is the i^{th} reference variable, u_i is the i^{th} manipulated variable, w_{x_i} is the weighting coefficient reflecting the relative importance of x_i, and w_{u_i} is the weighting coefficient penalising relative big changes in u_i.

A model of the process is obtained. This model is used to predict how certain actions will affect certain variables in the system. The model gives the ability to predict how certain actions will affect certain objectives. This can be done in real time. The predictions are optimised and the optimisation provides an action plan from the

present time ($t = t_k$) and into the future ($t = t_{k+1}$). This optimised plan can be implemented and after some time the system will give measurements. By using feedback it is now possible to use the measurements to obtain better predictions of the variables that are utilised in the model. This feedback is critical in the successful operation of the system. A new starting point is effectively created and from this it is again possible to optimise the predictions and obtain a new action plan. The control system effectively then consist of the repeated optimisation of the action plan followed by current state estimation based on the available measurements. Figure 31 illustrates the MPC scheme.

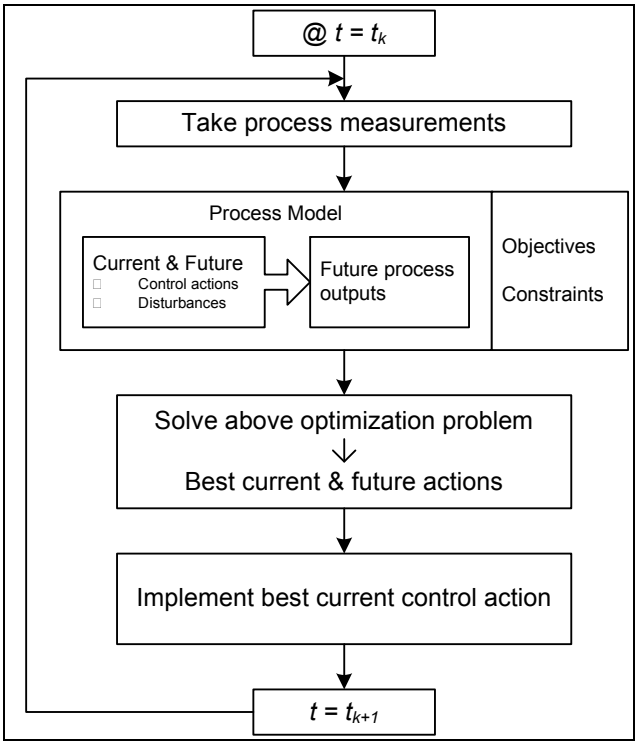

Figure 31: MPC scheme [17]

MPC is used in industry to manage large MIMO control problems. The basic principle of MPC is identifying a control action through continuous online solving of an optimal control problem.

The MPC is a control algorithm that utilises a dynamic state-space model to generate optimal control outputs. At each control interval the MPC algorithm attempts to optimise the future behaviour of the plant. The initial values are

introduced into the plant. The optimisation process is repeated at each control interval thereafter.

Nuclear power plants are very complex and non-linear. Developing a control system for a nuclear power plant is a challenging task due to the complexity of the process. Current nuclear power plants implement classical control schemes such as combined feedforward and feedback [16].

In this study a dynamic, state-space model is not available, but data obtained from a PWR nuclear reactor power plant simulator is used by the System Identification Toolbox™ to develop a data based model of the plant. This model will then be used in the MPC Toolbox™. Before the model can be used in the MPC Toolbox™ the System Identification Toolbox™ model that was created from the measured data must be converted to a LTI (Linear, Time-Invariant) object. This is automatically done by a built-in function of the System Identification Toolbox™. The MPC Toolbox™ fits in directly to MIMO plants. The plant can also have a unique number of inputs and outputs [13].

4.3.3.2 Matlab® Robust Control Toolbox™

Controllers can be designed for MIMO LTI models by using the Robust Control Toolbox™. With the Robust Control Toolbox™ uncertain LTI system models containing uncertain parameters and uncertain dynamics can be constructed. The Robust Control Toolbox™ also contains tools for analysing stability margins and worst case performance of MIMO systems [13].

4.3.3.3 Matlab® Control System Toolbox™

The Control System Toolbox™ in Matlab® also provides a type of MIMO controller. The LQR control and LQG control are modern state-space control strategies. More commonly it is used for designing optimal dynamic regulators and set-point trackers. This strategy gives less complexity to the design, with more performance and takes into account disturbances from the process and also measurement noise. Figure 32 shows the feedback configuration for a LQR problem. The feedback is negative and there is no reference signal for configuration which is one of many.

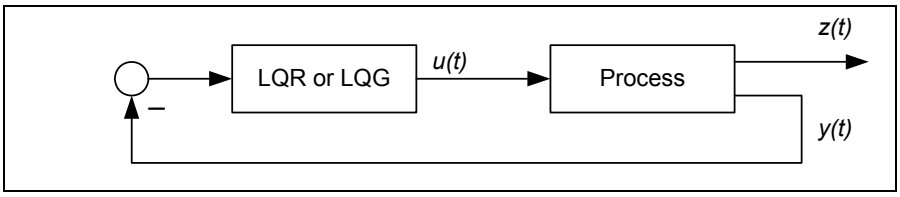

Figure 32: LQR feedback configuration (Regulatory control example) [21]

In this configuration, the state-space model for the process shown will be in the following form:

$$\dot{x} = Ax + Bu \text{ ,} \quad \textbf{(4.16)}$$

$$y = Cx \text{ , and} \quad \textbf{(4.17)}$$

$$z = Gx + Hu \quad \textbf{(4.18)}$$

The two outputs of the process are the measured output $y(t)$ corresponding to the signals that can be measured therefore available for control. The other output is the controlled output $z(t)$ and it corresponds to the signal that should be made as small as possible as quick as possible [13, 21].

4.3.4 Simulink®

Simulink® is a block diagram based tool that is used for modelling, simulating, and analysing dynamic systems. It caters for linear and nonlinear systems and systems can be modelled in continuous time and discrete time. Models and data from the Matlab® environment are seamlessly transferred to Simulink®. The Simulink® environment will be used to verify the MIMO controller once it is developed. The validation and comparison of conventional and MIMO control will also be graphically represented in Simulink®. Finally the results will be analysed using the Simulink® environment [13].

4.4 Conclusion

For this study a model of the system is required. System identification is chosen as the method for deriving the system model. This chapter provided information regarding system identification and MPC. Information is given on the system identification procedure. Selected model structures available in the Matlab® System Identification Toolbox™ is described along with explanations of the validation techniques that are to be used for the verifying the system model.

Further information was provided in this chapter further on a selection of MIMO controller strategies available in Matlab®. Simulink® and its contribution in simulation tool for the testing and validation of the controller is given.

The theory given in this chapter provides the knowledge of the skills and tools required to successfully develop the MIMO controller. In CHAPTER 5 system identification is used to derive a system model using measured data from the PWR simulator described in 1.1.3. In CHAPTER 6 the controller is developed, tested against conventional controllers and evaluated using the ITAE performance index

CHAPTER 5. SYSTEM MODEL DERIVATION

In this chapter, the System Identification Toolbox™ in Matlab® is used to obtain models for the MIMO system of the PWR simulator. The first section provides information on the selection of the input and output variables. This section includes detailed explanations of the PWR control systems. The second section explains the PWR working regions as observed from the simulator data. The last section includes information regarding the system identification, models obtained and the verification of these models.

5.1 Identification of plant variables

Before any system identification can be performed certain plant variables have to be identified that are to be used as the inputs and outputs of the identified plant model. For this study keep in mind that the same model identified here is to be used in the Simulink® model as the plant to be controlled by the MPC controller. It is important that the model captured via System Identification be of low order, but still contains the dominant dynamics. To prevent the model from being too complex the variables to be used as input to the plant model should not be more than the number of MPC controller manipulated variables. The different variables of the control systems should be evaluated first when selecting the variables to be used for identifying the plant model. In this section the plant variables are described and identified with regards to the different control systems.

5.1.1 Turbine control system

The electrical power output of a power plant is controlled by the steam flow to the turbine. A PWR's overall control system is based on the fact that the reactor power follows the turbine steam demand. The electrical power is increased by allowing more steam to flow through the turbine. Reactor power will therefore be raised to meet the turbine load. The turbine control system adjusts the speed and the load of the turbine/generator. The speed of the turbine/generator is measured in revolutions per second and is related to electrical frequency by

$$N = \frac{60 \times f_s}{n}, \tag{5.1}$$

where N is the rotational speed in revolutions per minute, f_s is the frequency of the output voltage and n is the number of pole pairs of the generator.

The frequency is therefore directly related to the rotational speed and the number of poles is fixed. Load increases and load decreases affect the rotational speed and therefore also the frequency of the system. A load increase on the network would result in the frequency starting to decrease. The turbine and generator starts to rotate slower and the turbine control system is required to supply more power in the form of steam flow to the turbine to keep the output frequency of the turbine/generator constant and meet the increased demand in power from the large grid. The turbine control system is mainly responsible to maintain a constant system frequency. By maintaining a constant system frequency, the turbine control system is performing load following. Therefore to meet the changing load demand (frequency) the steam flow to the turbine is the variable required to be controlled. The relationship between the turbine power output and the revolutions of the turbine is given by

$$P = \dot{m}.\Delta v_w.\pi.N.D, \tag{5.2}$$

where P is the power of the turbine, $\dot{m}$ is the mass flow rate of the steam entering the turbine, Δv_w is the change in velocity in the whirl direction, N is the revolutions per second and D is the diameter. In order to change the power P while maintaining a constant number of revolutions per second, N, the mass flow rate of the steam entering the turbine $\dot{m}$ is required to be maintained.

The turbine inlet and outlet temperatures also affect the power delivery of the turbine. The rest of the plant control systems will however try to maintain the secondary plant temperatures at constant values [9].

5.1.2 Steam dump

The steam dump system design is such that a high reactor coolant temperature is prevented as a result of a rapid secondary system heat load reduction. A rapid decrease in the load results in more energy being transferred to the reactor coolant water by the core than what is being removed by the secondary system in the steam generators. The reactor coolant temperature and volume increases, the pressuriser

water level increases and therefore the pressure in the primary system increases. As long as the sudden load reduction is inside the design limits of the different components, the transient will be allowed. For assisting the normal control system, the steam dump system creates an artificial temporary steam load. This artificial load reduces the sudden load decrease from a transient easily by the normal control system. The steam is exhausted from the steam headers to the main condenser shells or to the atmosphere. Steam dump is essentially used during large turbine load rejections or following a turbine trip [9].

5.1.3 Steam generator water level control system

The steam generator water level control system maintains a sufficient water inventory in the steam generator by controlling the feedwater supply to the steam generator. This inventory is required for ensuring that the necessary water inventory is present to remove heat from the reactor coolant system. The steam generator water level control system actually consists of three different control systems; each described briefly [9].

5.1.3.1 Main feed regulating valve control system

This system is used when the reactor power is greater than 15%. The steam generator level is controlled by regulating the main feed regulating valve. The feedwater and steam flows are used as inputs to this control system. These two flows are required to be equal. The deviation of the water level from a preset level is also used as an input [9].

5.1.3.2 Bypass feed regulating valve control system

This system is used when the reactor power is less than 15%. The bypass feed regulating control valve is controlled according to the reactor power. During normal operation this valve is closed at around 15% power. From there as mentioned, the main feed regulating valve system takes over [9].

5.1.3.3 Feed pump speed control system

The rate of the feedwater pump is controlled as a function of the total steam flow. With an increasing steam flow the feedwater pump speed will increase. The steam flow to the turbine is therefore an input to this control system [9].

A simple layout of the three control systems as they are discussed are illustrated in Figure 33.

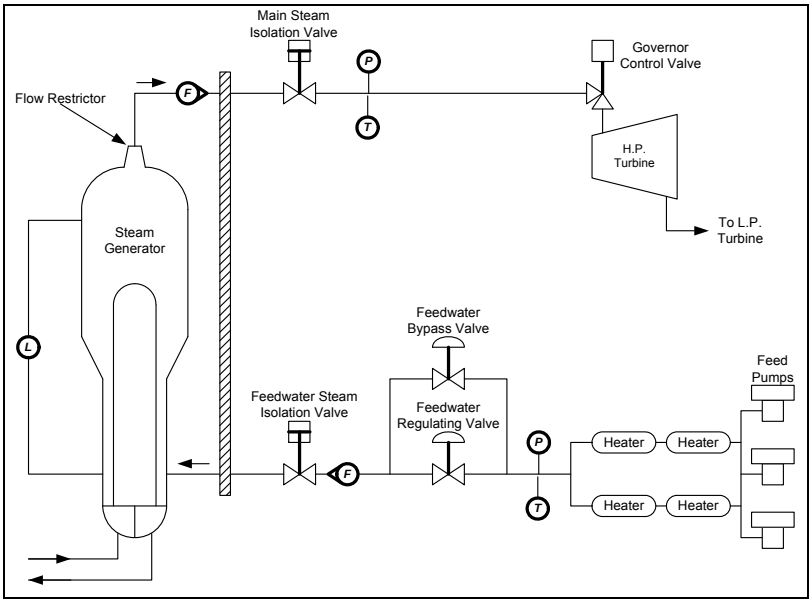

Figure 33: Basic steam generator feed and steam systems [9]

5.1.4 Pressuriser pressure and level control system

The pressuriser is responsible for maintaining the pressure in the primary circuit preventing the reactor coolant from boiling. The reactor coolant system pressure is prevented from going above its designed limits. The pressuriser pressure is controlled by electrical heaters, spray valves and relieve valves. When a pressure drops below a certain point the electrical heaters are energised. The heaters heat the water causing it to expand and as a result increase the pressure. The pressure is again reduced when required by sprays in the pressuriser spraying cold water from the cold leg of the reactor coolant system. The steam is condensed in the pressuriser cavity and the pressure is reduced. An even further increase in pressure will cause the pressuriser relieve valves to open to the pressuriser relieve tank, reducing the pressure. A simple layout of a pressuriser pressure and level control system is illustrated in Figure 34. In the figure the heater and spray valve can be seen. It is seen that the pressure and level inside the pressuriser is measured [9].

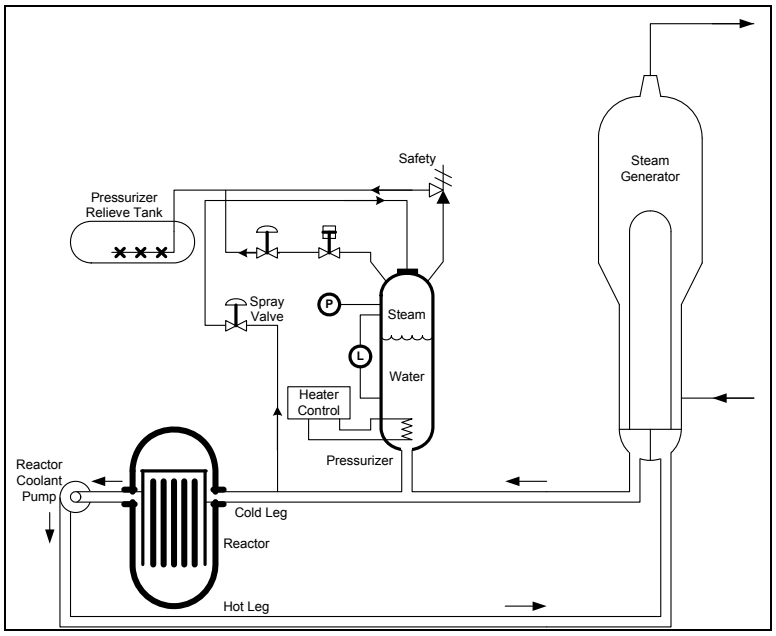

Figure 34: Pressuriser pressure and level control [9]

5.1.5 Rod control system

Reactor core power is regulated by controlling the neutron density available for fission to occur. Reducing the number of neutrons reduces the number of fissions that can take place, therefore reducing the number of neutrons released even more and the power is reduced. Three basic methods of accomplishing this are through burnable poison rods, soluble chemical neutron absorbers and control rods. The first two as mentioned previously are used for long term control to compensate for excess reactivity. As the control rods are inserted into the core they absorb neutrons causing fewer neutrons to fission and as described above reduce the core thermal power. As the control rods are removed from the core fewer neutrons are absorbed causing more neutrons to fission and therefore increase the core thermal power. The power produced by the core is not controlled by the control rods, but by the steam demand from the steam generators. The control rods are responsible for controlling the average temperature of the reactor coolant. This can be explained through the following example. As the load on the reactor turbine is reduced the turbine control system will reduce the steam flow to the turbine. Less energy is now being removed from the reactor coolant in the steam generator. Reactor coolant temperature will now increase causing a reduction in the neutron fissions due to the negative

temperature coefficient. The reactor rod control system will insert the control rods to decrease the coolant temperature.

There are two modes of control that can be used for the rod control system for controlling the reactor power. T_{Avg} is the difference between the reactors inlet- and the outlet temperatures. The constant T_{Avg} mode maintains the average temperature of the reactor outlet and inlet temperatures constant at all power levels. This means that the secondary plant temperature and pressures need to be adjusted resulting in poor turbine performance. The constant steam temperature mode provides very good turbine performance. An increase in the power demand of the secondary plant requires additional thermal energy transfer from the primary circuit to the secondary circuit in the steam generators. Now with the secondary circuit temperature kept constant the primary circuit is required to adjust its temperatures. With this mode it is assumed that the pressuriser control system is capable of maintaining the pressure of the coolant volume changes [9].

5.1.6 Final variable selection

The four main control systems are evaluated individually. The inputs and outputs required to perform system identification is selected according to the information provided in the preceding sections.

When considering all the control systems four variables are identified that have to be maintained at specified set-points in order to control the various parts of the plant. These variables are, as discussed in the previous sections, the load of the power turbine, the steam generator water level, the pressuriser pressure and level and the reactor neutron fission power.

Although these four variables were identified, problems were encountered with the pressuriser level and control variables during preliminary system identification efforts. A discussion on this topic is provided in Appendix A. As a result the pressuriser pressure and level control is not to be included in the model to be identified. This leaves three variables to be controlled.

The controller will manipulate a set of variables known simply as manipulated variables. The controller uses these manipulated variables to control the output

variables at their specified set points. These manipulated/input variables are the steam mass flow rate to the turbine, the feedwater mass flow rate to the steam generator and the control rod reactivity of the reactor. Figure 35 shows a diagram indicating the inputs and outputs used in the system identification of the plant model.

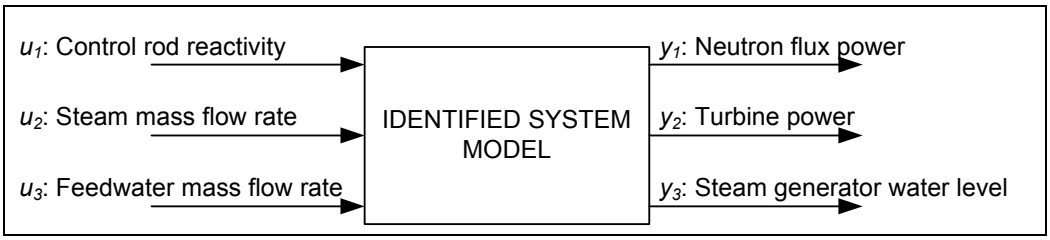

Figure 35: System identification input and output variables

The variables u_1, u_2 and u_3 are the input or manipulated variables to the system model that will be controlled by the MPC controller. The variables y_1, y_2 and y_3 are the output variables that are required to be maintained using certain reference inputs. These variables are inputs to the controller and internally used as feedback.

5.2 Simulations

The PWR simulator from Micro-Simulation Technology was used to generate the data required for system identification. Initially data was generated for the entire possible load following spectrum assumed for this study to be from 30% to 100% at a 10%/min load change. The data generated showed that the plant reacted differently for load changes in certain regions of the power output. These regions are identified for load changes between 30% and 40%, 40% and 50%, 50% and 60%, 60% and 70%, 70% and 80%, 80% and 90%, and 90% and 100% of full power. In these regions the data indicated that the system characteristics acted differently for the same size (10% of full power) in load change. From this it was decided to focus on specific region for the purpose of this study. The region selected is for load changes between 90% and 100% of full power. The simulator was used to generate seven sets of data. Each data set is unique and captures as far as possible all the dynamics of the variables used. The data sets can be viewed in Appendix B.

5.3 System identification of the PWR simulator model

The System Identification Toolbox™ in Matlab® is used to identify a model from the PWR simulator data. The nonlinear ARX model structure is used to identify a model of the PWR. This model is linearised and converted to state-space form. Seven sets of data are used and therefore seven models are obtained. From these seven models the best performing state-space model is identified following appropriate verification methods. This state-space model is later to be used to construct the MPC controller.

5.3.1 Non-linear ARX model identification and verification

The nonlinear ARX model identification structure in the System Identification Toolbox™ in Matlab® is used to identify system models from the seven different sets of generated data. The system models *nlarx1* to *nlarx7* is obtained and verified against each of the seven sets of data referred to as *DS1* through to *DS7*. The verification results are shown in Table 3, Table 4 and Table 5.

Table 3: Non-linear ARX model fits for output y_1 : Neutron flux power

	Output y_1 (Reactor power, %)						
	nlarx1	**nlarx2**	**nlarx3**	**nlarx4**	**nlarx5**	**nlarx6**	**nlarx7**
DS1	93.30%	81.36%	87.53%	92.52%	**93.55%**	89.66%	87.63%
DS2	94.19%	**96.92%**	92.35%	94.70%	93.10%	90.29%	85.31%
DS3	95.19%	93.26%	**98.02%**	95.77%	94.60%	91.04%	86.73%
DS4	93.70%	93.22%	90.16%	**97.34%**	92.49%	91.10%	83.93%
DS5	90.24%	83.30%	91.42%	87.36%	**98.07%**	95.10%	88.76%
DS6	90.15%	81.81%	90.16%	88.51%	95.99%	**97.94%**	88.87%
DS7	**96.79%**	91.11%	90.85%	95.40%	94.05%	90.78%	95.59%

Table 3 shows good results for all the models and data sets for the reactor power output y_1.

Table 4: Non-linear ARX model fits for output y_2 : Turbine load

	Output y_2 (Turbine load, %)						
	nlarx1	**nlarx2**	**nlarx3**	**nlarx4**	**nlarx5**	**nlarx6**	**nlarx7**
DS1	**92.66%**	-76.92%	64.22%	29.36%	92.16%	92.43%	89.94%
DS2	87.88%	**90.31%**	41.46%	46.43%	87.87%	87.94%	85.25%
DS3	91.24%	-1.50%	**92.99%**	48.96%	91.36%	91.46%	89.36%
DS4	90.48%	-24.45%	56.41%	**93.16%**	90.49%	90.52%	88.74%
DS5	95.55%	-40.07%	6.78%	-26.75%	**97.72%**	97.65%	97.20%
DS6	95.63%	-65.20%	32.93%	-26.65%	96.98%	**97.10%**	96.11%
DS7	97.19%	12.66%	56.06%	66.52%	99.19%	99.08%	**99.77%**

Table 4 shows a number of good results and also a number of bad results for all the models and data sets for the turbine load output y_2.

Table 5: Non-linear ARX model fits for output y_3: Steam generator water level

	Output y_3 (Steam generator water level, %)						
	nlarx1	**nlarx2**	**nlarx3**	**nlarx4**	**nlarx5**	**nlarx6**	**nlarx7**
DS1	**73.51%**	-12.18%	-64.80%	28.21%	-93.45%	38.02%	57.00%
DS2	72.58%	57.45%	41.89%	58.96%	3.78%	71.02%	**78.13%**
DS3	73.88%	42.38%	37.88%	55.92%	33.82%	67.61%	**84.26%**
DS4	70.87%	29.22%	-20.67%	73.00%	75.33%	69.53%	**75.79%**
DS5	-53.41%	-148.10%	-229.80%	-61.63%	-293.00%	-25.57%	**-0.88%**
DS6	-158.40%	-328.10%	-496.90%	-142.20%	-1378.00%	-124.30%	**-60.51%**
DS7	44.25%	60.82%	28.51%	57.90%	66.38%	54.31%	**99.67%**

Table 5 shows very bad results for almost all models for all data sets for output y_3.

5.3.2 Linearisation and verification

To ultimately end up with a state-space model that can be used in the MPC Tool of the MPC Toolbox™ the nonlinear ARX models are converted to linear models. *lm_1* to *lm_7* are obtained for each non-linear ARX model *nlarx1* to *nlarx7*. Each models' corresponding data sets are used.

To verify the accuracy of the linear ARX models they are transferred to the System Identification Tool™ and verified using the best fit technique using the same data sets. The verification results are shown in Table 6, Table 7 and Table 8.

Table 6: Linear ARX model fits for output y_1: Neutron flux power

	Output y_1 (Reactor power, %)						
	lm_1	**lm_2**	**lm_3**	**lm_4**	**lm_5**	**lm_6**	**lm_7**
DS1	91.73%	92.15%	92.20%	92.30%	92.27%	**92.42%**	89.58%
DS2	87.08%	87.75%	87.63%	**87.94%**	87.82%	**87.94%**	83.52%
DS3	90.07%	91.26%	91.24%	91.32%	91.36%	**91.46%**	88.32%
DS4	89.62%	90.25%	90.21%	**90.58%**	90.48%	90.52%	87.16%
DS5	93.71%	97.26%	97.42%	96.97%	**97.68%**	97.65%	97.03%
DS6	93.44%	96.67%	96.93%	96.48%	97.05%	**97.09%**	96.05%
DS7	95.94%	98.38%	98.63%	98.50%	99.26%	99.08%	**99.76%**

The results for Table 6 are similar to those obtained for the verification of the non-linear models in Table 3.

Table 7: Linear ARX model fits for output y_2 : Turbine load

	Output y_2 (Turbine load, %)						
	lm_1	**lm_2**	**Lm_3**	**lm_4**	**lm_5**	**lm_6**	**lm_7**
DS1	-58.57%	-113.90%	-102.20%	-84.20%	-283.70%	**46.87%**	-307.70%
DS2	-128.00%	14.33%	24.76%	-62.35%	-132.10%	**39.28%**	-37.18%
DS3	-149.00%	-26.72%	14.89%	-72.15%	-132.80%	**19.56%**	-154.00%
DS4	-98.42%	-12.04%	0.23%	-34.82%	14.89%	**49.87%**	-119.10%
DS5	-1159.00%	-753.40%	-717.10%	-620.90%	**-155.00%**	-358.90%	-1185.00%
DS6	-1790.00%	-1309.00%	-1278.00%	-962.50%	-785.90%	**-954.90%**	-1993.00%
DS7	-152.40%	-31.75%	-11.14%	-132.40%	**47.91%**	26.90%	3.89%

The results for Table 7 are similar to those obtained for the verification of the non-linear models in Table 4.

Table 8: Linear ARX model fits for output y_3 : Steam generator water level

	Output y_3 (Steam generator water level, %)						
	nlarx1	**nlarx2**	**nlarx3**	**nlarx4**	**nlarx5**	**nlarx6**	**nlarx7**
DS1	**73.51%**	-12.18%	-64.80%	28.21%	-93.45%	38.02%	57.00%
DS2	72.58%	57.45%	41.89%	58.96%	3.78%	71.02%	**78.13%**
DS3	73.88%	42.38%	37.88%	55.92%	33.82%	67.61%	**84.26%**
DS4	70.87%	29.22%	-20.67%	73.00%	75.33%	69.53%	**75.79%**
DS5	-53.41%	-148.10%	-229.80%	-61.63%	-293.00%	-25.57%	**-0.88%**
DS6	-158.40%	-328.10%	-496.90%	-142.20%	-1378.00%	-124.30%	**-60.51%**
DS7	44.25%	60.82%	28.51%	57.90%	66.38%	54.31%	**99.67%**

The results for Table 8 are similar to those obtained for the verification of the non-linear models in Table 5.

5.3.3 Convert models to state-space and verify

The final step in preparing the models to be used in the MPC Tool is to convert them to state-space models. *lm_ss_1* to *lm_ss_7* are obtained for each linear model *lm_1* to *lm_7*.

To verify the accuracy of the state-space system models the models are again transferred to the System Identification Tool™ and verified using the best fit technique. The verification results are shown in Table 9, Table 10 and Table 11.

Table 9: State-space model fits for output y_1 : Neutron flux power

	Output y_1 (Reactor power, %)						
	Im_ss_1	**Im_ss_2**	**Im_ss_3**	**Im_ss_4**	**Im_ss_5**	**Im_ss_6**	**Im_ss_7**
DS1	**95.34%**	93.27%	92.53%	93.21%	95.28%	93.07%	90.55%
DS2	94.72%	94.52%	93.21%	94.35%	**94.96%**	93.60%	91.70%
DS3	**95.07%**	94.23%	94.26%	93.70%	94.85%	92.97%	91.74%
DS4	**94.99%**	93.81%	91.65%	94.26%	94.18%	93.75%	91.79%
DS5	92.55%	93.22%	92.32%	93.69%	**97.64%**	95.39%	92.93%
DS6	93.62%	95.16%	94.46%	95.97%	**97.60%**	96.76%	92.81%
DS7	**96.44%**	95.37%	94.93%	94.99%	96.00%	94.59%	85.26%

The results of the state-space models shown in Table 9 actually show slight improvement from that of the non-linear ARX and the linearised models from tables Table 3 and Table 6.

Table 10: State-space model fits for output y_2 : Turbine load

	Output y_2 (Turbine load, %)						
	Im_ss_1	**Im_ss_2**	**Im_ss_3**	**Im_ss_4**	**Im_ss_5**	**Im_ss_6**	**Im_ss_7**
DS1	91.77%	92.15%	92.20%	92.30%	92.27%	**92.42%**	89.58%
DS2	87.09%	87.75%	87.63%	**87.94%**	87.82%	**87.94%**	83.52%
DS3	90.07%	**92.26%**	91.24%	91.32%	91.36%	91.46%	88.32%
DS4	89.69%	90.25%	90.21%	**90.58%**	90.48%	90.52%	87.16%
DS5	93.74%	97.26%	97.42%	96.97%	**97.68%**	97.65%	97.03%
DS6	93.45%	96.67%	96.93%	96.48%	97.05%	**97.09%**	96.05%
DS7	96.10%	98.38%	98.63%	98.50%	99.26%	99.08%	**99.76%**

The results of the state-space models shown in Table 10 also show slight improvement from that of the non-linear ARX and the linearised models from tables Table 4 and Table 7.

Table 11: State-space model fits for output y_3 : Steam generator water level

	Output y_3 (Steam generator water level, %)						
	Im_ss_1	**Im_ss_2**	**Im_ss_3**	**Im_ss_4**	**Im_ss_5**	**Im_ss_6**	**Im_ss_7**
DS1	-49.86%	-113.50%	-102.20%	-83.73%	-43.84%	**58.82%**	-305.10%
DS2	-120.40%	17.83%	26.31%	-61.62%	15.61%	**57.72%**	-20.95%
DS3	-126.80%	0.86%	11.48%	-69.57%	5.07%	**54.86%**	-130.10%
DS4	-79.58%	-4.32%	3.96%	-32.71%	53.04%	**67.62%**	-104.80%
DS5	-1098.00%	-655.20%	-620.80%	-617.70%	**-127.00%**	-145.60%	-1127.00%
DS6	-1754.00%	-1250.00%	-1220.00%	-959.80%	-690.20%	**-682.90%**	-1958.00%
DS7	-129.80%	-10.05%	5.19%	-131.90%	**70.00%**	53.54%	31.57%

The results of the state-space models shown in Table 11 also show improvement from that of the non-linear ARX and the linearised models from tables Table 5 and

Table 8. The output y_3 again produced bad results and is believed to be as a result of the reason provided previously.

From the results presented in the tables the linearised state-space model *lm_ss_4* provided the best performance. Table 12 to Table 16 give the state-space matrices of *lm_ss_4*.

Table 12: State-space ***A*** matrix

1.4029	0	0	-0.41959	0	0	30.018	0.00050459	-0.0015451	-30.007	-0.00019595	0.0015322
0	0.0011762	0	0	0.0021568	0	-61.939	0.019835	-0.0073075	61.297	-0.0018817	0.0069722
0	0	1.8524	0	0	-0.85367	-39.861	0.00044048	-0.0034706	39.672	-0.00032453	0.0034511
1	0	0	0	0	0	0	0	0	0	0	0
0	1	0	0	0	0	0	0	0	0	0	0
0	0	1	0	0	0	0	0	0	0	0	0
0	0	0	0	0	0	0	0	0	0	0	0
0	0	0	0	0	0	0	0	0	0	0	0
0	0	0	0	0	0	0	0	0	0	0	0
0	0	0	0	0	0	1	0	0	0	0	0
0	0	0	0	0	0	0	1	0	0	0	0
0	0	0	0	0	0	0	0	1	0	0	0

Table 13: State-space ***B*** matrix

0	0	0
0	0	0
0	0	0
0	0	0
0	0	0
0	0	0
1	0	0
0	1	0
0	0	1
0	0	0
0	0	0
0	0	0

Table 14: State-space ***C*** matrix

1.4029	0	0	-0.41959	0	0	30.018	0.00050459	-0.0015451	-30.007	-0.00019595	0.0015322
0	0.0011762	0	0	0.0021568	0	-61.939	0.019835	-0.0073075	61.297	-0.0018817	0.0069722
0	0	1.8524	0	0	-0.85367	-39.861	0.00044048	-0.0034706	39.672	-0.00032453	0.0034511

Table 15: State-space ***D*** matrix

0	0	0
0	0	0
0	0	0

Table 16: State-space ***K*** matrix

1	0	0
0	1	0
0	0	1
0	0	0
0	0	0
0	0	0
0	0	0
0	0	0
0	0	0
0	0	0
0	0	0
0	0	0

5.4 Conclusion

In the results presented a fit of 100% would correspond to a perfect fit. A fit of 0% indicates that the fit is no better than guessing the output to be a constant ($\hat{y} = \bar{y}$).

As can be seen from the tables there are some very good fits, some bad fits and there are also fits that are negative. Negatives fits are possible because of the definition of the best fit. A negative value is worse than 0%. There are a number of reasons why a best fit can have a fit result worse than 0%. For example it is possible that the estimation algorithm failed to converge. The possibility also exists that the model was not estimated by minimising $|\hat{y} = \bar{y}|$. The best fit can be negative when one-step-ahead prediction during the estimation is minimised but the simulated output $\hat{y}$ is used to validate. Another possibility is that the data set used for the validation was not pre-processed in the same way as the data set used for the estimation.

The result from Table 5 appears to be very bad. One might consider the system model as inconclusive. It is however necessary to look at the outputs y_3 from the simulator provided in Appendix B. The reason for the bad fits may be a result of small deviations after an adjustment is made. The level diverts by a small value from its original value and then stabilises back at the original level. The poor results are therefore understandable. The results of Table 5 are therefore decided not to be used as an indication for the accuracy of the model. This is to be remembered for the linearisation and when converting to state-space models.

The model does not indicate any less accurate models than the original non-linear ARX system identification.

From the seven linear state-space models obtained the model selected to be used to develop the MPC controller using the MPC Tool is the state-space model *lm_ss_4*. This model provided the best results when looking at the average fit for every scenario. CHAPTER 6 will discuss how the system model *lm_ss_4* is used to develop a MPC controller using the MPC Tool.

The State-Space matrices of lm_ss_4 can be viewed in Table 12 to Table 16. From the matrices it is shown that ***A*** is a 12×12 matrix, ***B*** is a 12×3 matrix, ***C*** is a 3×12 matrix and ***D*** is a 3×3 matrix. Therefore, this results in $n=12$ states (this is also the order of the system), $m=3$ number of inputs and $r=3$ number of outputs. These matrices conform to the basic forms for matrices ***A***, ***B***, ***C*** and ***D*** as presented in (4.7) and (4.8).

CHAPTER 6. MODEL PREDICTIVE CONTROL

In the following chapter, the MPC Tool of the MPC Toolbox™ in Matlab® is used to develop the MPC controller. In the first section the controllability and observability of the model is calculated. The following section describes the development of the controller itself. In the next section Simulink® is used to test and evaluate the controller, and finally the controller is compared to the conventional control using the ITAE (Integral of Time multiplied by the Absolute value of Error) performance index.

6.1 MPC design

The MPC Toolbox™ is used to design the MPC controller from the state-space model obtained. The MPC design tool is a visual environment for rapid MPC design. The state-space model *lm_ss_4* is imported into the MPC tool directly from the Matlab® workspace. After all settings are completed the controller is exported back to the Matlab® workspace. From the Matlab® workspace the controller can be used in any toolbox for evaluation.

Before an attempt can be made to develop a controller it is necessary to establish whether it is possible to control the system model. For this purpose the controllability and observability of the system model have to be analysed. The controllability of a system indicates if it is possible to force the system into a specific state by using an appropriate control signal.

Observability however indicates the possibility to observe the state of a system through output signals. For a state that is unobservable, the controller can not determine the behaviour of the state and the system will be unstable.

6.1.1 Controllability and observability

Controllability and observability are important properties of a dynamic system. A system is controllable if, given an initial state x_i a final state x_f and a fixed time T, it is possible to find an input signal $u(t)$ that takes the state of the system from x_i to x_f in the time interval $0 \le t \le T$ [22], [26]. This means that a system is controllable if the rank of the controllability matrix is equal to the size n of the state vector. The controllability matrix is given by

$$C = \begin{vmatrix} B & AB & A^2B & \dots & A^{n-1}B \end{vmatrix}. \quad \textbf{(6.1)}$$

A system is observable if the initial condition $x(0)$ can be determined by observing the input signal $u(t)$ and the output signal $y(t)$ in the time interval $0 \le t \le T$ [22], [26]. This means that a system is observable if the rank of the observability matrix is equal to the size n of the state vector. The observability matrix is given by

$$O = \begin{vmatrix} C \\ CA \\ CA^2 \\ \vdots \\ CA^{n-1} \end{vmatrix}. \quad \textbf{(6.2)}$$

Matrices of the state-space model are given in 5.3.3. There it is shown that the size of the state vector is $n = 12$. Using the Matlab® functions explained above the following ranks were determined:

For the controllability matrix a rank of 12 was calculated. This is equal to $n = 12$ and the system is therefore ***controllable***.

For the observability matrix a rank of 6 was calculated. This is not equal to $n = 12$ and the system is therefore not ***observable***.

If a system is not observable as in the current situation, it means that the present values of some of its states cannot be determined through its output sensors. This has the implication that their values are unknown to the controller and the initial state can not be observed from the knowledge of the input and output. The controller will be unable to perform the control specifications of these outputs. For advanced control design it is however not necessary to look at a system's observability. For most systems with more than a handful of states the observability matrix will have a rank that is numerically singular. For more information regarding this subject refer to [13] and [22].

6.1.2 Using the MPC tool

This section describes how the MPC controller is developed using the MPC tool. Different configurations were tested and evaluated to eventually end up with the best

performing controller. A number of controllers were developed and evaluated. The controller finally selected is exported as *MPC11*.

6.1.2.1 Specifying signal properties

Figure 36 shows the main window of the MPC tool. In the main window the signal types are selected and signal names and units are given. A description of each signal is also given. The controller's signal properties are specified as it is shown in Figure 36.

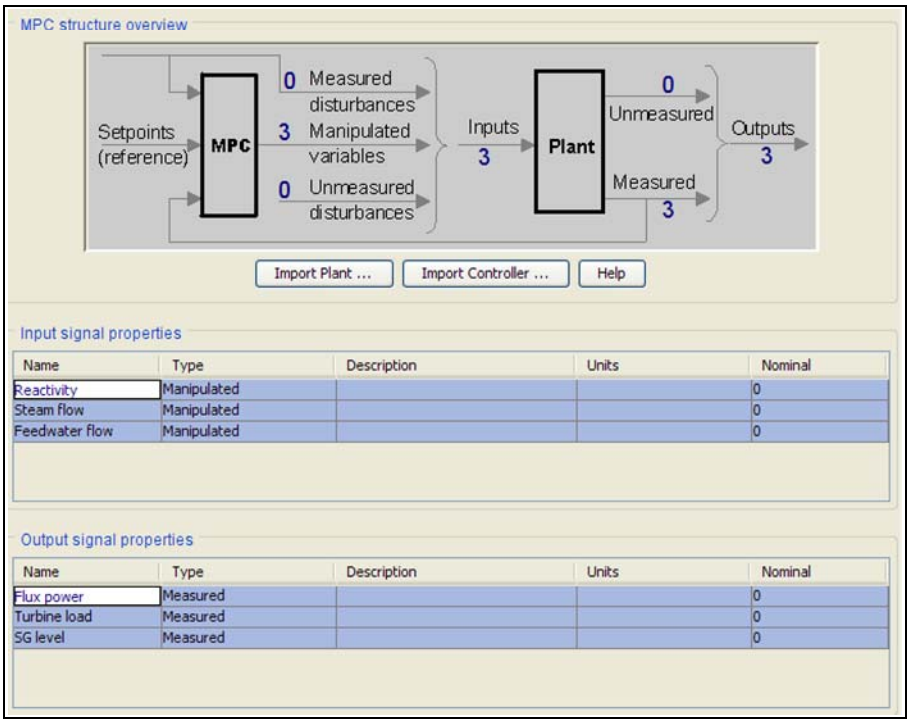

Figure 36: MPC design tool main window

6.1.2.2 Specifying controller properties

The controller's properties are viewed and edited in the MPC tool. Controller properties are divided into four groups, each dedicated to a specific design aspect.

In the first group, the plant model that the controller uses for its predictions are specified. The plant model to be used is the imported state-space model *lm_ss_4*. Controller horizons are also specified here. The first setting to be selected in the horizon field is the controller interval. This setting sets the time between consecutive controller moves. The next setting is the prediction horizon setting. This option sets the number of control intervals that the controller uses to predict its output. The last

setting in the horizon field is the control horizon setting. This option sets number of moves computed. The model and horizon settings for *MPC11* are specified as it is shown in Figure 37.

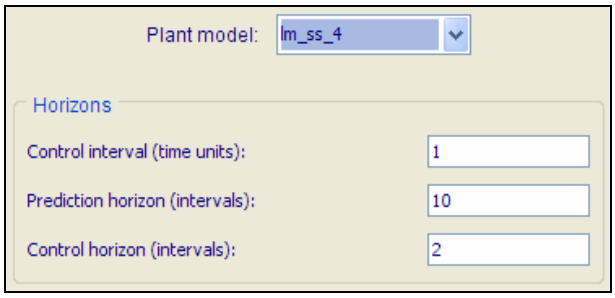

Figure 37: MPC controller plant model selection and horizons

The second of the four groups is the model constraints. These include the constraints on manipulated variables and the constraints on output variables. Constraints are the values that bound the manipulated variables and the outputs. The constraints for the controller are specified as it is shown in Figure 38. The constraints for this controller are not given a specific value. For *MPC11* no constraints have been set and the values are indicated as it is shown in Figure 38.

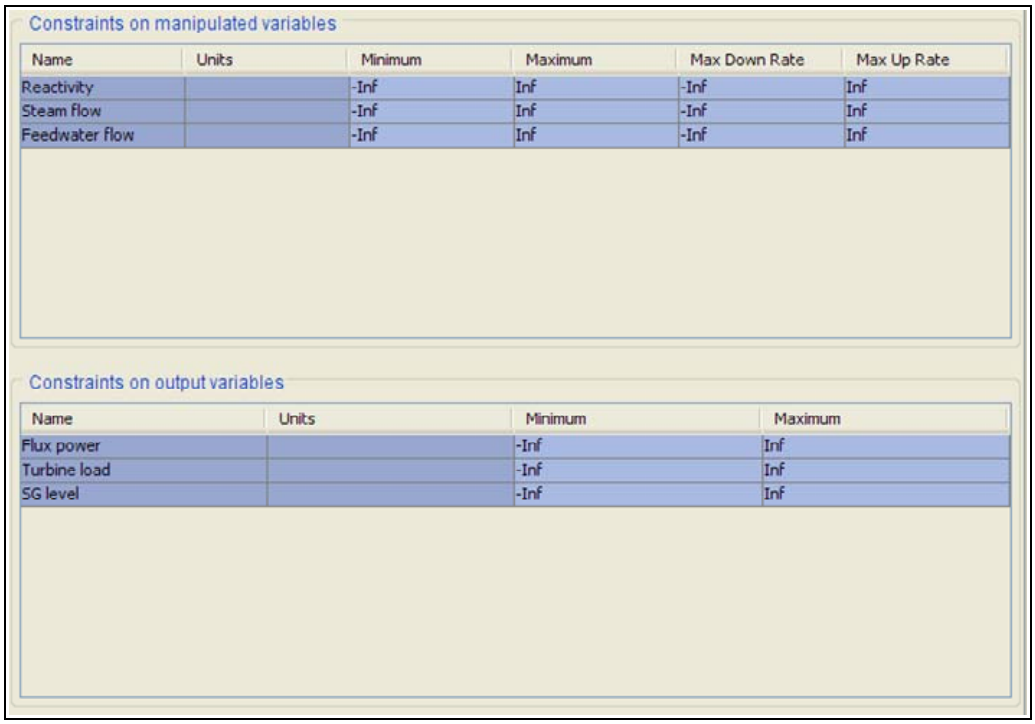

Figure 38: MPC controller model constraints on manipulated variables

The third of the four groups is the weight tuning values. These include the overall weight, the input weights and the output weights. For *MPC11* the controller weights are specified as it is shown in Figure 39.

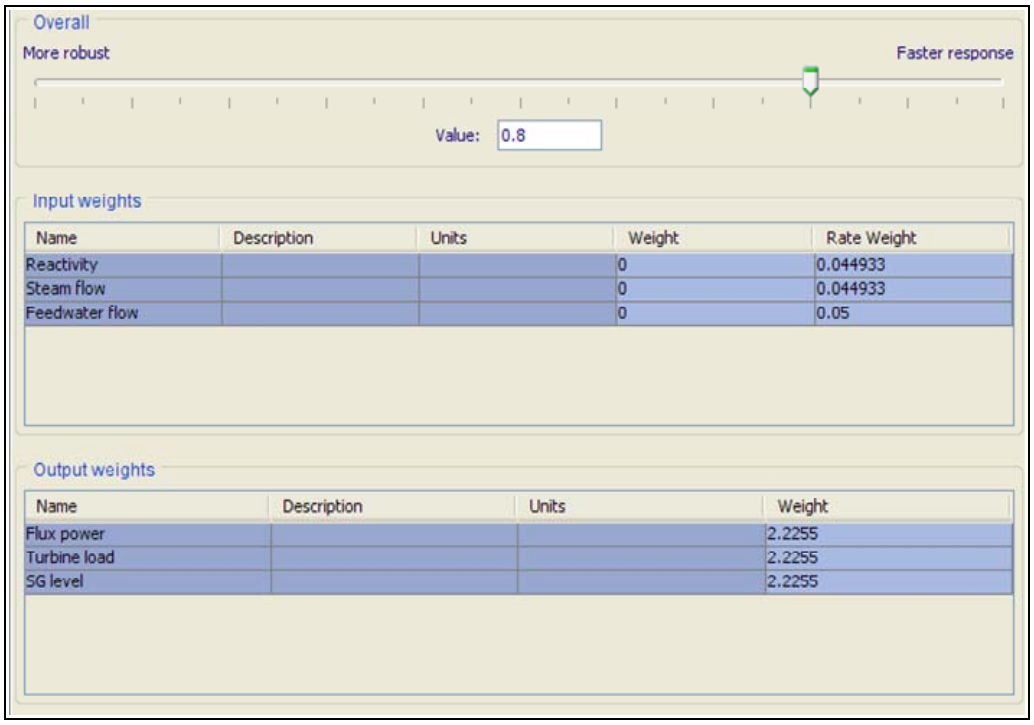

Figure 39: MPC controller overall, input and, output weight tuning

The last of the four groups is estimation. The estimation allows the response of the controller to unmeasured disturbances to be adjusted. This is ignored for this specific tab and left to default.

6.2 Simulink® model

6.2.1 Setup

To evaluate the MPC controller a Simulink® model is created using various function blocks available in Simulink®. Figure 40 shows the Simulink® model. The main parts of the model are the linear state-space model in the form of an *idmodel* object, and the MPC controller. The three outputs of the linear state-space model are connected to the measured output (*mo*) of the MPC controller as a single vector. Similarly the manipulated variable (*mv*) outputs from the MPC controller are connected as the vector input to the linear state-space model. Reference values are given as input to the MPC controller. The MPC controller attempts to control the measured outputs to

the values given to it as reference values. This is achieved by manipulating the manipulated variables going to the linear state-space plant model.

To be able to store, view and evaluate the data from the model, the input and output signals are separated. The Demux block extracts the components of an input signal and outputs the components as separate signal, and conversely the Mux block combines its inputs into a single vector output. To evaluate the linear state-space plant model and the MPC controller against the PWR simulator data, *iddata* sources are created containing information collected from the PWR simulator. A similar *iddata* object is created and used as the reference input to the MPC controller. This is the reference signal for both the turbine power and reactor power. A constant block source is used as an input to the steam generator water level reference signal for the MPC controller. Scope blocks are used for quick analysis of the output signals. The scope blocks are also used to export the Simulink® model data to the Matlab® workspace. The Simulink® model, PWR simulator data and reference values can be simultaneously viewed and compared.

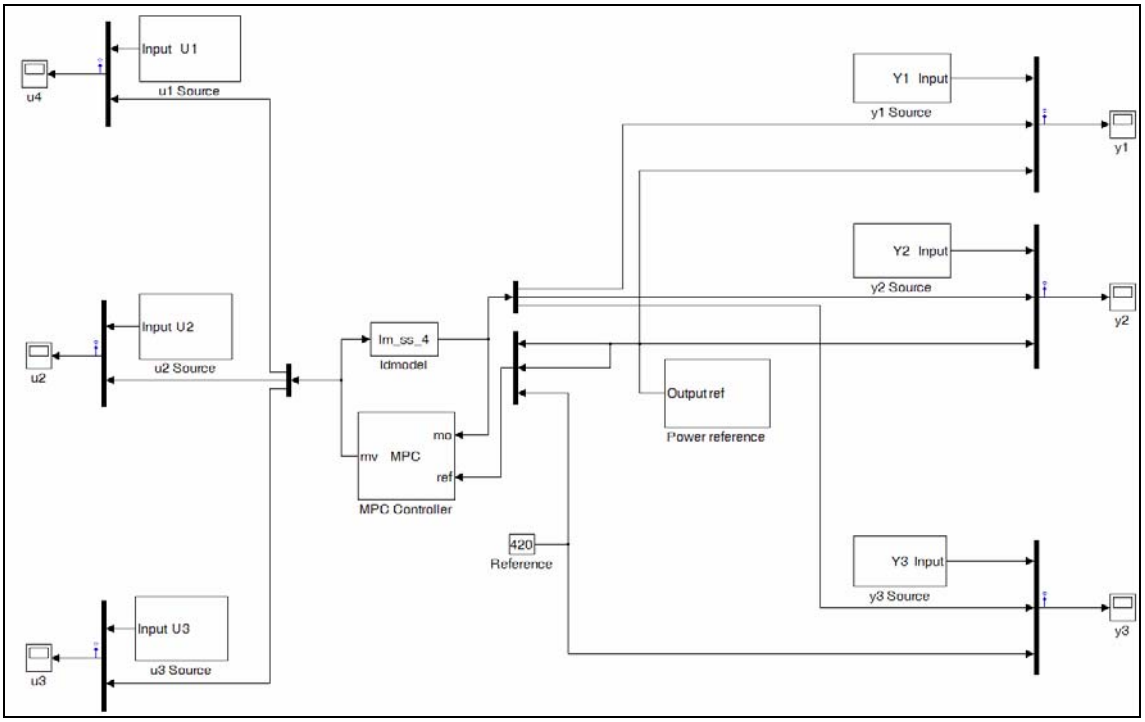

Figure 40: Simulink® model graphic illustration

6.2.2 Results

Figure 41 shows the signal used as reference input to the MPC controller for both the turbine load and reactor power. For the steam generator a constant reference signal is given to the MPC controller.

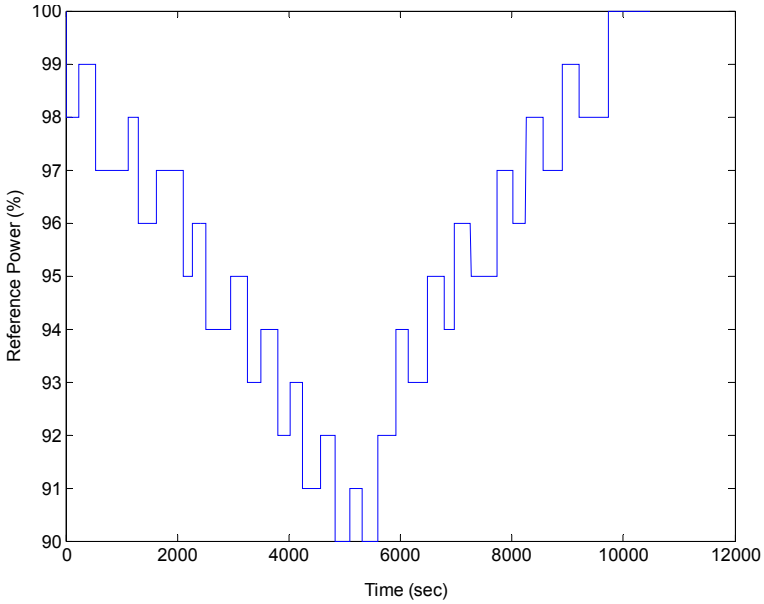

Figure 41: Turbine load and reactor power reference signal

Figure 42 shows the output of the reactor power. The blue line represents the conventional plant control. The green line is the measured output from the state-space model for the reactor power. This is the output controlled by the MPC controller. The red line is the reference signal given to the MPC controller.

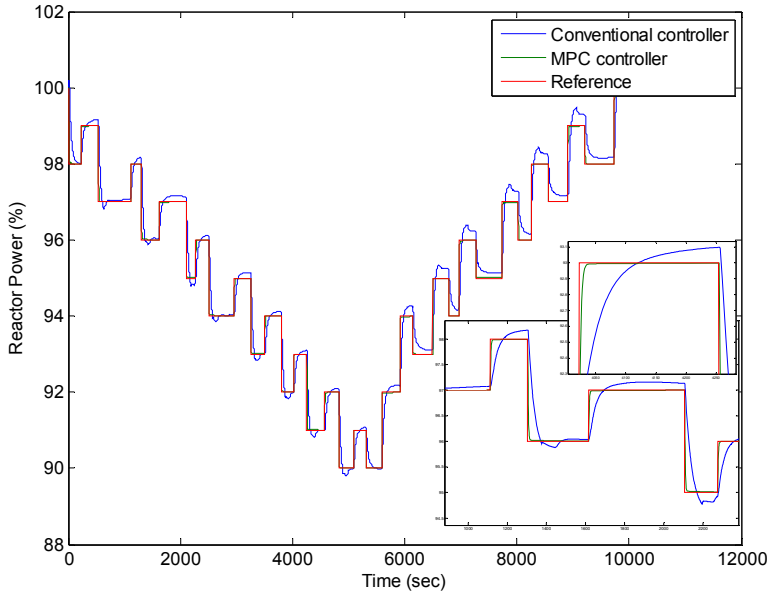

Figure 42: Compare conventional & MPC controllers for reactor power

The MPC controller performs much better than the conventional controller. The MPC controller response is faster and settles faster than the conventional controller and shows almost no overshoot. The load changes experienced are approximately 6%/minute. This change is within the capabilities of a PWR as it can go as high as 10%/minute. Figure 43 provides the percentage error experienced for Figure 42.

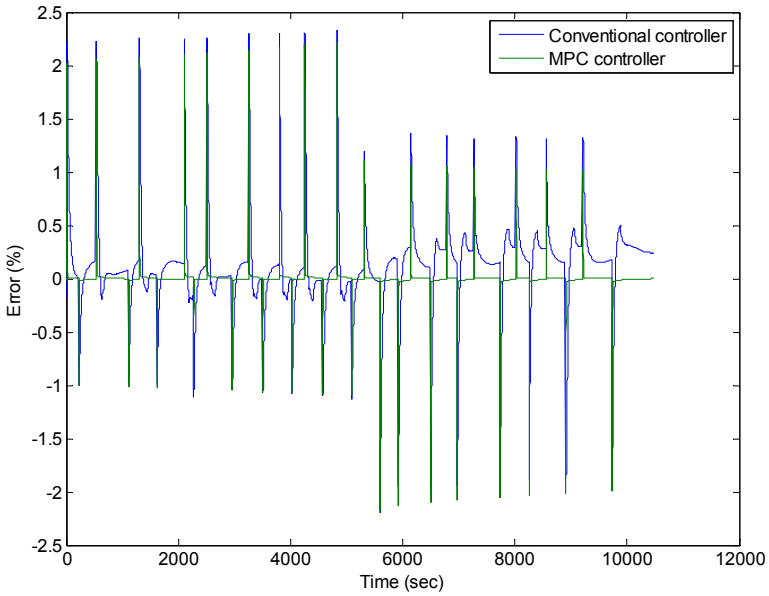

Figure 43: Conventional & MPC controllers' % error for reactor power

Figure 44 shows the output of the turbine load. The blue line represents the conventional plant control. The green line is the measured output from the state-space model for the turbine power. This is the output controlled by the MPC controller. The red line is the reference signal given to the MPC controller.

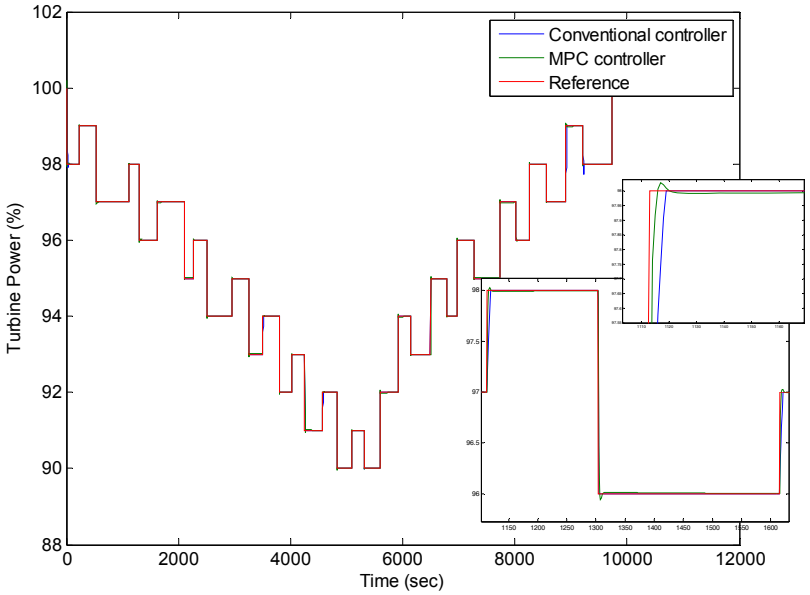

Figure 44: Compare conventional & MPC controllers for turbine load

The MPC controller does perform slightly better than the conventional control. Both controllers responded and settled very quickly to any changes made to the turbine load. Figure 45 provides the percentage error experienced for Figure 44.

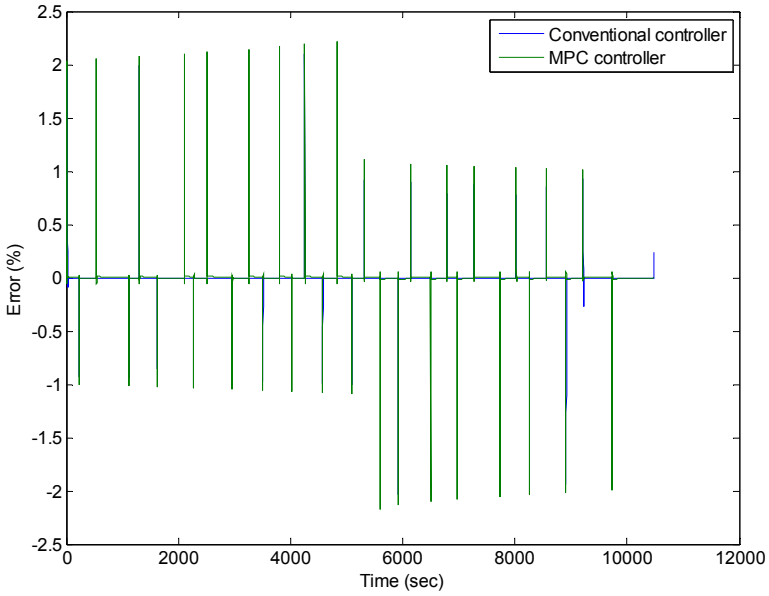

Figure 45: Conventional & MPC controllers' % error for turbine load

Figure 46 shows the output of the steam generator water level. The blue line represents the conventional plant control. Green is the measured output from the state-space model for the steam generator water level. This is the output controlled by the MPC controller. The red line is the reference signal given to the MPC controller.

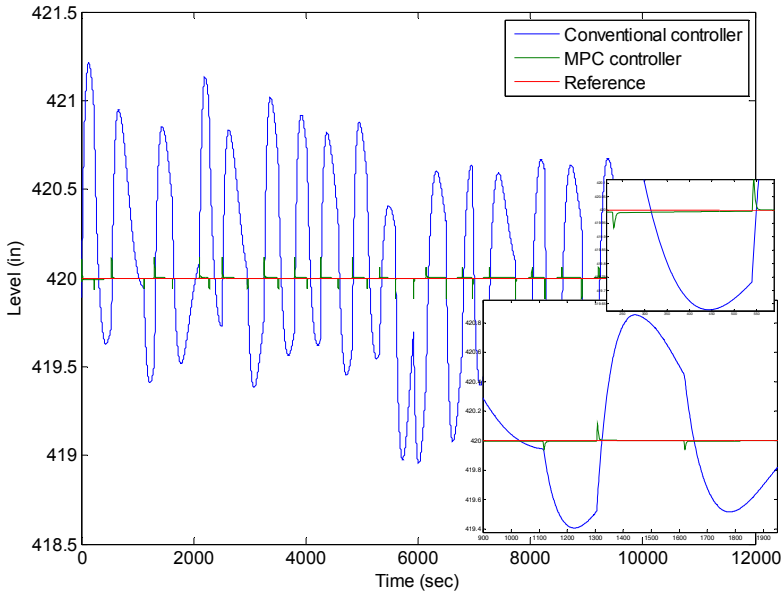

Figure 46: Compare conventional & MPC controllers for steam generator level

The MPC controller responds much faster than the conventional controller to changes in the steam generator water level. The conventional controller responds slowly to changes in the steam generator water level. Figure 47 provides the percentage error experienced for Figure 46.

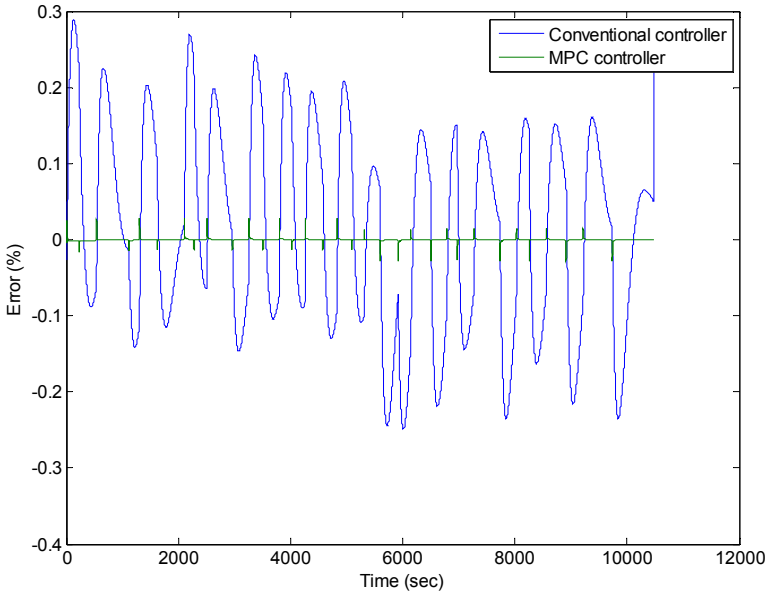

Figure 47: Conventional & MPC controllers' % error for steam generator level

Figure 48 shows the manipulated variable for the control rod reactivity. The blue line is the conventional plant control and the green line is the manipulated variable from the MPC controller for the control rod reactivity.

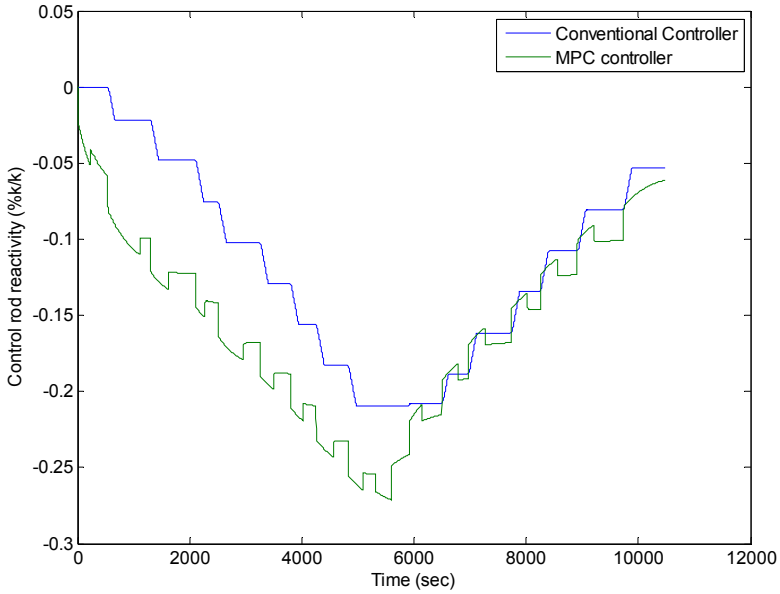

Figure 48: Compare conventional & MPC controllers for control rod reactivity

The MPC controller values differ from that of the conventional controller. This is expected as the reactor power output presented in Figure 42 response is different. The values are not unacceptable although they go down lower than the conventional controller. This can have implications on the reactivity constraint.

Figure 49 shows the manipulated variable for the steam mass flow rate. The blue line represents the conventional plant control. The green line is the manipulated variable from the MPC controller for the control rod reactivity.

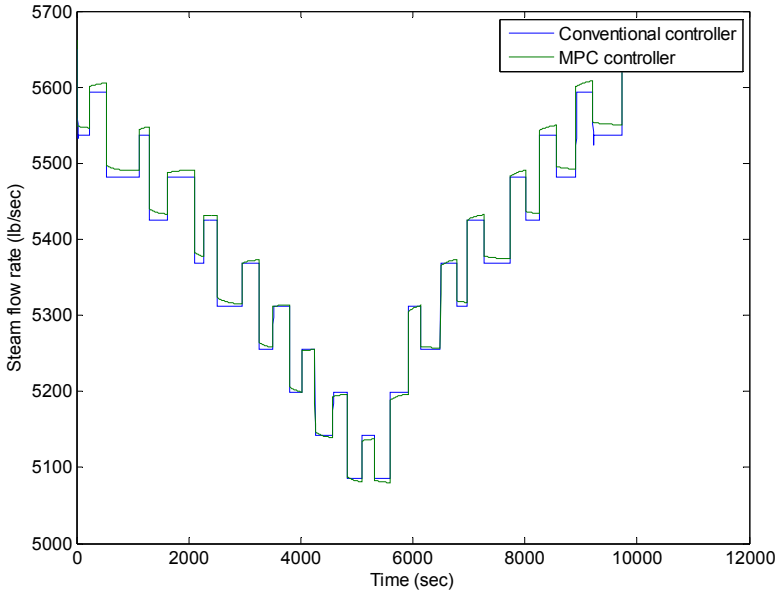

Figure 49: Compare conventional & MPC controllers for steam mass flow

The MPC controller illustrates similar values for the steam supply to the turbine. This corresponds to the good result obtained for the turbine load presented in Figure 44.

Figure 50 shows the manipulated variable for the feedwater mass flow rate. The blue line represents the conventional plant control. The green line is the manipulated variable from the MPC controller for the control rod reactivity.

Figure 50 shows the feedwater supply to the steam generator. It is seen that the feedwater mass flow rate experiences large, rapid changes at every load change. The change in feedwater mass flow rate is approximately 26.5lb/s^2 (12kg/s^2). This is within limits and completely acceptable if it is considered that the total mass flow rate is in the order of around 5511lb/s (2500kg/s), approximately 640kg/s per loop for a three loop system. A change in feedwater mass flow rate of 8.8 lb/s^2 (4kg/s^2) per

loop is the result. This can be achieved by the system. The sharp rises in the mass flow rate is therefore acceptable.

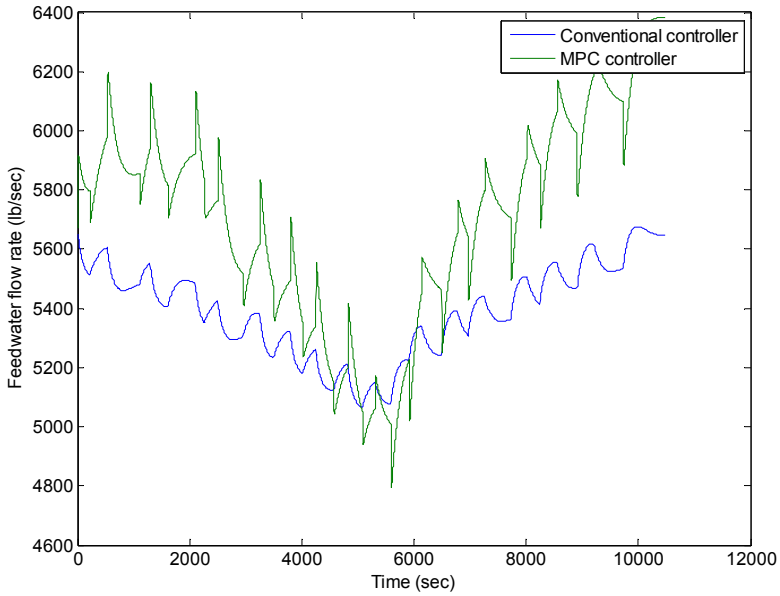

Figure 50: Compare conventional & MPC controllers for feedwater mass flow

The one concern in this case is the high flow rate values that the MPC controller reaches. These values should be similar to that of the conventional controller. The flow rates differ by approximately 300lb/s (136kg/s). It is also observed that at the lower power ranges the MPC controller flow rates are similar to that of the conventional system.

6.3 Simulink® ITAE performance index

To compare the performance of the conventional control and the MPC controller the ITAE performance index is used. An additional performance index library is included into Simulink®. This performance index library includes three performance indices: the integral of the squared error (ISE), the integral of the absolute value of error (IAE), and the integral of time multiplied by the absolute value of error (ITAE). Figure 51 shows the parameters of the ITAE function block. The ITAE function block has no parameters that can be set. The input to the ITAE function block is the error between the value of the controlled variable and the value of the reference signal. The ITAE value is displayed using a display block. The display block format is set to short to display a 5-digit scaled value with fixed decimal point [27].

Figure 51: ITAE function block parameters

6.3.1 Setup

Figure 52 shows the ITAE function block applied to the Simulink® simulation. An ITAE value is generated for each of the three measured outputs for both the conventional control and the MPC controller.

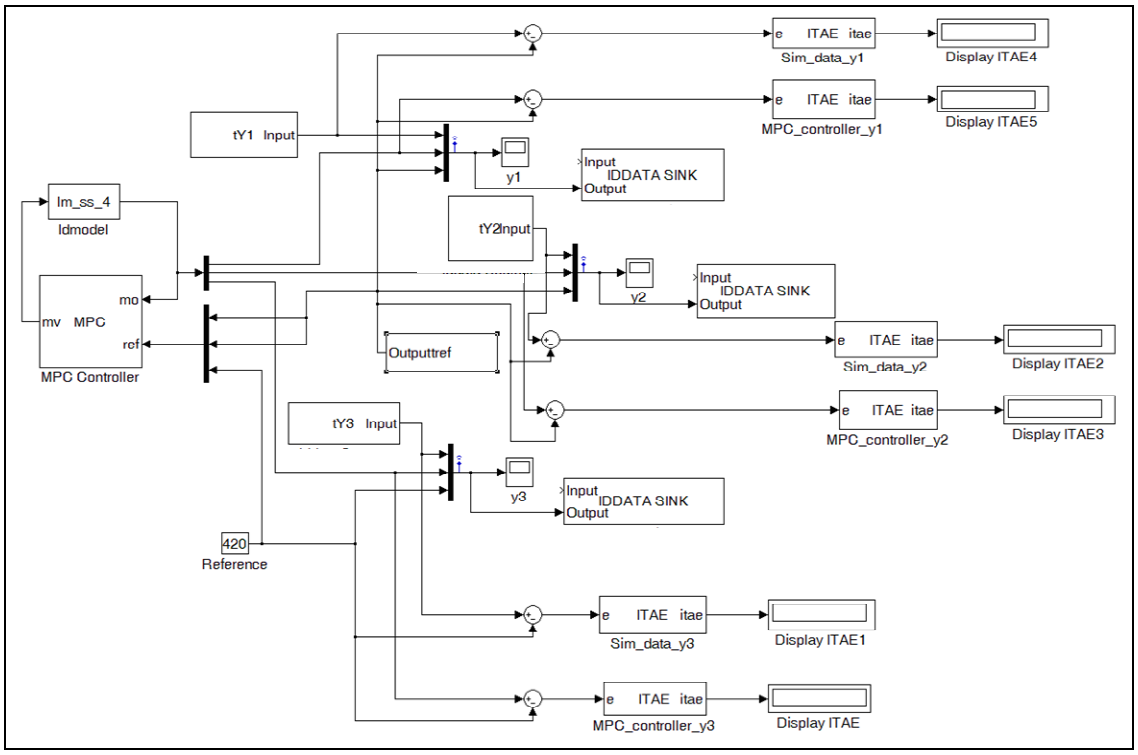

Figure 52: Simulink® ITAE performance indexing

6.3.2 Results

The ITAE is calculated for four different situations. The first is for a load change from 100% of full power to 90% of full power. The power is changed from 100% to 90% and the ITAE is determined for both the conventional control and the MPC controller of the Simulink® model. The second is for a load change from 90% back to 100% of full power. The power is changed from 90% to 100% and the ITAE is determined for both the conventional control and the MPC controller of the Simulink® model. The third is a smaller load change from 100% of full power to 95% of full load power. The

power is changed from 100% to 95% and the ITAE is determined for both the conventional control and the MPC controller of the Simulink® model. The fourth is again for a load change from 95% back to 100% of full load power. The power is changed from 95% to 100% and the ITAE is determined for both the conventional control and the MPC controller of the Simulink® model. The results for each of the abovementioned scenarios are given in Table 17.

Table 17: ITAE values for conventional and MPC controller

		ITAE value 100%-90%	ITAE value 90%-100%	ITAE value 100%-95%	ITAE value 95%-100%
y_1	Conventional controller	11600	7697	3716	5633
	MPC controller	3449	4096	1837	1822
y_2	Conventional controller	6613	6633	22.14	870.7
	MPC controller	2298	2708	1176	1171
y_3	Conventional controller	452100	289700	112800	112700
	MPC controller	239.2	333.5	100.8	96.89

Table 17 shows that for all four cases for the reactor power (y_1) the MPC controller produced much better performance than the conventional controller. For the turbine load (y_2) the performance of the conventional controller was better for the load changes between 100% and 95% of power. The steam generator water level (y_3) control for the MPC controller showed good results.

6.4 Conclusion

The results indicate that the MPC controller controlled the outputs of the model very well. The MPC controller was given a power reference value and a steam generator water level reference value. The MPC controller controlled the outputs much better than the conventional controller. It responded much faster and also settled much quicker than the conventional controller. The ITAE performance index also supported this statement.

For the turbine load the conventional controller and the MPC controller performed quite similar. Figure 44 shows that the MPC controller does perform slightly better than the conventional control, but the difference is not as significant as that of the reactor power. Both controllers responded and settled very quickly to changes made to the turbine load. For the turbine load the rate of change is not questionable as the

PWR simulator indicated similar, and in some cases even slightly faster load changes than what the MPC controller achieved.

The response of the conventional controller to the steam generator water level is quite slow and the MPC controller is very fast and is performing much better. The slow response of the conventional controller is not an indication of bad control strategy, only that the philosophy was not to control the level fast, but within certain limits. The steam generator water level can be allowed to settle over a long time as is shown in the figures presented in the results.

The only concern with the results produced is the feedwater flow rates. In an attempt to improve the feedwater flow rate figures, the MPC controller configuration was changed by giving the feedwater mass flow rate a constraint on it's up and down rates of change. This constraint did decrease the rate at witch the mass flow rate changes and ultimately the values. This however had negative implications on the outputs of the reactor power and the turbine load. The performance of the MPC controller on these two outputs decreased. The ITAE performance index also indicated a decrease in the MPC controller performance when this constraint was included.

Table 17 shows that the MPC controller overall performance using the ITAE performance index. Table 17 shows that the MPC controller shows increased performance when compared to the conventional controller. There is one case where the conventional controller showed better performance than the MPC controller. This was when a load change from 100% to 95% was made. In all other cases however the MPC controller performed better. It is however noted above and indicated in Figure 44 that both the conventional and MPC controllers perform very well for the control of the turbine load.

CHAPTER 7. CONCLUSIONS & RECOMMENDATIONS

7.1 Introduction

During this study a MPC controller was developed for the load following of a PWR plant. Normal operating conditions were assumed and the plant's main control functions were included. The controller was developed for a specific power range of the PWR plant. The controller was tested and evaluated against the conventional PWR control strategies. Many different tools were used to develop the controller. In this final chapter an overview of the work that was done is given. Conclusions are drawn from the work performed and the results obtained. Finally, contributions made by this study are provided along with recommendations for future research. The study is closed of with a closure explaining that the purpose of the study was achieved.

7.2 Overview

In this study a MPC controller is developed for the control of a PWR plant during load following operations. In order to develop a MPC controller a model of the plant is required. A model is developed from measured data taken from a PWR plant simulator. This process is known as system identification. For this study several sets of measured data from a PWR simulator is collected, and using the System Identification Toolbox™ available in Matlab®, several non-linear models are derived for the plant. The non-linear models were linearised and transformed to linear state-space models. These models are verified using the best fit approach where a percentage value is calculated for each of the outputs of each model. The percentage value gives an indication of how well each model output fits the corresponding output values of the measured data. Each model is evaluated against each set of measured data. The best performing model is selected and used as the input for developing the controller. An MPC controller is developed using the MPC toolbox™ available in Matlab®. Several MPC controllers are developed using the best performing identified linear state-space model. These controllers are evaluated on the identified plant model. A Simulink® simulation is also created to evaluate the performance of the MPC controller against the data from the PWR simulator representing the conventional control of a PWR plant. The performance of the

conventional control and the MPC are further evaluated using the ITAE performance index. A Simulink® simulation is used for this purpose.

7.3 Conclusion

The first conclusion drawn from this study is that system identification is a feasible method to be used for creating a model of a PWR plant and can further be used to develop control strategies for the plant. The results of CHAPTER 4 showed that the identified plant models reproduced the outputs of the measured data to acceptable levels. See Appendix B for examples of model fits. Not all the derived models were useful. For this reason more than one model was developed and evaluated to identify the best performing plant model.

Limitations of the methodology of the study are observed where the input and output variables for the model is selected. It would be preferred to select more inputs than outputs as this provides more measured inputs for the model to produce the outputs. Although possible to do this, creating the Simulink® model would not be possible as the variables selected as inputs to the identified model would either have to come from the controller as manipulated variables or be introduced to the model via external data sources obtained from the PWR simulator. Due to the approach followed only the MPC controller manipulated variables were available as input to the plant model. This approach made it possible to create and run the Simulink® simulation without any external data inputs.

The next conclusion drawn from this study is that the MPC controller developed controlled the outputs of the model exceptionally. There are however improvements that can be made regarding the testing and implementation of the MPC controller. The values for the feedwater flow rate manipulated variable were slightly higher than what is expected. The cause for the small variances in deviation of this variable is due to the quality model used for testing the MPC controller in the Simulink® simulation. The rest of the manipulated variables showed good performance. Despite the problems and limitations, the MPC controller performed well and controlled the outputs of the model to the reference value. This action was performed quickly for all three the outputs, and upon any change in the reference

values the MPC controller responded instantly. All values were within acceptable limits with regards to the physical capabilities of a PWR plant.

7.4 Contribution of this study

The outcomes of this study demonstrate that a MPC controller is a viable solution for PWR plant control. It is also showed that a plant model obtained through system identification process can be used to create the MPC controller. The MPC controller derived for the PWR plant had better performance than the conventional controllers for a PWR plant. It is shown that system identification can successfully generate a model of a non-linear system like a PWR plant.

7.5 Recommendations for future research

It is believed that the identified plant model used to develop the MPC controller contains sufficient dynamics for the purpose of developing such a MPC controller. The controller should be evaluated on a plant model created from first principles or even on a PWR plant.

Separate specialised research studies into the two topics system identification and MPC controllers is recommended for fine-tuning the methods of creating the plant models and the MPC controllers. Further research is essential to eventually produce a controller for practical applications.

7.6 Closure

The purpose of this study was to develop a single MIMO controller for the load following of a PWR plant. The controller was to include all control functions of a PWR power plant as far as possible. This objective was achieved by developing a MPC controller for the PWR plant. The required control functions: nuclear reactor power control, steam generator water level control, and control of the turbine steam supply are included into the MPC controller. The MPC controller successfully controlled the PWR plant and outperformed the conventional controller in two of the three main control functions and showed equal performance in one of the three.

LIST OF REFERENCES

[1] M.J.H. Sterling, *Power system control*. University of Sheffield.

[2] IAEA, *Interaction of grid characteristics with design and performance of nuclear power plants*. Vienna, 1983.

[3] IAEA, *Modern instrumentation and control of nuclear power plants: A guidebook*. Vienna, 1999.

[4] J.R. Lamarsh and A.J. Baratta, *Introduction to nuclear engineering*, 3rd Edition: Prentice Hall, 2001.

[5] F. Zhao, J. Ou, and W. Du, *Simulation modelling of nuclear steam generator water level process – a case study*. Isa Transactions 39, 2000

[6] A.P. Sage and J.L. Melsa, *System identification*. Information & control science centre institution of technology, Southern Methodist University, Dallas, Texas, 1971.

[7] J.A. Bernard, *Reactor operation at power*. MIT Nuclear reactor laboratory.

[8] J. Lewins, *Nuclear reactor kinetics and control*. Pergamoon Press.

[9] Koeberg Westinghouse designed reactor operator manuals. Westinghouse nuclear reactor operator course, Volume 1A – 6B.

[10] W.O Erasmus, *Modelling the pebble bed modular reactor using system identification techniques*. Potchefstroom Universiteit vir Christelike Hoër Onderwys, 2003

[11] F.J.E Laubscher, *Ontwerp van die beheeralgoritmes vir die stoomvoorsieningstelsel van 'n drukwaterreaktor*. Universiteit van Pretoria, 1989.

[12] L. Ljung, *System identification: Theory for the user, 2nd Edition*. Linköping University, Sweden, 1999.

[13] Matlab® Version 7.4.0.287, Help Files, 2007.

[14] C.S. Fazekas, G. Szederkènyi, and K.M. Hangos, *A simplified model of the primary circuit in VVER plants for controller design purposes*. Process control research group, Systems and control laboratory, Computer and automation institute, Hungary academy of science, 2006.

[15] M. Gopal, *Modern control system theory*. Department of electrical engineering, Indian institute of technology, Delhi, 1984.

[16] A. Cammi, F. Casella, L. Luzzi, A. Milano, M. Ricotti, *A model predictive control approach for the Italian LBE-XADS*. Energy Department, Nuclear Engineering Devision (CeSNEF), Politecnico di Milano, Italy, 2008.

[17] M. Nikolaou, *Model Predictive Controllers: A Critical Synthesis of Theory and Industrial Needs*. Chemical Engineering Department, University of Houston.

[18] J.P. Hespanha, *Undergraduate Lecture Notes on LQR/LQG Controller Design*. Electrical & Computer Engineering Department, University of California, 2007.

[19] M. Gyunna and I. Hwang, *Design of a PWR power controller using model predictive control optimized by a genetic algorithm*. Department of Nuclear, Chosun University, 2005.

[20] P. Bendotti and B. Bodenheimer, *Identification and H∞ control design for a pressurised water reactor*. Department of Electrical Engineering, California Institute of Technology, Pasadena, 1994.

[21] J.P. Hespanha, Undergraduate lecture notes on *LQR/LQG controller design*. University of California, Santa Barbara, 2007.

[22] C.C. Paige, *Properties of numerical algorithms related to computing controllability.* IEEE transaction on automatic control, vol. AC-26, No.1, 1981.

[23] L. Balbis, R. Katebi, and A. Ordys, *Model predictive control design for industrial applications*. University of Strathclyde.

[24] T.Wildi, *Electrical machines, drives and power systems, 4th Edition*. Prentice Hall, 2000.

[25] Y. A. Cengel and R. H. Turner, *Fundamentals of thermal-fluid science, 2nd Edition,* McGraw Hill, 2005.

[26] R.E. Pruneda, C. Solares, A.J. Conejo, and E. Castillo, *An efficient algebraic approach to observability analysis in state estimation*, Elsevier, 2009.

[27] F.G. Martins, *Tuning PID controllers using ITAE criterion*. Faculty of Engineering, Universoty of Porto, 2005.

[28] M. Lundh and M. Molander, *State-space in model predictive control.* ABB Automation Products AB, 721 59 Västerås.

[29] M. Boroushaki, M. B. Ghofrani, C. Lucas, and M. J. Yazdanpanah, *An intelligent nuclear reactor core controller for load following operations, using recurrent neural networks and fuzzy systems.* Pergamon, 2003.

[30] H. Akkurt and U Colak, *PWR system simulation and parameter estimation with neural networks*. Pergamon, 2002.

[31] S. Shyu, *A robust multivariable feedforward/feedback controller design for integrated power control of nuclear power plant.* Department of Mechanical an Nuclear Engineering, Pennsylvania state University, 2001.

[32] M. Boroushaki, M. B. Ghofrani, C. Lucas, *Identification of a nuclear reactor core (VVER) using recurrent neural networks.* Pergamon, 2002.

[33] P. la Cour Christensen, *Description of the real time PWR power plant model PWR-PLASIM*. Danish atomic energy commission,1974.

[34] H. J. van Antwerpen, *Modelling a pebble bed high temperature gas-cooled reactor using a system CFD approach.* School of Mechanical engineering, North West University, 2007.

[35] H. R. Pota, *MIMO systems – Transfer function to state-space.* IEEE transactions on education, vol. 39, 1996.

[36] N. Song, *Multivariabl controller design for power plant steam temperature control*. Tennesee Technological University, 2004.

[37] S. S. Khorramabadi, M. Boroushaki, and C. Lucas, Emotional learning based controller for a PWRnuclear reactor core during load following operation. Elsevier, 2008.

[38] Micro-simulation Technology. (undated). [Online]. Viewed 2009 February 12. Available: http://www.microsimtech.com/

APPENDIX A: ADDITIONAL INFORMATION

A.1 Why non-linear ARX system identification?

Why is a nonlinear model identified and converted to state-space models if linear state-space models can be identified from the start?

Although both linear and nonlinear models were identified the nonlinear models could not be used as the MPC Toolbox™ requires linear state-space models to work. This was not a problem as both linear and nonlinear models produced good results. The linear models however did not perform as good as the nonlinear models when they were applied to data sets out of its identified power ranges, therefore they could only be used for specified power ranges. This also is not a problem as for this study, the power range limits could be used, as it was only required to test the possibilities that are available. The difficulty with the linear identified models was that, when performing the system identification the state-space model, contained a D-matrix, which is also known as the feedforward matrix. This feedforward led to an error message produced by the MPC tool due to the direct feedtrough that was present. This affected the principle of the working of a MPC controller.

The previous results led to a revision of using the linear identified models. The nonlinear models were now considered. It was noted that, if the nonlinear models are linearised and converted to state-space models, they produced a zero feedtrough matrix. Therefore, these models could be linearised and used to develop the MPC controllers required using the MPC Toolbox™ and direct feedtrough would not be possible anymore. This again produced no problems as the linearised models when validated using the data sets produced good results and also when these models were converted to state space models they produced satisfactory results.

A.2 Pressuriser pressure and level model identification

During the system identification process it was observed that the pressuriser pressure and level that was originally identified as one of the main control systems could not be included in the identification process. During the attempt to identify suitable model structures for simulating the outputs of pressuriser heater and spray

mass flow rate, it was observed that by using the measured data it was not possible to generate model structures that would replicate the measured data sets. In all cases that were attempted the models only gave reasonable fits when the same measured data set was used for identification and for validation. If any one of the remaining data sets was used for verification the models did not produce satisfactory fits. To get insight into the problem, the working of a pressuriser pressure and level control philosophy was studied in more detail than before. The findings are discussed here.

A.1.1 Pressuriser pressure and level control system

The purpose of the pressuriser is to maintain a pressure high enough to prevent the reactor coolant from boiling. In the case of a PWR this coolant is water. It is also required to maintain the pressure below the system design limits.

Three components are responsible for controlling this pressure: Electrical heaters, spray valves, and relief valves.

The heaters are energised when the pressure drops below a certain pressure set point. Once the pressure goes above the pressure set point the heaters are switched off.

The pressure controller receives two values, the actual pressure and a reference pressure. An error signal is then used to control the power output of the heaters. As the actual pressure rises above the reference pressure the heater power is reduced linearly. As actual pressure drops below the reference pressure, the heater power is increased linearly until the maximum heater power is reached.

Pressuriser spray valves are opened as the pressure starts to increase above a certain pressure set point. These spray valves spray water from the reactor coolant system (RCS) cold leg onto the water inside the pressuriser. A further increase in the pressure results in the relief valves being opened into a relief tank. The spray valves are responsible to recover moderate pressure increases. As the pressure rises above the reference the spray valves start to open until fully open. Any larger pressure increases will see the relief valves being used.

The pressuriser level is allowed to increase and decrease as the reactor power/temperature is increasing and decreasing. Keeping a constant level would be difficult as coolant would be required to be extracted and introduced on a continuous basis. This process would be very costly. Instead, a level set point is determined depending on the average coolant temperature. A Chemical and Volume Control System is responsible for maintaining the set level inside the pressuriser. This is done according to a set level for specific average temperatures. It is assumed that the pressuriser level controller maintains the level in the pressuriser at the required set point. This is assumed as the level in the pressuriser does not contribute to any dynamics of any of the systems. It is basically for safety to ensure that the coolant loops always have a sufficient volume of coolant present [9].

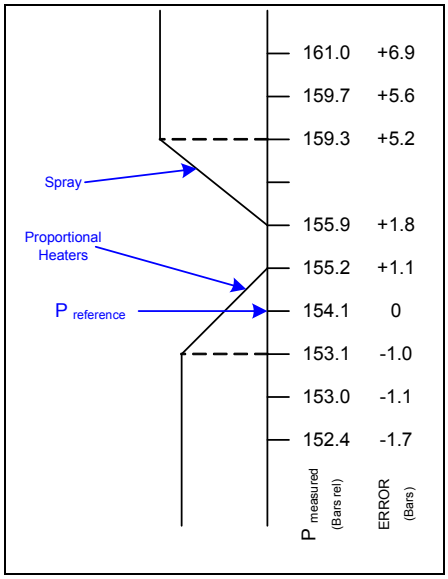

Figure 53: Pressuriser pressure control system illustration [9]

Figure 53 illustrates the principle of the Pressuriser Pressure Control System. The values indicated in Figure 53 are values obtained from the Koeberg operating and training manuals. It shows the values of heater and spray set points as they have been described.

The primary system pressure, the pressuriser heater power and pressuriser spray mass flow of the measured data sets was studied. All the data sets were looked at.

A.1.2 Pressuriser data analysis results

For all the simulated data sets, the heater power and spray mass flow rate was plot against the primary pressure. The result is shown in Figure 54 and Figure 55. Figure 54 shows the heater power (kW) plotted against the system primary pressure (MPa). Figure 55 shows exactly what is illustrated in Figure 53 and what is described in the paragraphs above. From the simulator it is known that the set point is 15.51MPa. The main pressuriser heaters are switched on at about 15.51MPa and increase linearly to about 15.41MPa where the main heaters maximum power of 315kW is reached.

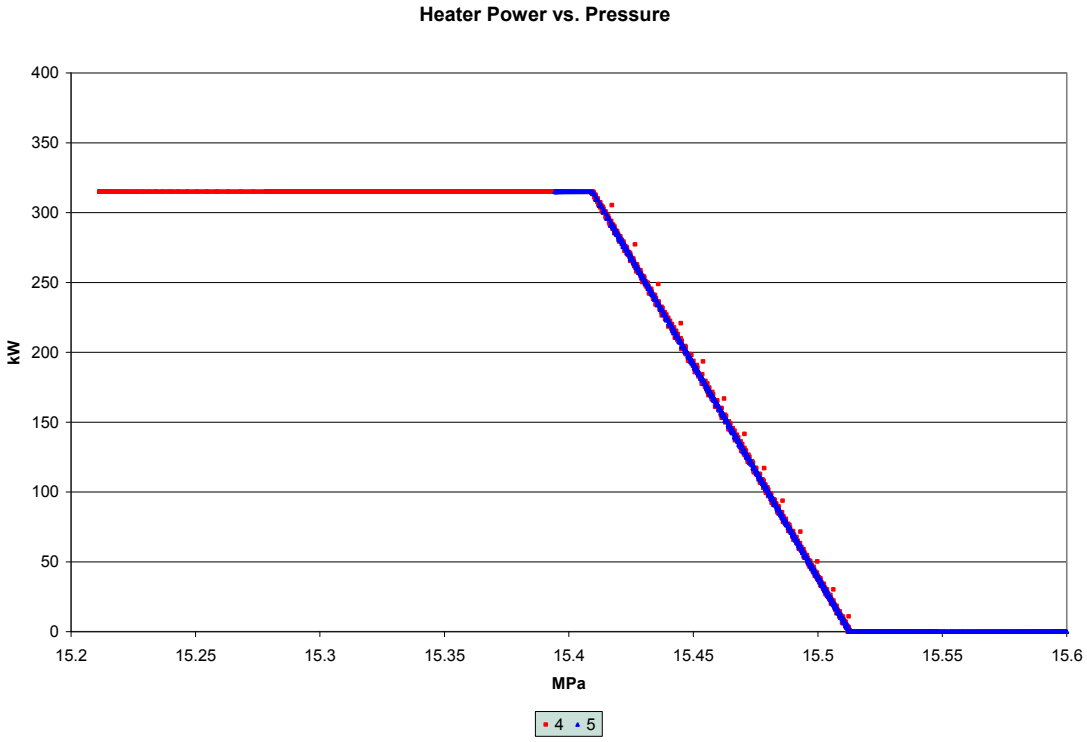

Figure 54: Pressuriser heater power vs. primary pressure

Figure 55 shows the spray mass flow rate plotted against the system primary pressure (MPa). Figure 55 shows exactly what is illustrated in Figure 53 and what is described in the paragraphs above. From the simulator it is known that the set point is 15.51MPa. The pressuriser spray valves are opened at a minimum value and increase linearly to a maximum value. In none of the simulated data sets could a maximum value for the spray mass flow be reached.

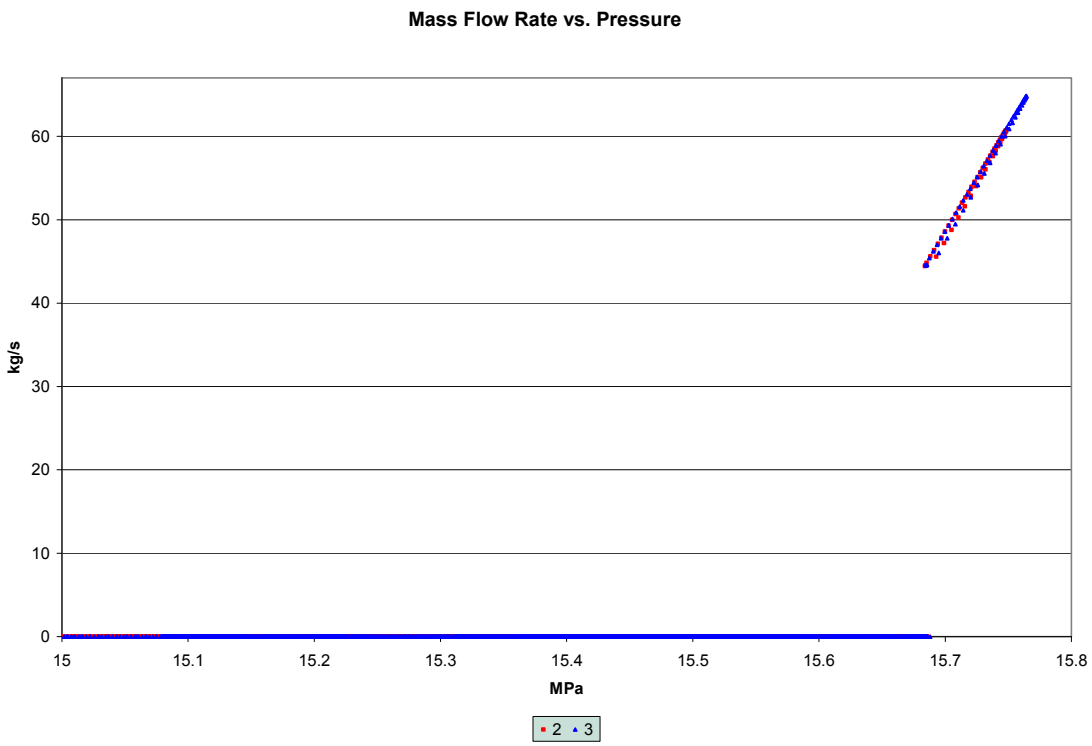

Figure 55: Pressuriser spray mass flow rate vs. primary pressure

As can be seen from Figure 54 and Figure 55 and as was physically proven by identification attempts on the data, system identification can not identify a model structure that would reproduce the same values as a simulation for this part of the system. It does not include any system dynamics but is rather completely preset for all possible primary system pressure values that normal operating conditions will observer. Figure 54 and Figure 55 contain all information required to be able to produce a model for the pressuriser pressure control system.

APPENDIX B: SUPPORTING FIGURES

B.1 Simulated input and output data

Each of the following sections, B.1.1 to B.1.7, provides the data used for system identification. Each section represents a set of data obtained from the PWR simulator. For each of the simulations the output y_2 (turbine load) was changed. The resulting inputs and outputs were then obtained. As the appear in order the output y_1 is the reactor power (%), the input u_1 is the control rod reactivity (%k/k), the output y_2 is the turbine load (%), the input u_2 is the steam mass flow rate (lb/s), the output y_3 is the steam generator water level (in), and the input u_3 is the feedwater mass flow rate (lb/s).

B.1.1 Measured data set 1

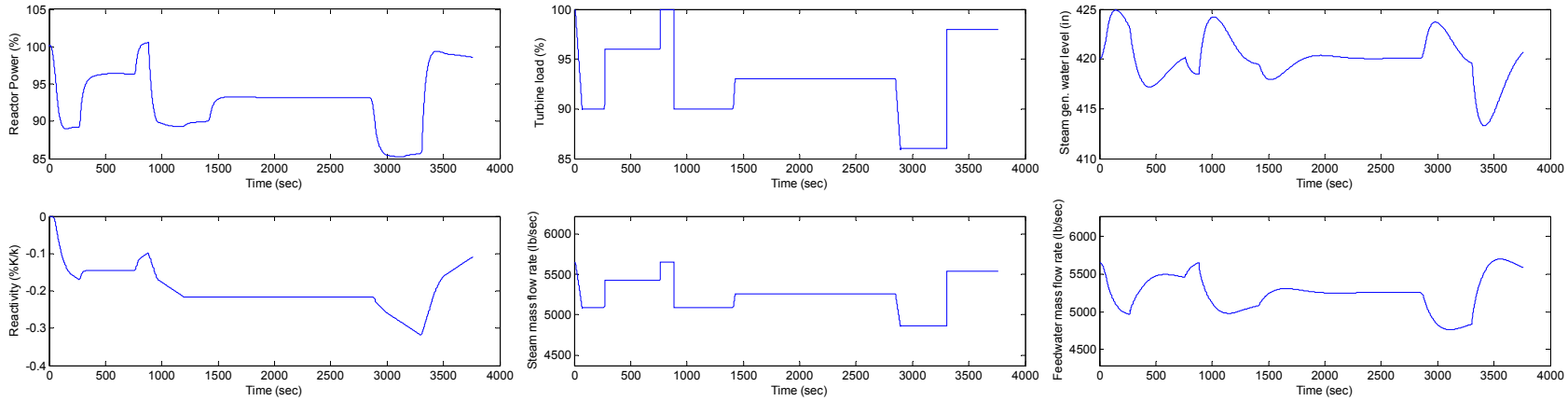

Figure 56: Measured data set 1 inputs & outputs

B.1.2 Measured data set 2

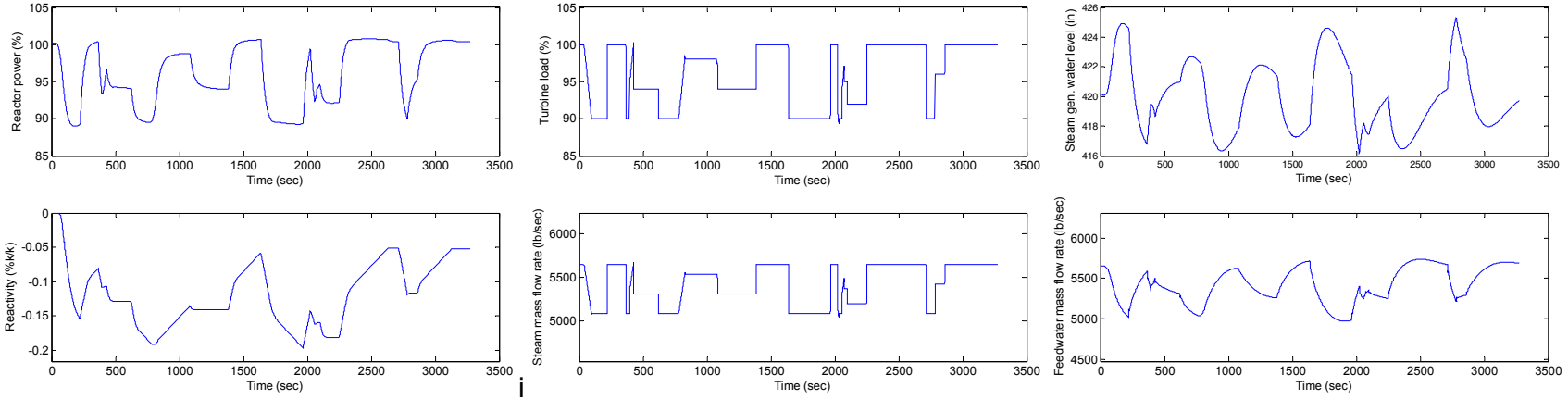

Figure 57: Measured data set 2 inputs & outputs

B.1.3 Measured data set 3

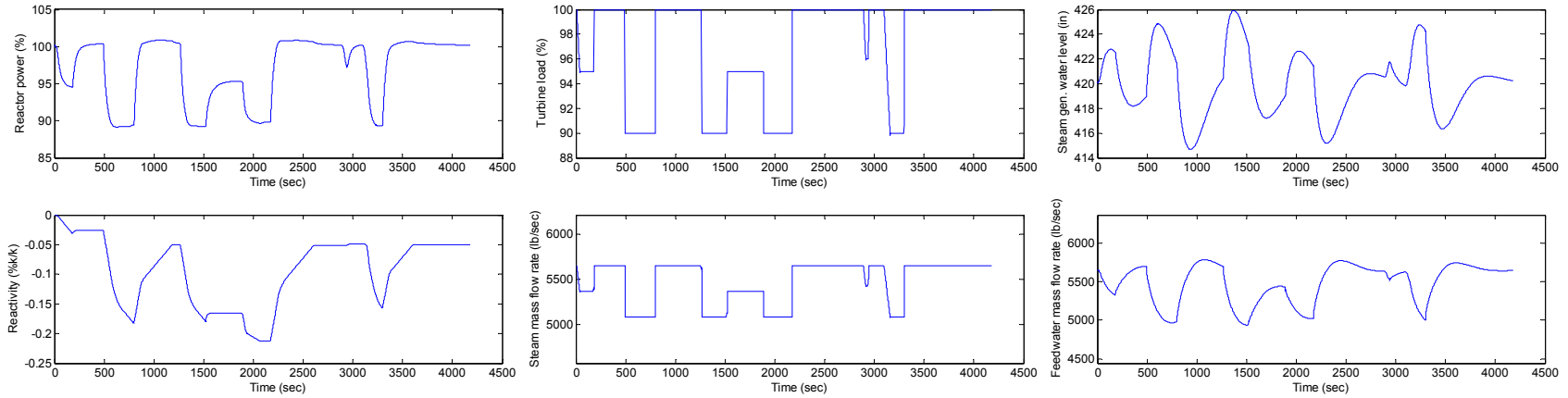

Figure 58: Measured data set 3 inputs & outputs

B.1.4 Measured data set 4

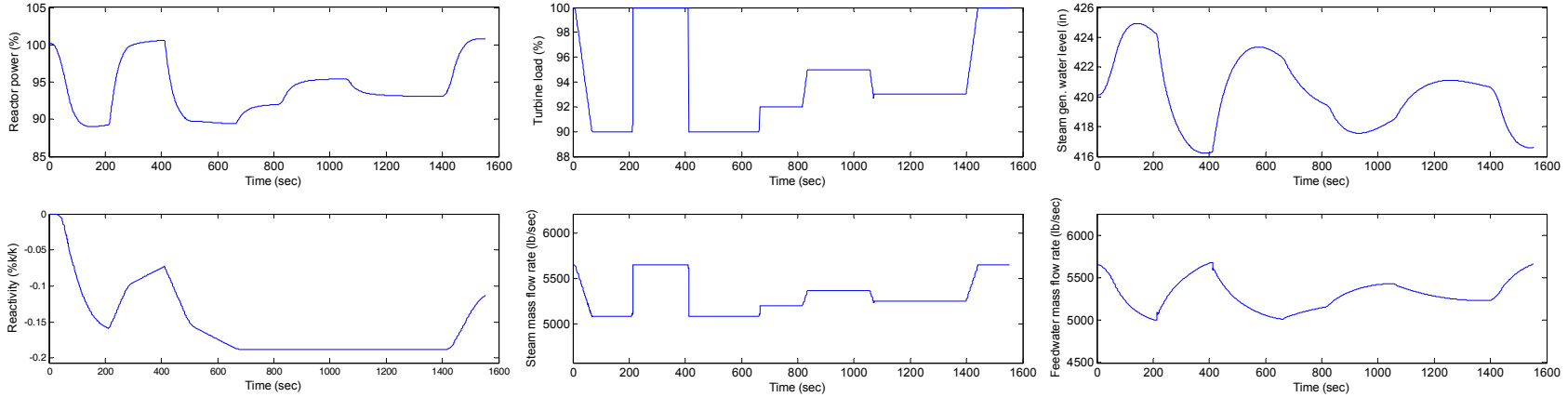

Figure 59: Measured data set 4 inputs & outputs

B.1.5 Measured data set 5

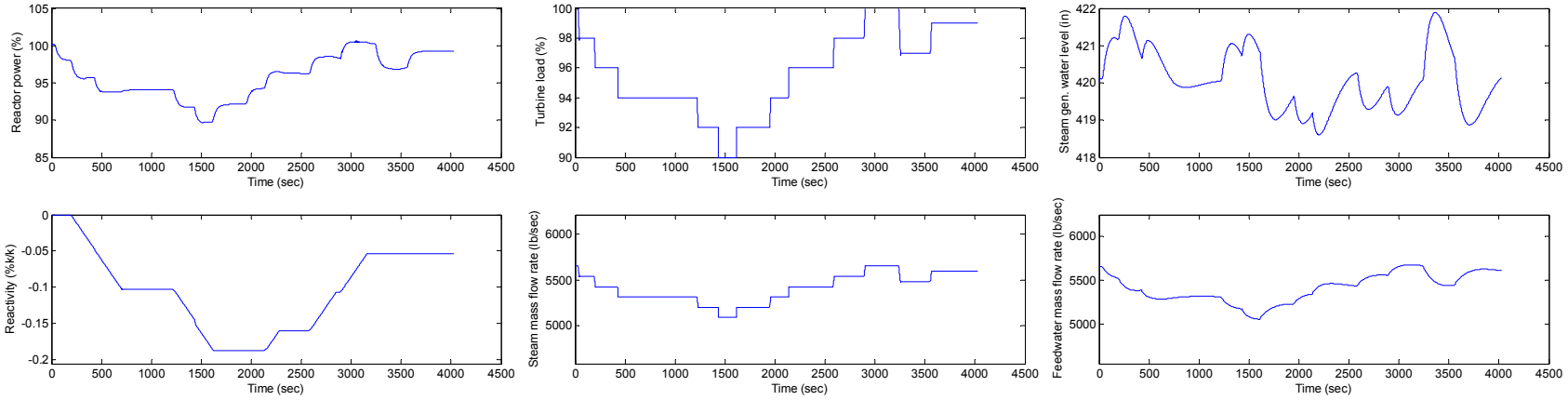

Figure 60: Measured data set 5 inputs & outputs

B.1.6 Measured data set 6

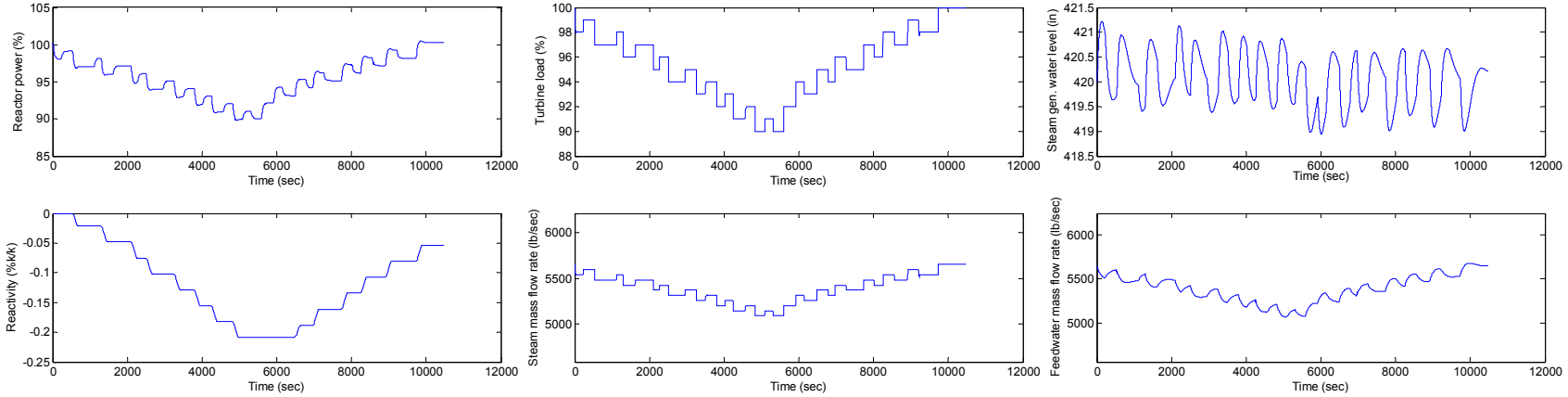

Figure 61: Measured data set 6 inputs & outputs

B.1.7 Measured data set 7

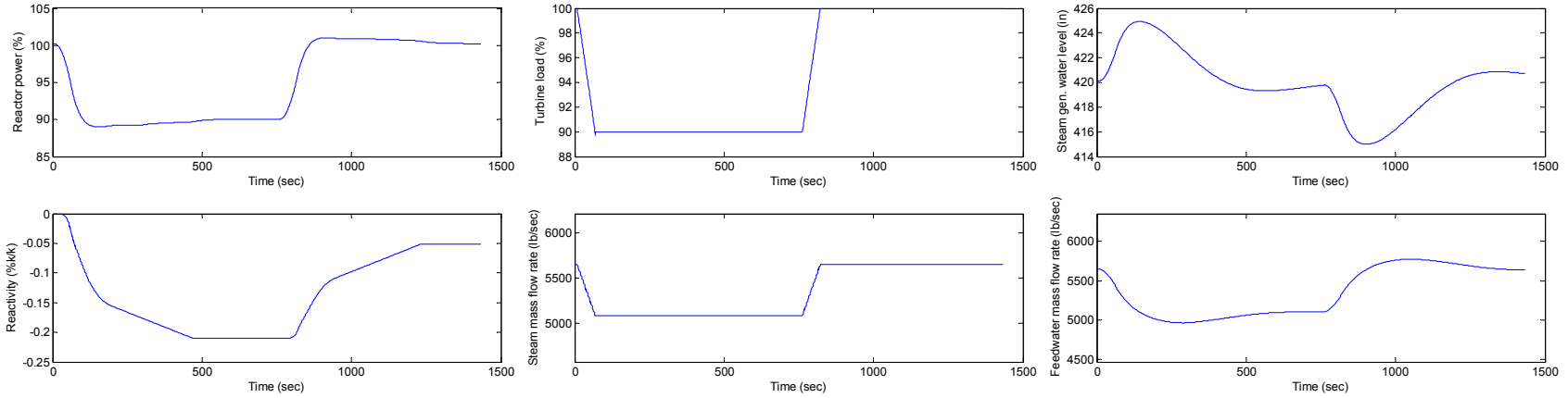

Figure 62: Measured data set 7 inputs & outputs

B.2 Examples of model outputs illustrating percentage fit

The figures below illustrate the output models that were obtained from the system identification of the data set *DS4* given in Figure 59. Figure 63, Figure 64 and Figure 65 provide the outputs y_1, y_2 and y_3 model fits for *nlarx4*, *lm_4* and *lm_ss_4* validated with the data set *DS4* each time. Figure 66, Figure 67 and Figure 68 provide the outputs y_1, y_2 and y_3 model fits for *nlarx4*, *lm_4* and *lm_ss_4* validated with the data set *DS6* each time. Figure 69, Figure 70 and Figure 71 provide the outputs y_1, y_2 and y_3 model fits for *nlarx4*, *lm_4* and *lm_ss_4* validated with the data set *DS7* each time.

B.2.1 Validation with *DS4*

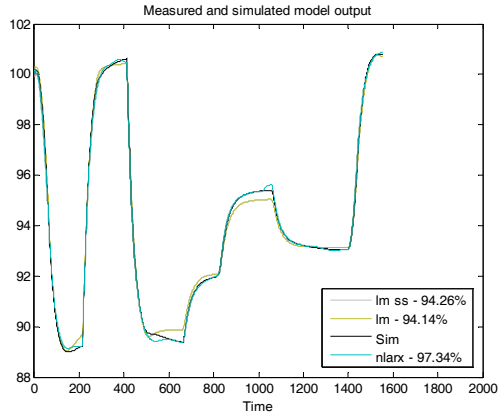

Figure 63: Output y_1 for DS4

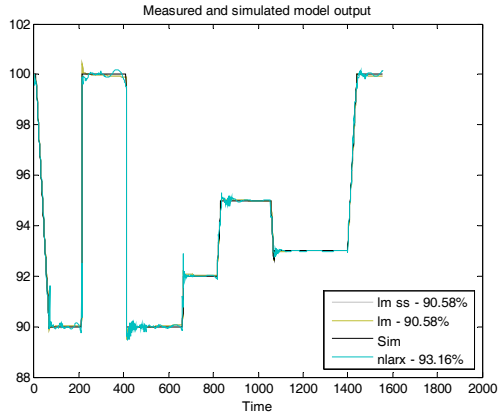

Figure 64: Output y_2 for DS4

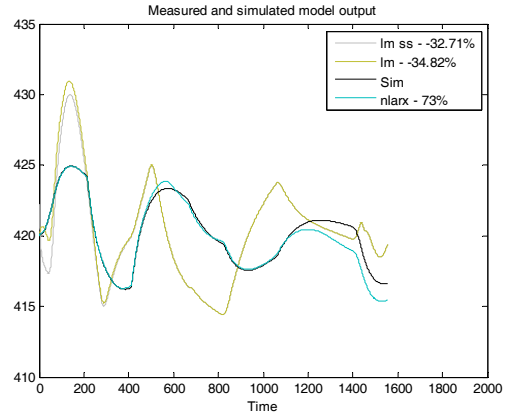

Figure 65: Output y_3 for DS4

B.2.2 Validation with *DS6*

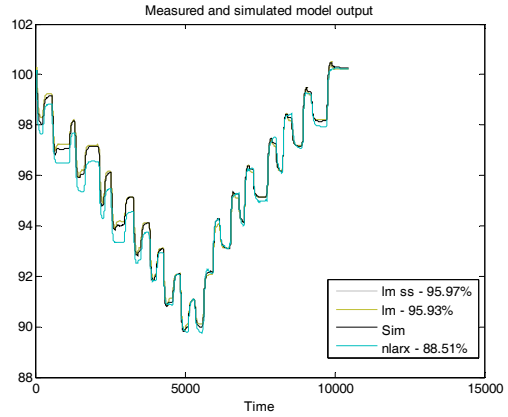

Figure 66: Output y_1 for DS6

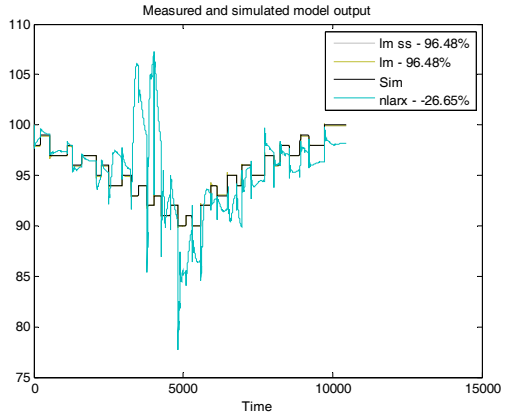

Figure 67: Output y_2 for DS6

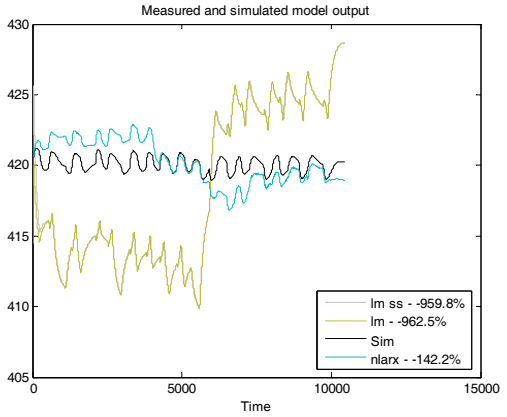

Figure 68: Output y_3 for DS6

B.2.3 Validation with DS7

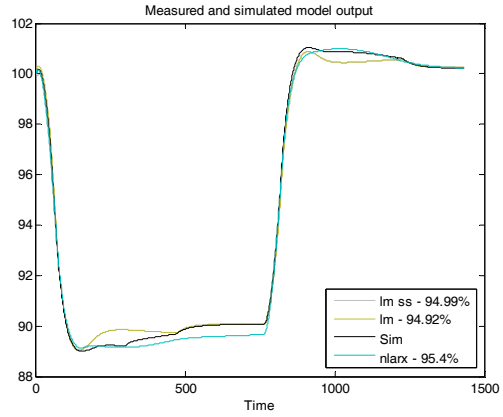

Figure 69: Output y_1 for DS7

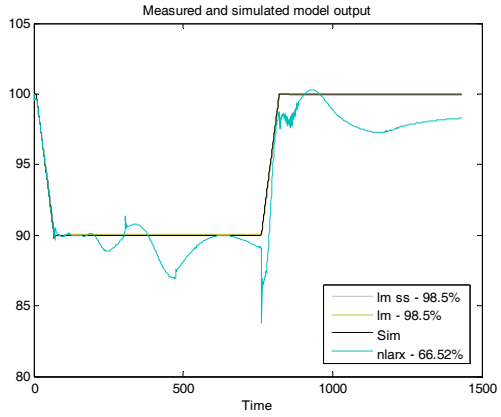

Figure 70: Output y_2 for DS7

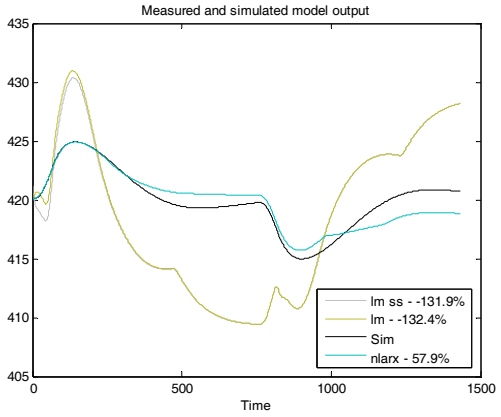

Figure 71: Output y_3 for DS7

APPENDIX C: MODEL STRUCTURES

C.1 Non-linear ARX system model

The model identified has 3 outputs and 3 inputs:

Input names: u_1, u_2 and u_3

Output names: y_1, y_2 and y_3

The model standard regressors corresponding to the orders:

$$n_a = [2 \quad 0 \quad 0; 0 \quad 2 \quad 0; 0 \quad 0 \quad 2],$$

$$n_b = [2 \quad 2 \quad 2; 2 \quad 2 \quad 2; 2 \quad 2 \quad 2], \text{ and}$$

$$n_k = [1 \quad 1 \quad 1; 1 \quad 1 \quad 1; 1 \quad 1 \quad 1].$$

No custom regressors were included.

The nonlinear regressors are as follows:

For output y_1:

$y_1(t-1)$, $y_1(t-2)$, $u_1(t-1)$, $u_1(t-2)$, $u_2(t-1)$, $u_2(t-2)$, $u_3(t-1)$ and $u_3(t-2)$

For output y_2:

$y_2(t-1)$, $y_2(t-2)$, $u_1(t-1)$, $u_1(t-2)$, $u_2(t-1)$, $u_2(t-2)$, $u_3(t-1)$ and $u_3(t-2)$

For output y_3:

$y_3(t-1)$, $y_3(t-2)$, $u_1(t-1)$, $u_1(t-2)$, $u_2(t-1)$, $u_2(t-2)$, $u_3(t-1)$ and $u_3(t-2)$

The nonlinearity estimators used re as follows:

For output y_1: wavenet with 16 units

For output y_2: wavenet with 62 units

For output y_3: wavenet with 30 units

C.2 Linear ARX system model

The linear ARX system model obtained is given by

$$\begin{aligned} &A0\times y(t)+A1\times y(t-T)+A2\times y(t-2T)+\ldots+A4\times y(t-4T) \\ &=B0\times u(t)+B1\times u(t-T)+B2\times u(t-2T)+B3\times u(t-3T). \end{aligned} \quad \textbf{(8.1)}$$

The tables below give the matrices of (8.1).

Table 18: Linear ARX A0 Matrix

1	0	0
0	1	0
0	0	1

Table 19: Linear ARX A1 Matrix

-1.4029	0	0
0	-0.0012	0
0	0	-1.8524

Table 20: Linear ARX A2 Matrix

0.4196	0	0
0	-0.0022	0
0	0	0.8537

Table 21: Linear ARX B0 Matrix

0	0	0
0	0	0
0	0	0

Table 22: Linear ARX B1 Matrix

30.0175	0.0005	-0.0015
-61.9389	0.0198	-0.0073
-39.8608	0.0004	-0.0035

Table 23: Linear ARX B2 Matrix

-30.0066	-0.0002	0.0015
61.2971	-0.0019	0.007
39.6718	-0.0003	0.0035

C.3 State-space system model

The state-space model matrices are presented in the document in the conclusion of CHAPTER 5 SYSTEM .

APPENDIX D: MATLAB® AND SIMULINK® PROGRAM

Refer to the attached CD for the Matlab® and Simulink® files containing all the information and programs developed throughout the course of the study.

APPENDIX E: GENERAL RULES AND ASSUMPTIONS

Mainly based on the explanations of section 5.1 of CHAPTER 5, and following remarks noted throughout the document, the following assumptions are made for the purpose of this study:

- Start-up and shutdown operations are not included as these do not form part of normal reactor load following operations.

- Reactor has been running for a sufficiently long time after a start-up in order to avoid the conditioning period. This is not part of the normal reactor load following operations.

- The load changing region to be considered when collecting data is selected at 30% to 100% of reactor full power up to a maximum rate of 10% per minute. This is considered as the normal load changing range of a PWR as described by most of the sources. For the purpose of this study, only the 90% to 100% region will be simulated and identified in detail. The rest of the load following region will only be looked at and mentioned if interesting findings are made and/or if time allows.

- Slow acting effects are neglected. Only fast acting effects are considered. Therefore, Xenon effects and boron addition are not considered. Xenon and boron effects are considered long term and normal load following takes place in minutes to even seconds. With the term slow is used there is referred to seconds and minutes and long refers to hours and longer.

- The limitation of a maximum rate of power change of 10% per minute is sufficient to assume any design limitations will not need to be considered. This limit can be used as the maximum as it is not a control plant limitation but a mechanical limitation on the power plant components.

- The steam dump system will not be included as it is used in large load rejections and following turbine trips. These are not considered as normal load following operations.

- The bypass feed regulating control system will not be considered as it is only used below 15% power. The feed regulating valve and feed water pump is however essential in the steam generator water level control system.

- The pressuriser pressure and level control system model will not be identified. The reason for this is described in more detail in Appendix A.